



**NORMALISED UNDRAINED SHEAR STRENGTH AND
DEFORMATION PROPERTIES OF REMOULDED
KESWICK CLAY**

By

MD. ZAHURUL ISLAM

B.Sc. Engg. (B. U. E. T.), Dhaka, Bangladesh

Thesis submitted for the degree of Master of Engineering Science

in

The University of Adelaide

(Department of Civil and Environmental Engineering)

Australia

June 1994

Awarded 1995

To

Late Nurun Nahar Begum, grandmother and Late Md. Iman Ali Mondal, grandfather.

ACKNOWLEDGMENTS

The author expresses his deepest gratitude to Dr. G. W. S. Kaggwa, Senior Lecturer, in the Department of Civil and Environmental Engineering, who supervised this research project. He has been a constant source of inspiration in carrying out the whole project. His extensive comments, constructive suggestions and close supervision helped enrich the thesis.

The author is also grateful to Mr. M. B. Jaksa, Lecturer, in the Department for his valuable comments and friendship. It was not possible to carry out the experiments without Laurie Collins, Colin Haese, Robert Kelman, Bruce Lucas, Tad Sawosko, and Stan Woithe. The author would like to thank all these people for their timely help during the experiments. He also wishes to thank all fellow postgraduates particularly, to Mathew Burnet, Anthony Garreffa, Abir Ghosh, Ranjani Jha, and Paul Morgan for their friendship and cooperation over the period of his candidature. The initial help of Anthony Garreffa in the laboratory, and the effort of editing the whole thesis by Paul Morgan is greatly appreciated.

The author is extremely grateful to his parents and friend, Rita Afsar for their love and encouragement during the hard time of research.

Finally the author expresses his thanks to Department of Civil and Environmental Engineering for providing computing and other facilities which enabled the successful completion of the course. The scholarship provided by the Australian International Development Assistance Bureau is gratefully acknowledged. The author is also thankful to Quamrul Islam Siddique, Chief Engineer, Local Government Engineering Department, Bangladesh for providing study leave during the whole course.

STATEMENT OF ORIGINALITY

This work contains no material which has been accepted for the award of any other degree or diploma in any university or other tertiary institution and, to the best of my knowledge and belief, contains no material previously published or written by another person, except where due reference has been made in the text.

I give consent to this copy of my thesis, when deposited in the University Library, being available for loan and photocopying.

SIGNED:

DATE: 29.06.94

Abstract

This research project was undertaken to determine the normalised undrained shear strength and normalised deformation parameters of remoulded Keswick Clay using laboratory tests. The test results were then used to evaluate the in situ soil parameters, followed by analysis of field loading conditions.

Isotropically consolidated undrained triaxial tests were carried out on normally consolidated samples using effective consolidation pressures between 100 kPa and 400 kPa. For overconsolidated samples an effective consolidation pressure of 400 kPa was used followed by reduction of effective consolidation pressure to achieve overconsolidation ratios between 2 and 13. The results from these tests show that the normalised soil parameters are dependent on the overconsolidation ratio.

The normalised soil parameters were extended to determine the in situ parameters of a typical soil deposit with or without surcharge which were then used to calculate the settlement and bearing capacity of a circular footing under different loading conditions. The in situ parameters were used in finite element analyses to determine the time-settlement behaviour of the footing. Footing settlement and bearing capacity, and applied surcharge were used to determine the minimum surcharge needed to ensure that the footing would perform satisfactorily.

Contents

Acknowledgments		i
Statement of Originality		ii
Abstract		iii
Contents		iv
List of Figures		viii
List of Tables		xii
Principal Notation		xiv
Chapter	1	Introduction..... 1
	1.1	Introduction 1
	1.2	Objective and scope 4
	1.3	Thesis layout..... 5
Chapter	2	Triaxial testing of cohesive soils 7
	2.1	Introduction 7
	2.2	Triaxial testing 8

	2.3	Testing equipment.....	9
	2.4	Types of triaxial shear tests	10
	2.4.1	Consolidated drained test (CD).....	10
	2.4.2	Consolidated undrained test (CU).....	12
	2.4.3	Unconsolidated undrained test (UU).....	13
	2.5	Summary.....	15
Chapter	3	Normalised behaviour of cohesive soils	24
	3.1	Introduction.....	24
	3.2	Review of factors affecting the properties of cohesive soils.....	26
	3.2.1	Sample disturbance.....	26
	3.2.2	Initial consolidation.....	28
	3.2.3	Effect of anisotropy	29
	3.2.4	Strain rate.....	30
	3.3	Concept of normalised behaviour.....	31
	3.3.1	Normalisation of soil parameters.....	31
	3.3.2	Normalised behaviour	32
	3.4	The SHANSEP method.....	35
	3.4.1	Laboratory shear tests in the SHANSEP method.....	36
	3.4.2	Testing procedure for normalised soil parameters.....	37
	3.4.3	Representation of various NSP in SHANSEP method.....	38
	3.4.4	Steps involved in SHANSEP method to extend laboratory data to field conditions.....	46
	3.4.5	Assessment of the SHANSEP method in practice.....	48
	3.5	Summary	49
Chapter	4	Description of soil used and experimental program.....	65
	4.1	Introduction	65

	4.2	Soil profile within the Adelaide metropolitan area.....	66
	4.3	Description and properties of Keswick Clay from available literature	67
	4.4	Source of Keswick Clay used in testing program	69
	4.4.1	Preparation of remoulded clay.....	70
	4.5	Preliminary tests on Keswick Clay.....	71
	4.6	Laboratory testing program	74
	4.7	Testing procedure	75
	4.7.1	Choice of sample size.....	75
	4.7.2	Preparation of the sample and set up.....	76
	4.7.3	Sample saturation stage	77
	4.7.4	Consolidation stage.....	79
	4.7.5	Compression stage.....	80
	4.8	Summary.....	82
Chapter	5	Triaxial test results and analysis.....	91
	5.1	Introduction	91
	5.2	Consolidated undrained triaxial test results	92
	5.2.1	Deviator stress and excess pore water pressure versus axial strain	94
	5.3	Analysis of test results	95
	5.3.1	Undrained shear strength	96
	5.3.2	Undrained stress-strain modulus.....	98
	5.3.3	Effective stress paths during undrained loading	100
	5.3.4	Validity of normalised behaviour.....	102
	5.3.5	Normalised soil parameters with different OCR.....	103
	5.4	Comparison of test results with available literature	106
	5.4.1	Normalised undrained shear strength with OCR	106

	5.4.2	Normalised deformation parameter with OCR.....	108
	5.4.3	Pore pressure parameter with OCR.....	109
	5.5	Summary.....	110
Chapter	6	Application of test results to field problems	133
	6.1	Introduction	133
	6.2	The field problem	134
	6.2.1	Typical OCR profile of natural deposit.....	134
	6.2.2	Effects of surcharging	135
	6.3	Determination of soil design parameters	136
	6.3.1	Lateral earth pressure coefficient.....	136
	6.3.2	Effective normal stress versus depth.....	137
	6.3.3	In-situ soil design parameters	137
	6.4	The finite element method	140
	6.4.1	Descritisation of problem	141
	6.5	Results of analysis	142
	6.5.1	Settlement of circular footing.....	142
	6.5.2	Bearing capacity of circular footing.....	144
	6.5.3	Recommendations for design pressure.....	146
	6.6	Summary.....	146
Chapter	7	Summary and conclusions.....	164
	7.1	Summary.....	164
	7.2	Future research	166
	7.3	Conclusion.....	167
References		168

List of Figures

Figure 2.1	Cylindrical soil sample and application of stresses in triaxial testing	17
Figure 2.2	Schematic diagram showing different components of triaxial apparatus	18
Figure 2.3	Typical results from drained triaxial tests on Weald Clay	19
Figure 2.4	Stress path of CD test on normally consolidated and overconsolidated Weald Clay	20
Figure 2.5	Typical stress-strain curves from CU tests on Weald Clay (a) Normally consolidated clay. (b) Overconsolidated clay (OCR =8)	21
Figure 2.6	Effective stress paths from CIU tests on Weald Clay (a) Normally consolidated clay. (b) Overconsolidated clay	22
Figure 2.7	Representation of results of UU test on saturated soil samples	23
Figure 3.1(a)	Triaxial compression test data for $\sigma'_c = 200$ and 400 kN/m^2	52
Figure 3.1(b)	Normalised plot of triaxial test data	53
Figure 3.2	Normalised undrained shear strength for overconsolidated Boston Blue Clay	54

Figure 3.3	Consolidation procedure in the laboratory.....	55
Figure 3.4	Stress system for in situ modes of failure.....	56
Figure 3.5	Variations of normalised undrained shear strength with OCR.....	57
Figure 3.6	Relative increase in undrained shear strength ratio with OCR from CK ₀ UDSS tests.....	58
Figure 3.7	Idealised undrained behaviour in triaxial compression test.....	59
Figure 3.8	Normalised undrained modulus versus OCR.....	60
Figure 3.9	Normalised undrained modulus for Sydney Kaolin.....	61
Figure 3.10	The variation of the pore pressure parameter at failure with OCR.....	62
Figure 3.11	Effective stress path for Marine Clay.....	63
Figure 3.12	Soil conditions of a soil profile at Portland.....	64
Figure 4.1	Typical soil profile beneath Adelaide Metropolitan area.....	85
Figure 4.2	Map of Adelaide city area showing the location of Myer Building.....	86
Figure 4.3	Particle size distribution of Keswick Clay sample.....	87
Figure 4.4	Plasticity chart for Keswick Clay sample.....	88
Figure 4.5	Consolidation curve for Keswick Clay.....	89
Figure 4.6	Relationship between the normalised undrained shear strength and strain rate.....	90
Figure 5.1	Stress-strain and excess pore water pressure-strain curves of remoulded normally consolidated Keswick Clay.....	116
Figure 5.2	Stress-strain and excess pore water pressure-strain curves of remoulded overconsolidated Keswick Clay.....	117
Figure 5.3	Relationship between effective residual mean normal stress and residual shear stress.....	118
Figure 5.4	Relationship between undrained shear strength of Keswick Clay and effective consolidation pressure.....	119

Figure 5.5	Effective stress path for normally consolidated remoulded Keswick Clay	120
Figure 5.6	Effective stress path for overconsolidated remoulded Keswick Clay	121
Figure 5.7	Relationships between $(1+e_f)$, p'_f , and q_f for normally consolidated clay .	122
Figure 5.8	Relationships between $(1+e_f)$, p'_f , and q_f for overconsolidated clay	123
Figure 5.9	Relationships between $(1+e_f)$, (p'_f/p'_e) , and (q_f/p'_e) for Keswick Clay.....	124
Figure 5.10	Normalised behaviour from the stress-strain data of normally consolidated remoulded Keswick Clay	125
Figure 5.11	Variation of normalised undrained shear strength with overconsolidation ratio	126
Figure 5.12	Variation of normalised undrained Young's modulus of elasticity with overconsolidation ratio	127
Figure 5.13	Variation of Normalised undrained modulus (E_u/s_u) with overconsolidation ratio	128
Figure 5.14	Relationship between pore pressure parameter and overconsolidation ratio.....	129
Figure 5.15	Relationship between normalised mean normal stress, p'/p'_e , and normalised shear stress, q/p'_e	130
Figure 5.16	Comparison between experimental and m - based theoretical curve of undrained shear strength ratio of remoulded Keswick Clay.....	131
Figure 5.17	Comparison between experimental and Λ - based theoretical curve for undrained shear strength ratio of remoulded Keswick Clay.....	132
Figure 6.1	Different stress conditions which are used to determine the soil properties	149
Figure 6.2	Relationship between OCR and depth of the deposit	150
Figure 6.3	Relationship between effective vertical stress, σ'_v , for different surcharges with depth of the deposit	151

List of figures

Figure 6.4	Variation of K_0 with depth of the deposit	152
Figure 6.5	Relationship between mean effective stress, p'_0 , and depth of the deposit.....	153
Figure 6.6	Relationship between undrained shear strength, s_u , and depth of deposit	154
Figure 6.7	Relationship between undrained Young's modulus, E_u , and depth of the deposit.....	155
Figure 6.8	Finite element mesh detail	156
Figure 6.9	Relationship between settlement and elapsed time at the centre of a circular footing for 12 kPa loading	157
Figure 6.10	Relationship between settlement and elapsed time at the centre of a circular footing for 24 kPa loading	158
Figure 6.11	Relationship between settlement and elapsed time at the centre of a circular footing for 48 kPa loading	159
Figure 6.12	Relationship between settlement and elapsed time at the edge of a circular footing for 12 kPa loading	160
Figure 6.13	Relationship between settlement and elapsed time at the edge of a circular footing for 24 kPa loading	161
Figure 6.14	Relationship between settlement and elapsed time at the edge of a circular footing for 48 kPa loading	162
Figure 6.15	Variation of long term settlement and safe and bearing pressure of 4 m diameter footing with surcharge pressure	163

List of Tables

Table 3.1	Computation of in situ undrained shear strength s_u , from Figure 3.5.....	51
Table 4.1	Comparison between Keswick Clay and London Clay	83
Table 4.2	Results of Atterberg limit tests	84
Table 4.3	Summary of testing program	84
Table 4.4	Suggested maximum particle size for triaxial samples	84
Table 5.1	Initial sample conditions, OCR and final water contents for CIUTC tests on remoulded Keswick Clay.....	112
Table 5.2	Axial loading data for CIUTC tests on remoulded Keswick Clay	112
Table 5.3	Undrained shear strength and undrained shear strength ratios from CIUTC tests of remoulded Keswick Clay.....	113
Table 5.4	Undrained Young's modulus at different stress level from CIUTC tests	113
Table 5.5	Data of specific volume at residual state, $(1+e_f)$, peak shear stress, q_f , peak normal stress, p'_f , normalised peak shear stress, q_f/p'_e , and normalised effective mean normal stress, p'_f/p'_e , from CIUTC tests	114

List of tables

Table 5.6	Variation of normalised undrained Young's modulus (E_u/s_u) with OCR from CIUTC tests.....	114
Table 5.7	Variation of experimental undrained shear strength ratio with theoretical undrained shear strength ratio	115
Table 6.1	Summary of in situ undrained shear strength, undrained and drained Young's modulus of elasticity for no surcharge	148
Table 6.2	Summary of in situ undrained shear strength, undrained and drained Young's modulus of elasticity for surcharge of 30 kPa.....	148
Table 6.3	Summary of in situ undrained shear strength, undrained and drained Young's modulus of elasticity for surcharge of 60 kPa.....	148

Principal Notation

The following symbols are used in this thesis:

A_f	= pore pressure parameter at failure
A_o	= initial area
A_r	= pore pressure parameter at residual state
A_u	= pore pressure parameter during sampling
b_c, b_q, b_γ, b'_c	= base factors used in bearing capacity analysis
B	= Skempton's pore pressure parameter
C_c	= compression index
C_s	= swelling index
c'	= effective cohesion intercept
c'_r	= residual effective cohesion
d_c, d_q, d_γ, d'_c	= depth factors used in bearing capacity analysis
e	= void ratio
e_f	= void ratio at failure
E'	= drained Young's modulus of elasticity

Principal notation

E_i	= initial Young's modulus of elasticity
E_u	= undrained Young's modulus of elasticity
$E_{u(j)}$	= undrained Young's modulus at stress level j
E_{ui}	= initial undrained Young's modulus of elasticity
E_{u25}	= undrained Young's modulus of elasticity at 25% stress level
E_{u50}	= undrained Young's modulus of elasticity at 50% stress level
g_c, g_q, g_γ, g'_c	= ground factors used in bearing capacity analysis
G_s	= specific gravity of solids
i	= hydraulic gradient
i_c, i_q, i_γ, i'_c	= inclination factors used in bearing capacity analysis
I_l	= liquidity index
I_p	= plasticity index
k	= hydraulic permeability
K	= slope of the swelling line (isotropic condition)
K_c	= effective consolidation ratio
K_o	= coefficient of earth pressure at rest
$K_o(OC)$	= K_o for overconsolidated clay
$K_o(NC)$	= K_o for normally consolidated clay
L	= original length of the sample
m_{vc}	= volume compressibility
m_{vs}	= volume expansibility
M	= slope of critical state line
N_c, N_q, N_γ	= bearing capacity factors
OCR	= overconsolidation ratio
\bar{p}	= mean normal effective stress
p_c	= maximum effective consolidation pressure
p_e	= effective equivalent pressure
p'_f	= effective peak mean normal shear stress

Principal notation

p_o'	= effective mean normal stress
p_r'	= residual effective mean normal stress
p_s'	= mean effective normal stress on critical state line
p_x'	= mean effective normal stress at critical state on swelling line
q	= shear stress
q_f	= peak shear stress
q_r	= residual shear stress
q_{ult}	= ultimate bearing capacity
Q	= flow rate
r	= spacing between the normal consolidation line and the critical state line
R	= overconsolidation ratio
s_c, s_q, s_γ, s_c'	= shape factors used in bearing capacity analysis
s_u	= undrained shear strength
s_{ur}	= undrained residual shear strength
V_s	= volume of solids
w	= moisture content
w_l	= liquid limit
W_s	= weight of solids
ϵ	= axial strain
ϕ'	= effective shearing angle (effective stress analysis)
ϕ_r'	= residual effective shearing angle
ϕ_u	= undrained shearing angle (total stress analysis)
λ	= slope of the normal consolidation line
σ'_{1c}	= effective vertical consolidation pressure
σ'_{1f}	= effective major principal stress
σ_3	= confining pressure
σ'_{3c}	= effective lateral consolidation pressure
σ'_{3f}	= effective major principal stress

Principal notation

σ'_c	= effective confining pressure
σ_d	= deviator stress
σ'_p	= pre-consolidation pressure
σ'_r	= residual mean effective normal stress
σ'_{ps}	= effective stress after sampling
σ'_{vm}	= effective maximum past pressure
σ'_{vo}	= effective overburden pressure
τ/τ_f	= shear stress level
$\Delta\sigma_h$	= lateral stress increment
$\Delta\sigma_v$	= vertical stress increment
Δu	= change in pore pressure
Δv	= change in specific volume
Λ	= plastic volumetric strain ratio



Chapter 1

Introduction

1.1 Introduction

The need for shelter and leisure facilities to support the increasing human population has resulted in situations all around the world where quality construction sites for buildings and other infrastructure are rare. In order to accommodate the varied infrastructure requirements, engineers have to design foundations on many sites where the soil conditions are unfavourable, requiring extensive site investigations. One group of soils that pose a range of problems to the designer are cohesive or clay soils. Clays are generally weak and soft, and are susceptible to large movements upon loading. In cities such as Mexico City and Bangkok, engineers have accumulated extensive experience of building on clay soils, although problems abound. The challenges that the engineer faces arise due to the geological history and locations of clays in areas to be traversed by highways, and in

marginal lands where sporting arenas and new high-rise developments are being constructed.

In order to minimise the risk of damage to structures, the soil properties that influence the stability and movements of footings need careful investigation. These investigations have to employ high quality testing procedures that allow proper simulation of the in situ conditions. Also, a clear understanding of soil behaviour is necessary to enable correct interpretation of the test results. The emphasis should be on the determination of soil strength parameters, used in evaluating the stability of footings, and linear elasticity soil parameters for predicting soil movements.

The assessment of undrained shear strength and deformation properties of cohesive soils is a challenging task for geotechnical engineers because of the complexity of soil behaviour. In the field, the nature of a soil is determined by its geological history, which controls the size, shape, mineral composition and packing of the particles, the stress history of the deposit and pore fluid, etc. These properties tend to vary substantially both laterally and vertically within the ground due to micro fabric of the particles and quirks of history. Essentially, it is not feasible to develop a model that incorporates all the above factors in order to determine the undrained shear strength, deformation and pore pressure response under all types of loading conditions. As a result, in practice, three general approaches are adopted to evaluate the soil parameters, namely, laboratory tests, in situ tests and empirical correlations. The accuracy of the parameters obtained from these tests, plays a large part in the reliability of the field predictions.

Recent research demonstrates that the undrained shear strength, s_u , determined from unconsolidated undrained (UU) triaxial tests in the laboratory is susceptible to errors due to sampling disturbance, stress relief, stress anisotropy and strain rate effects. The effects of

sampling disturbance increase with depth of the deposit and cause large variation of undrained shear strength, s_u , over the profile. However, these factors are uncontrollable and often produce large scatter and make the design either unsafe or highly conservative. On the other hand, field vane (FV) test data can overcome the problems that are associated with UU tests, particularly sample disturbance effects. However, empirical correction factors are also required before FV data can be used in design. Accordingly, designs based on assessing soil properties from either UU tests or field vane tests are highly empirical. In order to avoid such empiricism improved methods are essential to investigate the undrained shear strength and deformation properties of cohesive soil that simulate closely the in situ stress conditions.

Therefore with regard to soil investigation, importance has been given to the normalised soil parameter, which is a dimensionless number, and can be correlated with other properties such as overconsolidation ratio (OCR) of the soil deposit. The underlying advantage is that the correlations obtained from the laboratory can be extended judiciously to determine the in situ soil properties. SHANSEP, an acronym for Stress History And Normalised Soil Engineering Properties, is a design method proposed by Ladd and Foott (1974) which determines the in situ undrained shear strength and deformation properties from the normalised soil parameters.

The method introduced an improved testing technique in the laboratory to determine the normalised soil parameters (s_u/σ'_c , E_u/σ'_c) which are related to the overconsolidation ratio. The laboratory testing procedure involved in this method overcomes sampling disturbance, which influences significantly the reliability of laboratory test data, by simulating the in situ conditions. Following the detailed steps of this method, the overall picture of the soil properties (undrained shear strength, s_u , and undrained Young's modulus of elasticity, E_u) within the soil profile can be identified.

It appears from the case studies published by Ladd and Foott (1974) that the SHANSEP method provides a good or slightly conservative indication of stability whereas the use of UU tests has been found to be either unsafe or highly conservative. Thus, it gives the geotechnical engineer a complete framework for analysis and design of footings in cohesive soils.

1.2 Objective and scope

The main objective of this study is to determine the normalised undrained shear strength and normalised deformation properties of remoulded Keswick Clay within the Adelaide metropolitan area using the SHANSEP approach. In order to achieve this objective, emphasis has been given to laboratory undrained triaxial tests. In addition, preliminary tests (index property, permeability and oedometer tests) were performed to characterise and compare the experimental results of Keswick Clay with published data on other cohesive soils.

The experimental program was conducted in the Geotechnical Research Laboratory of the Department of Civil and Environmental Engineering, University of Adelaide. Two series of isotropically consolidated undrained triaxial tests were conducted to determine the normalised soil parameters of remoulded Keswick Clay. In the first series of tests, samples were normally consolidated at effective consolidation pressures of 100 kPa, 200, kPa, 300 kPa and 400 kPa. These tests were performed to examine the normalised behaviour of the soil. The second series of tests were related to the overconsolidated state of the soil where the samples were consolidated with an effective consolidation pressure of 400 kPa and then the effective pressure reduced to achieve overconsolidation ratios of either 2, 4, 8, 10, or 13, prior to shearing.

The results were analysed to obtain design parameters. These parameters were then used to determine the settlement and bearing capacity of footings under typical field conditions.

1.3 Thesis layout

The first part of the thesis describes different types of triaxial tests, the behaviour of cohesive soils, and the factors that affect the undrained shear strength and deformation properties. The SHANSEP method, which includes laboratory testing procedures, and also representation and application of test results, is described. In the later Chapters, the index properties, laboratory testing program and the results of undrained triaxial tests are presented. These results are extended to determine the in situ soil properties which are then used to predict the settlement and bearing capacity of a circular footing supported by a typical soil deposit.

Chapter 2 presents various types of shear tests in the triaxial apparatus, including typical results obtained. This is done through a review of published work. Also included are some of the factors that are associated with the unconsolidated undrained (UU) triaxial tests which are known to affect the undrained shear strength, s_u .

Chapter 3 reviews the advances made in the understanding of the behaviour of cohesive soils. Particular attention is given to the SHANSEP method. This method was developed from the normalised soil behaviour concept with an improved testing procedure in the laboratory, for more reliable evaluation of soil properties. Procedures for extending the laboratory test results to in situ soil properties are also presented.

In Chapter 4, the results of preliminary tests on Keswick Clay are presented to characterise the soil which is subsequently used in the analyses of undrained triaxial tests. Also, the detailed triaxial testing program undertaken for the study is described.

Chapter 5 presents and analyses the results of the laboratory undrained triaxial tests on remoulded Keswick Clay carried out on normally consolidated and overconsolidated samples. The results, in terms of the stress-strain and pore pressure-strain curves, are presented. On the basis of these results the effective strength parameters (c' , ϕ'), undrained shear strength, s_u , and Young's modulus of elasticity, E_u , are determined. The normalised undrained shear strength, normalised deformation parameters and pore pressure parameters are then related to the overconsolidation ratio (OCR), which is the basis of the SHANSEP method. Finally, a comparison is made between the normalised soil parameters from Keswick Clay and those reported by various researchers, as reviewed in Chapter 3.

Interpretation of in situ soil properties is presented in Chapter 6 based on the SHANSEP method. In interpreting the results from the laboratory tests, a typical OCR profile of a natural deposit was chosen from the literature. These properties are then used to predict the settlement and bearing capacity of a circular footing of a typical soil deposit.

An overall summary of the whole study is presented in Chapter 7. In this Chapter, the conclusions drawn from the present study are also included along with recommendations for further study.

Chapter 2

Triaxial testing of cohesive soils

2.1 Introduction

Since the development of the triaxial apparatus during the 1930's, triaxial shear tests have been widely used in geotechnical engineering practice for measuring the mechanical properties of normally consolidated and overconsolidated soils (Saada and Townsend, 1981). The mechanical properties that are often determined from the triaxial shear tests include consolidation characteristics and shear strength of the soil. Triaxial shear testing is also used to understand the influences of stress history, strain rate, creep and cyclic loading upon soil response.

It is assumed that the behaviour of the soil sample in the triaxial shear test in the laboratory will simulate closely the state of the soil in the field. In order to obtain appropriate and representative soil properties of those in the field, the soil sample has to be collected from a relatively uniform deposit to ensure sample integrity. It should

be noted that some soil samples, such as very sensitive soils, may not accurately represent the field properties even if they are collected from uniform deposits. This is because the stress-strain and strength properties of a very sensitive soil will be significantly influenced by disturbances during the sampling, handling and transportation process which cannot be regenerated in the laboratory. However emphasis has been given in this research to the triaxial testing of saturated soils which do not have unusually high sensitivities.

As a background for later chapters of the thesis, this chapter briefly reviews triaxial testing, triaxial apparatus, the various types of triaxial tests and typical results obtained from different types of triaxial tests.

2.2 Triaxial testing

The triaxial test is normally carried out on a cylindrical soil sample as shown in Figure 2.1. The soil sample is sealed in a water tight rubber membrane which is enclosed in a cell. Firstly a confining pressure, σ_3 , is applied in the form of fluid pressure around the sample, and acts as an all round pressure on all planes of the sample. Then an additional stress difference or deviator stress, σ_d , is applied in the axial direction of the sample. It is important to note that on an element of soil in the field there acts three different principal stresses, namely σ_1 , σ_2 and σ_3 , but only two different principal stresses can be applied in the triaxial apparatus.

Failure is achieved in two ways, namely triaxial compression and triaxial extension. In triaxial compression, failure occurs by increasing the compressive axial stress acting on the sample. Under this condition the axial stress is the major principal stress, σ_1 , and the intermediate and minor principal stresses, σ_2 and σ_3 , are both equal to the cell pressure. On the other hand, in triaxial extension failure occurs by increasing the cell

pressure. Thus the major principal stress is equal to the intermediate principal stress, σ_2 , ($\sigma_1 = \sigma_2 =$ cell pressure). In the context of this thesis emphasis has been given to triaxial compression conditions.

2.3 Testing equipment

The principal features of triaxial apparatus are shown in Figure 2.2. The triaxial apparatus consists of three principal components. First, is the base of the apparatus that forms the pedestal of the cell where the sample rests. It is cylindrical in shape and is machined from a block of bronze, aluminium or stainless steel. In addition it contains three different connections. One of the connections is for filling the cell with water to apply the cell pressure and the other two connections are connected with the base and top of the sample to allow two-way drainage during consolidation. To measure the volume change of the sample during consolidation and the increase in pore water pressure during undrained compression tests, these connections are attached to volume change and pressure transducers.

The second component is a removable transparent perspex cylinder that acts as an enclosure to enable fluid pressure to be applied around the sample. During testing it is fitted at the base between o-ring seals. Generally a perspex cylinder of 102 mm diameter and 6.5 mm wall thickness is used to test 38 mm diameter and 76 mm high sample in the laboratory.

The third component is the loading ram by which the deviator stress is applied to the sample. The stiffness of the ram should be sufficient enough to withstand a wide range of axial loads without significant deformation. In this apparatus a 12.7 mm diameter stainless steel ram is used.

2.4 Types of triaxial shear tests

In order to duplicate the field drainage conditions in the laboratory, triaxial shear tests have been classified into three types. These are:

1. Consolidated drained (CD) tests
2. Consolidated undrained (CU) tests
3. Unconsolidated undrained (UU) tests

The above tests are carried out in the laboratory to determine the shear strength and deformation properties of soil. In consolidated drained tests, the drained shear strength properties, (c', ϕ') , drained Young's modulus of elasticity, E' , and drained Poisson ratio, ν' , can be determined. On the other hand, the undrained shear strength, s_u , and undrained Young's modulus of elasticity, E_u , are determined from CU and UU tests. It should be noted that the drained properties can also be obtained from CU tests. In the following sections, the main features of each test are discussed.

2.4.1 Consolidated drained test (CD)

The sample in a CD test is fully consolidated under the applied confining pressure and full drainage is allowed during the shearing stage. The shearing during the drained test is performed at a slow strain rate to ensure no excess pore water pressures are developed in the sample at any time, i.e. the change in excess pore water pressure, Δu , is equal to zero.

As no excess pore water pressure is generated throughout the test, the results of consolidated drained triaxial tests are presented in the form of stress versus axial strain and volume change versus axial strain graphs. A typical result from a consolidated drained test is shown in Figure 2.3 for both normally consolidated and

overconsolidated Weald Clay¹ (Henkel, 1956). The stress-strain curves show that both soil samples approach comparable failure stress ratios (q_f/σ'_c) at large strains. It can be seen from the figure that the overconsolidated soil is stiffer and has a higher maximum shear strength. The volume for the overconsolidated soil sample initially decreases and then increases, whereas for the normally consolidated soil the volume decreases throughout the test.

In order to determine the effective stress parameters c' and ϕ' , a series of samples are tested at different confining pressures (which gives different effective stresses) in the consolidated drained tests. The results are presented as a series of Mohr's circles for the failure stresses. Usually when the number of tests is more than three then it becomes quite difficult to draw a straight line failure envelope, tangential to all the Mohr's circles. A limitation of Mohr's circle is that it does not show the states of stress that exist at non-failure conditions. Thus, the changes in stress during shearing are expressed using stress paths. These curves show the variations of the mean normal effective stress, $p' = (\sigma'_1 + \sigma'_3)/2$ and shear stress, $q = (\sigma_1 - \sigma_3)$.

The stress paths for both normally and overconsolidated Weald Clay are shown in Figure 2.4. For normally consolidated soil the failure envelope passes through the origin, which means that the effective cohesion, c' , is zero, but the overconsolidated soil exhibits a small cohesion intercept. The effective cohesion for overconsolidated soil usually varies from 4.8 kPa to 24 kPa (Lambe and Whitman, 1979). Laboratory tests are usually carried out on partially disturbed soil samples which have initial effective stresses that are different from the in situ values. So, at low consolidation pressures the failure envelope of normally consolidated clay is curved rather than a straight line, and demonstrates overconsolidated behaviour as there has been partial stress relief from the in situ stress conditions.

¹The Weald Clay is an estuarine deposit of the Cretaceous period (Parry, 1960).

2.4.2 Consolidated undrained test (CU)

The soil sample in the consolidated undrained (CU) test is initially consolidated under either isotropic or anisotropic stress conditions. After the sample is fully consolidated the drainage is closed. During shearing, the pore pressure response is measured in addition to the stress-strain behaviour. At this stage, the CU test on a saturated soil sample can be characterised by zero volume change ($\Delta v = 0$) and varying excess pore pressure, ($\Delta u \neq 0$).

Since the drainage is closed during shearing, the water content, void ratio and the dry density remain constant, and equal to the values at the end of the consolidation stage. Typical results of stress-strain and effective stress paths for both normally consolidated and overconsolidated soil samples are shown in Figures 2.5 and 2.6. The stress-strain curves show that the deviator stress increases steadily for both soil samples until failure. It should be noted that for both soils failure occurs at relatively large strains. Furthermore, these figures show that the pore water pressure increases steadily for a normally consolidated soil while for an overconsolidated soil it increases initially but then decreases. Generally, in normally consolidated soils both peak (or maximum) deviator stress and pore water pressure increase with increasing consolidation pressure. In the case of an overconsolidated soil the higher the overconsolidation ratio (at constant consolidation pressure) the higher the maximum deviator stress and the lower the excess pore water pressure.

The mean normal effective stress, p' , for normally consolidated soil decreases during the CU test as shown in Figure 2.6. This is because the tendency for volume decrease is manifested by an increase in pore pressure during shearing, which reduces the mean effective stress. On the other hand, for heavily overconsolidated soil the mean effective stress, p' , increases markedly because the tendency for volume increase is manifested as a reduction in pore water pressure. The effect of this decreasing pore

pressure is to increase the effective stress, so that the sample suffers large strains before reaching the peak deviator stress, as shown in Figure 2.5.

From the analysis of effective stress path in Figure 2.6 the effective stress parameters c' and ϕ' can be determined. For a normally consolidated soil the failure envelope passes through the origin ($c' = 0$). An overconsolidated soil would exhibit some low cohesion. A salient characteristic of both the CU and CD tests is that the obtained effective stress parameters c' and ϕ' are identical provided comparable strain rates are used during the shearing stage. The main advantage of carrying out the consolidated undrained triaxial test over the drained test is that the duration of the test is much shorter than that involved in the consolidated drained test. Furthermore, CU tests give effective strength parameters such as, effective cohesion, c' , and effective friction, ϕ' , as well as total strength parameters such as, pore pressure parameter, A , and undrained shear strength, s_u .

2.4.3 Unconsolidated undrained test (UU)

The unconsolidated undrained (UU) triaxial test enables one to determine the "as is" undrained shear strength of cohesive soils. In the UU test the soil sample is subjected to either isotropic or anisotropic confining pressures but no drainage is allowed. It is important that in the UU test the shearing stage follows immediately after the application of the confining pressure. As the drainage is kept closed throughout the test there is no volume change for a saturated soil sample and the excess pore pressure is non-zero. Accordingly, for a saturated soil sample under undrained conditions, any increase in the all round pressure results in an equal increase in pore water pressure. Also the void ratio, water content and dry density of a saturated soil sample throughout the test will be constant and the same as those in the ground. The UU tests are usually carried out on "undisturbed" soil samples. It is assumed that the laboratory shear strength is equal to the in situ strength provided the sample suffers minimal mechanical

disturbance and no change in water content. The results are expressed in terms of total stress as shown in Figure 2.7. The failure envelope is horizontal for normally consolidated saturated clays, i.e. $\phi_u = 0$, and the undrained shear strength is given by $\tau_f = s_u$. For overconsolidated clay samples ϕ_u is greater than zero, typically by a few degrees.

It should be emphasised that the properties measured from "undisturbed" soil samples in unconsolidated undrained tests do not fully reflect the in situ soil behaviour. The factors that affect the undrained shear strength in UU tests are:

(a) The influence of sample disturbance

In order to obtain a representative soil sample for testing in the laboratory, it should be subjected to stresses in the laboratory that are similar to those in situ. It is very difficult to achieve this ideal condition in the laboratory. Though the water content of the sample may be kept constant, significant disturbance usually results from stress relief during sample removal from the ground. The UU test is more unreliable than CU and CD tests because sample disturbance causes a reduction in undrained shear strength, probably because shearing starts from a reduced stress as compared to the field. Ladd and Lambe (1963), for example found that the sample disturbance reduces the undrained shear strength by up to 20% - 50% of the perfect sample.

(b) The rate of testing

The undrained shear strength varies with the strain rate used during shearing. It has been found (Ladd and Foott, 1974) that in triaxial compression each log cycle decrease in strain rate is typically accompanied by a 5% - 10% decrease in undrained shear strength. That is, triaxial tests

on cohesive soils show higher strength with increasing strain rate or decreasing time to failure.

(c) The mode of testing

The mode of shearing is related to the applied stress system. Basic differences in the applied stress system occur with change in either the relative magnitude of the intermediate principal stress, defined by $b = (\sigma_2 - \sigma_3) / (\sigma_1 - \sigma_3)$ or the direction of the applied major principal stress related to the vertical direction, denoted by the angle δ . Changes in b or δ lead to different stress-strain responses as the state of the soil is anisotropic. Ladd et al (1977) stated that peak undrained shear strength, s_u , from plane strain testing is reduced by 5% to 10% in compression whereas triaxial extension corresponds to 15% to 20% decrease.

2.5 Summary

This chapter has presented the types of triaxial tests, namely CD, CU and UU, all of which are used to obtain the stress-strain-strength properties of saturated cohesive soils. It can be said that the mechanical properties of saturated cohesive soil can be better examined and evaluated in consolidated drained or consolidated undrained tests. In the UU test, it is difficult to obtain a representative soil sample in the laboratory because of soil disturbance that leads to under-estimating the field properties. In the CD test total stress analyses cannot be done which indicates that it is not possible to predict the undrained shear strength and deformation properties. Interestingly, CU test provides both drained and undrained properties of soil and the duration of testing takes much shorter time compared to CD test. Thus the CU test is the most appropriate for obtaining data for stress-strain-strength studies of cohesive soils.

Apart from the mechanical properties of cohesive soils, triaxial testing is also used to determine correlations between the overconsolidation ratios and different soil parameters. A detailed review of the literature on the behaviour of cohesive soils with regard to the overconsolidation ratio is presented in the following chapter.

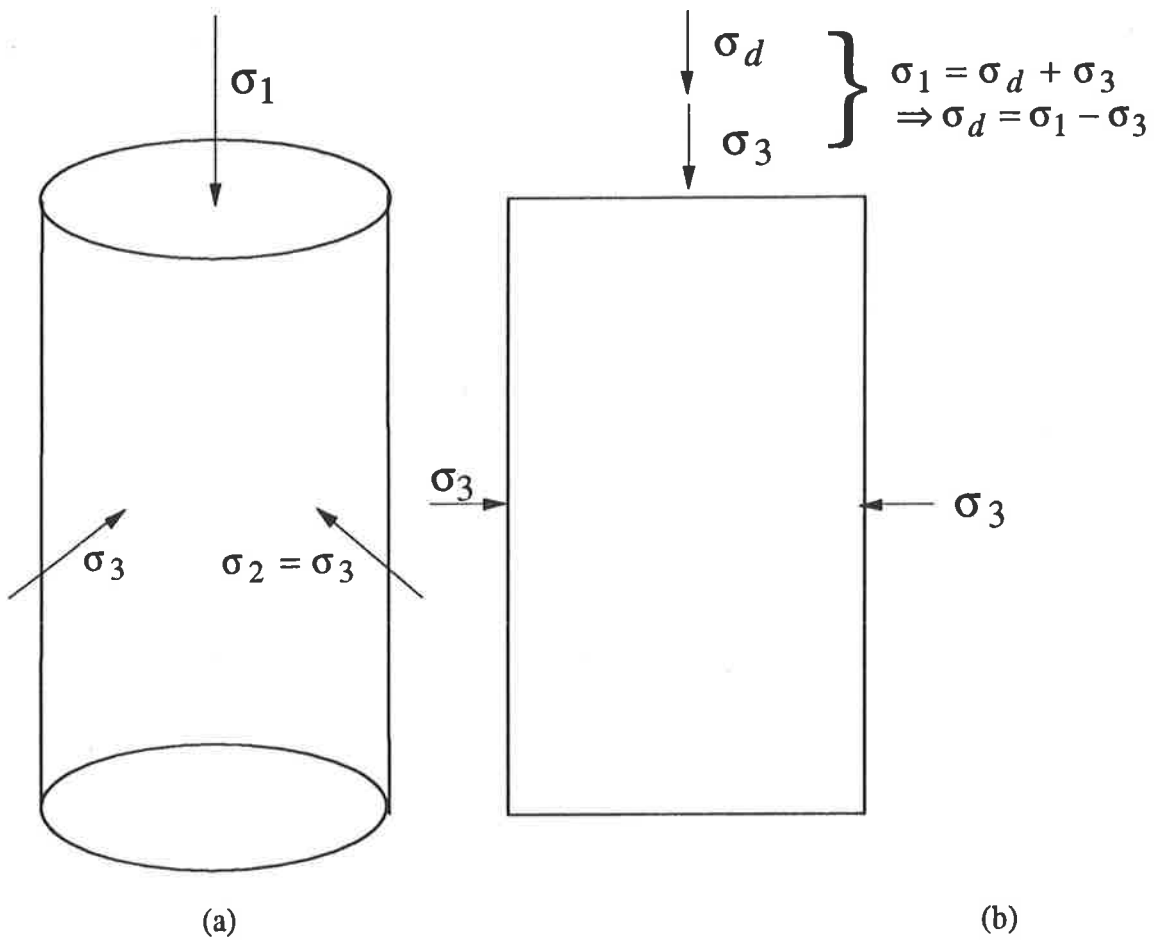


Figure 2.1. Cylindrical soil sample and application of stresses in triaxial testing

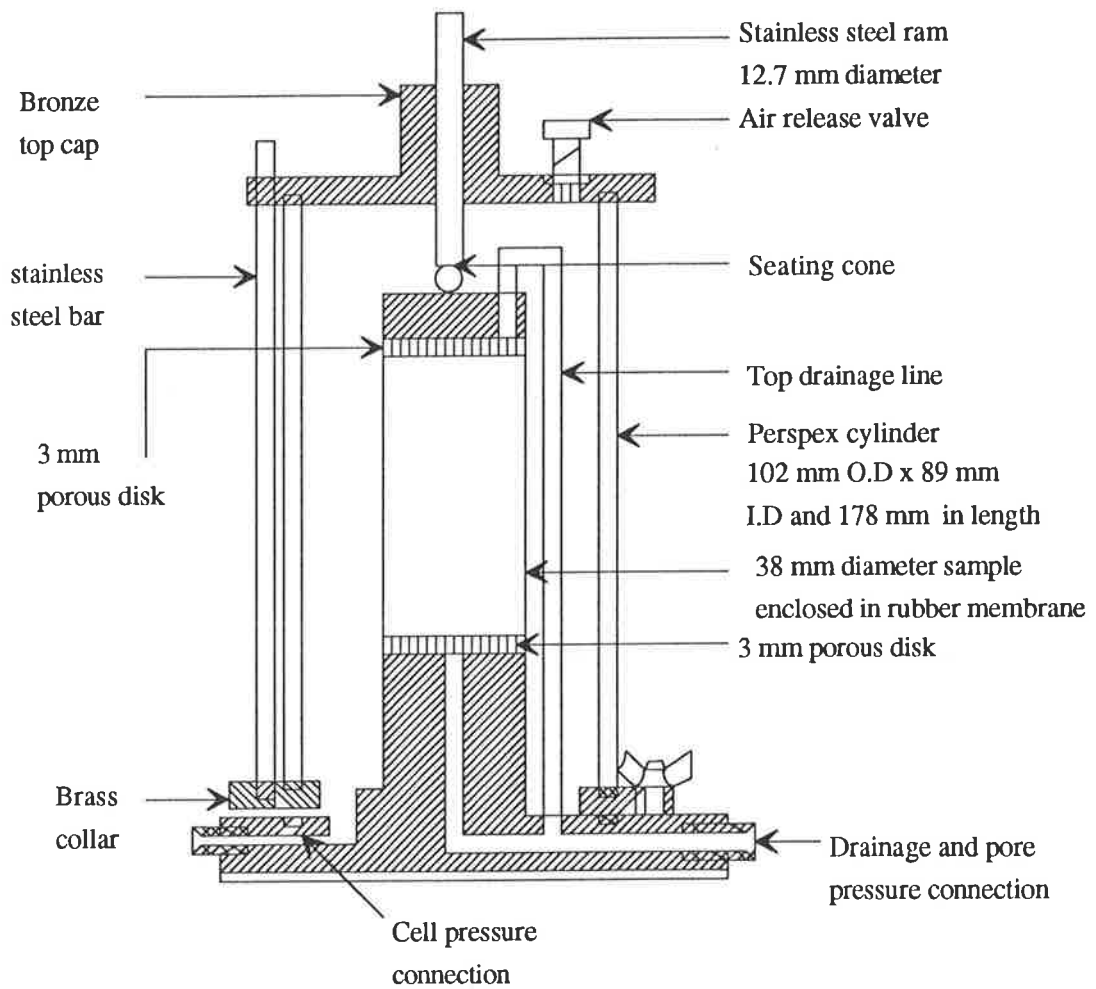


Figure 2.2 Schematic diagram showing different components of triaxial apparatus

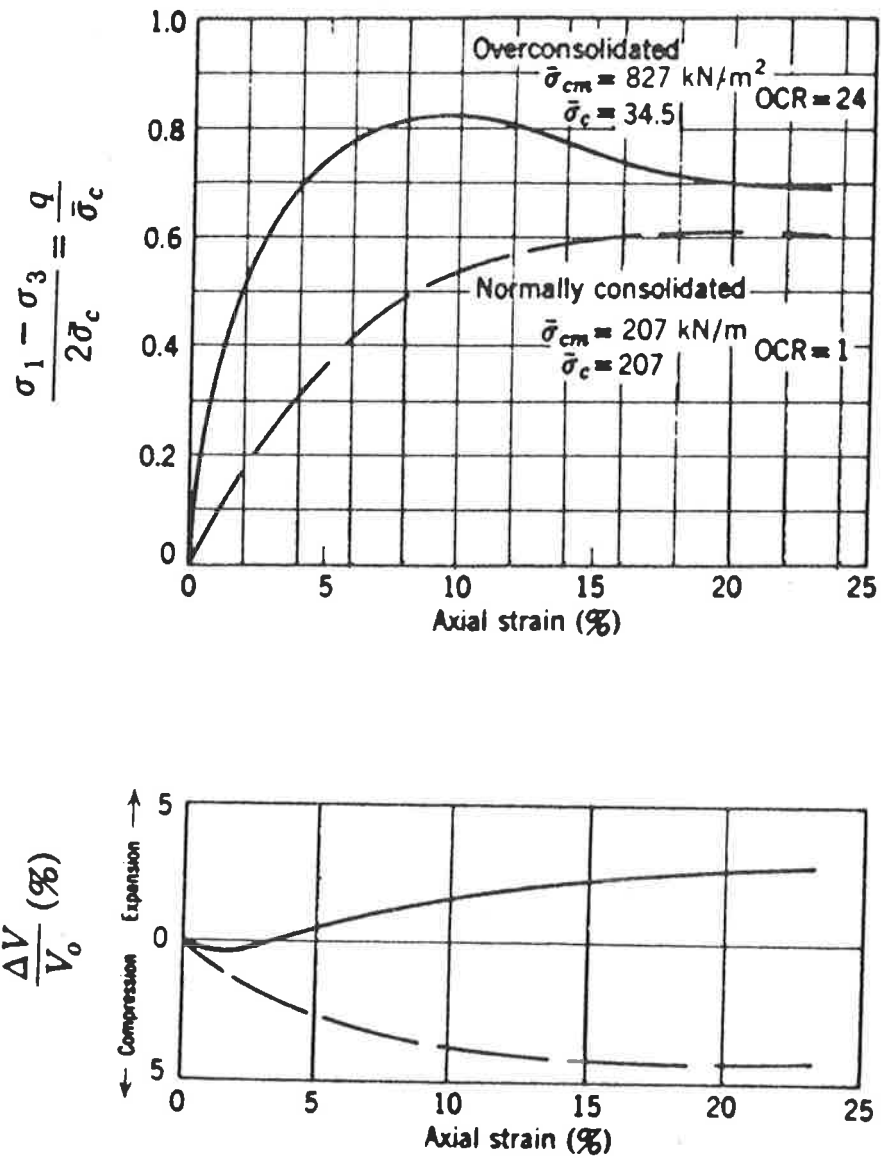


Figure 2.3. Typical results from drained triaxial tests on Weald Clay
(after Henkel, 1956)

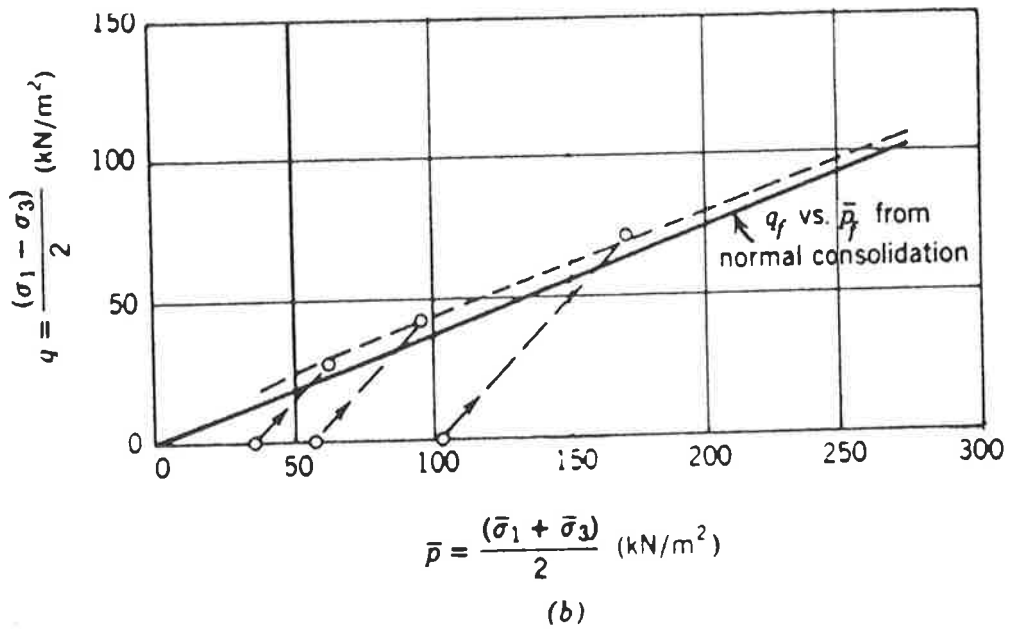
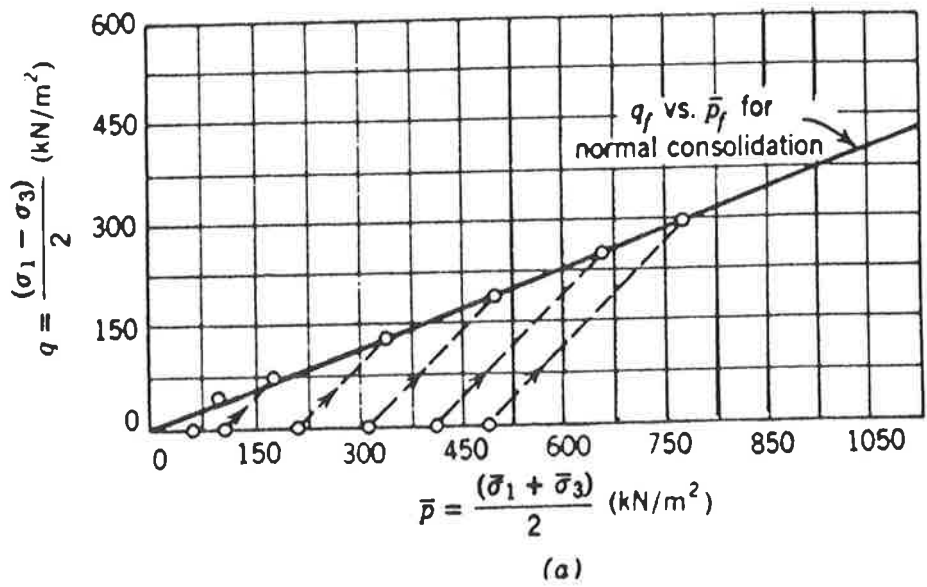


Figure 2.4. Stress path of CD test on normally consolidated and overconsolidated Weald Clay (after Lambe and Whitman, 1979)

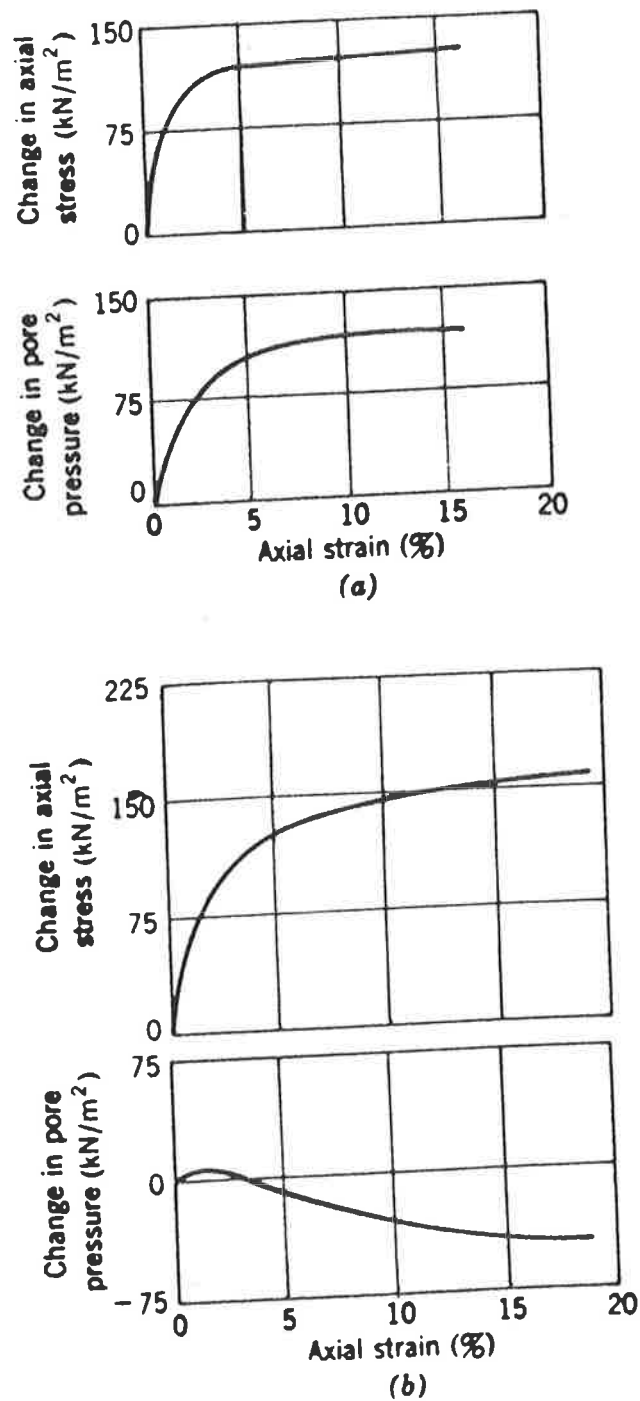


Figure 2.5. Typical stress-strain curves from CU tests on Weald Clay
 (a) Normally consolidated clay. (b) Overconsolidated clay (OCR = 8)
 (after Lambe and Whitman, 1979).

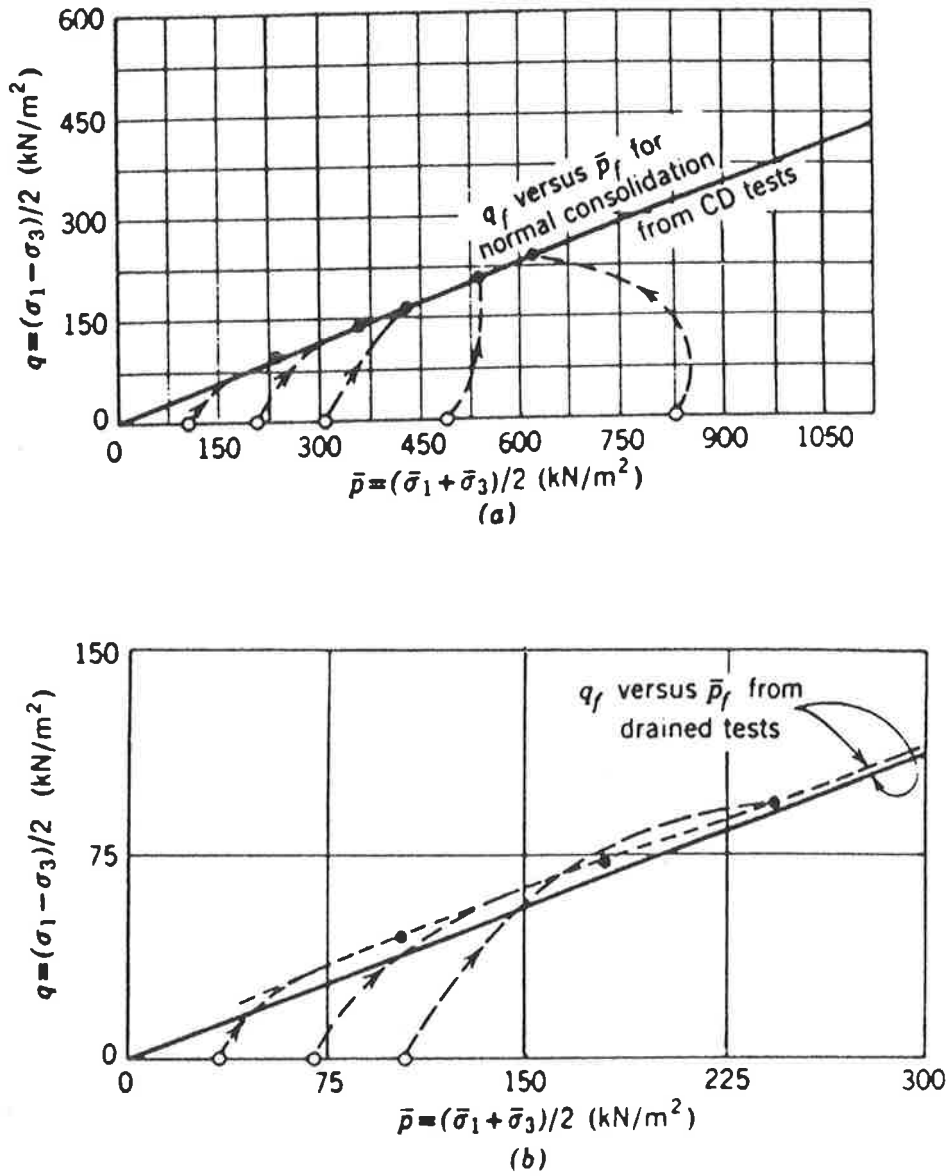


Figure 2.6. Effective stress paths from CIU tests on Weald Clay (a) Normally consolidated clay. (b) Overconsolidated clay (after Lambe and Whitman, 1979).

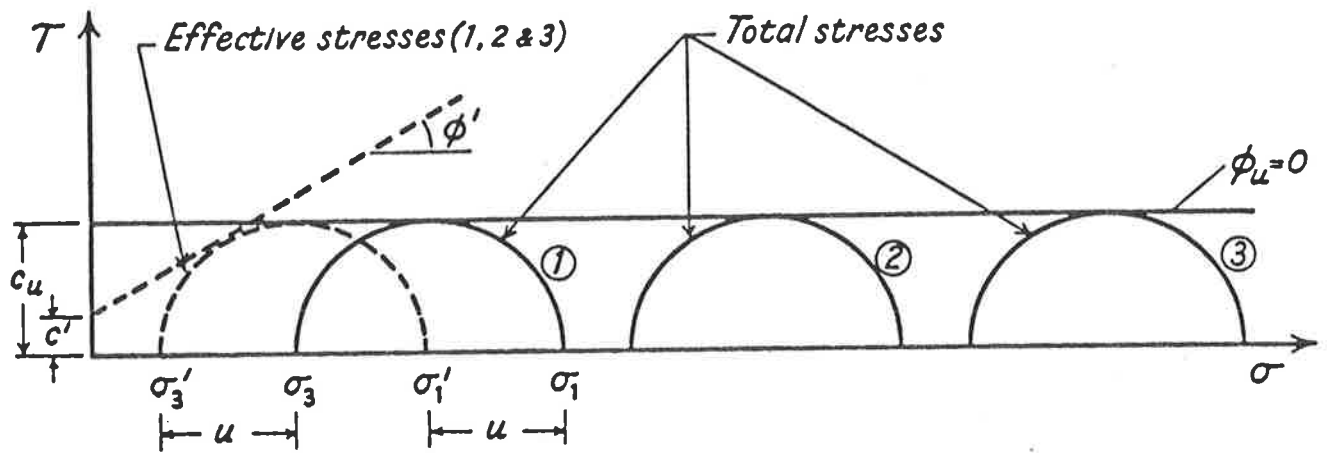


Figure 2.7. Representation of results of UU test on saturated soil samples
(after Lade, 1986)

Chapter 3

Normalised behaviour of cohesive soils

3.1 Introduction

In the last chapter the CU test was identified as the preferred procedure to evaluate undrained soil properties. In this chapter an analytical method for normalised soil behaviour called SHANSEP, is described in detail. Particular attention is given to its use with the CU test.

Normalised behaviour plays an important role in understanding the characteristics of cohesive soil with respect to modelling in situ soil properties. A soil parameter is said to be normalised when it is expressed as a dimensionless ratio of some other variable (e.g. effective overburden pressure, σ'_{v0}) with the same units. The concept of normalised behaviour is applicable to those soil deposits which show constant values of normalised soil parameters for a given overconsolidation ratio.

The soil properties can be evaluated in a number of ways. Due to the variation and uncertainty of soil properties, the process of assessment of the stress-strain and strength characteristics of a normally consolidated and overconsolidated soil can be complex. The undrained shear strength in the laboratory from unconsolidated undrained (UU) tests do not reflect the in situ behaviour of a soil under field conditions. In order to determine representative in situ undrained shear strength and deformation properties, the SHANSEP method was introduced by Ladd and Foott (1974).

It is generally accepted that the state of the soil is always altered to some extent due to sampling disturbance. To overcome the sampling disturbance effects and also obtain a known overconsolidation ratio (OCR), the laboratory testing technique involved in this method is to consolidate the sample beyond the pre-consolidation pressure and then to allow the sample to swell under a lower consolidation pressure corresponding to a predetermined OCR. For a soil that shows normalised behaviour, it is possible to perform a series of tests at different overconsolidation ratios which are then used to establish a relationship between the normalised soil parameter (NSP) and the overconsolidation ratio (OCR). From the obtained relationship the in situ soil properties can be determined, provided the in situ OCR is known.

In the following sections of this chapter the important factors influencing the behaviour of cohesive soils are reviewed, namely, sample disturbance, initial consolidation, strength anisotropy and strain rate effects. The normalised behaviour of cohesive soils is then summarised. A general review of the testing procedure for developing normalised soil parameters, typical values of NSP from the SHANSEP method and the steps involved in determining the in situ soil properties are also presented.

3.2 Review of factors affecting the properties of cohesive soils

The $\phi = 0$ method of analysis is commonly used to determine the undrained shear strength and deformation properties of saturated clays. It was considered by Skempton (1948) that the in situ undrained shear strength uniquely depended on its natural water content that could be determined accurately in the laboratory from unconsolidated undrained compression (UUC) tests. Bishop and Bjerrum (1960) verified the concept by analysing numerous end-of-construction failures concerning foundations in the cohesive soils. From their analysis, they concluded that the undrained shear strength could be reliably predicted from field vane (FV) tests or from the widely used UUC tests carried out on undisturbed samples at their natural water contents. However, other studies (for example, Hansen and Gibson, 1949; Casagrande and Wilson, 1951; Ladd and Lambe, 1963; Richardson and Whitman, 1963; Ladd, 1964; Ladd, 1965; Shibata and Karube, 1965; Duncan and Seed, 1966; Donaghe and Townsend, 1978; Mitachi and Kitago, 1979; Mayne, 1985; Germaine and Ladd, 1988) have revealed a number of factors by which the in situ undrained shear strength and deformation properties of soils can be better understood. These factors are briefly described below.

3.2.1 Sample disturbance

The undrained properties of saturated "undisturbed" clay can be evaluated from unconsolidated undrained (UU) and consolidated undrained (CU) tests in the laboratory. To simulate the in situ conditions in the laboratory, the moisture content and the effective stresses of the sample have to be similar to those in the field. The samples in UU tests suffer from inevitable stress relief during sampling although the moisture content may remain unaltered. In CU tests, the samples are sheared at the in situ effective stresses but the moisture content is different from that in the field. Due to variations of moisture content and effective stresses in the two different tests the results tend to be different. From the results of CU tests and UU tests of normally

consolidated and overconsolidated soils, which include, Boston Blue Clay, Plastic Clay at Lagunillas, Mexico City Clay, Varved Clay, etc., Ladd and Lambe (1963) concluded that the undrained shear strength obtained from UU tests were between 40 to 97 per cent of that of CU tests, and attributed this to sampling disturbance.

Ladd and Lambe (1963) suggested 'perfect sampling' to measure the undrained properties of cohesive soils. The term 'perfect sampling' was applied to a sample which is subjected to no disturbance other than relief of in situ stresses. During sampling the total stress is reduced to zero and the sample develops negative pore pressure. So the perfect sample is subjected to an isotropic effective stress, σ'_{ps} , which is given by the following equation,

$$\sigma'_{ps} = \sigma'_{v0} [K_0 + A_u(1 + K_0)] \quad (3.1)$$

where σ'_{v0} is the effective overburden pressure, K_0 denotes the coefficient of earth pressure at rest, and A_u represents the pore pressure during sampling procedure, which varies typically from -0.1 to 0.3 for medium to soft clays. It should be noted that the undrained shear strength of a perfect sample may be between 0% and 10% less than the actual value in the field and this also affects the stress-strain characteristics of the soil. This is because in the laboratory, shear starts in a perfect sample from an isotropic rather than an anisotropic stress state. A wide range of tests on low to moderate sensitivity clays indicate that the undrained shear strength from UU tests were found 20% to 50% less than that of perfect samples. In addition to the stress relief during sampling, storage and handling procedures also cause soil disturbance, further reducing the undrained shear strength. For the case of undrained Young's modulus of elasticity, E_u , Ladd (1964) concluded that sampling disturbance was the most important variable affecting modulus of elasticity from UU tests, especially with the tube samples of normally consolidated clays. Results of "undisturbed" Kawasaki and Lagunillas Clay

from isotropically consolidated undrained tests indicated that the moduli of elasticity were five to six times higher than those of confined UU tests. 'Perfect sampling' also significantly alters the modulus of elasticity since shear starts from isotropic rather than K_0 conditions (Ladd and Lambe, 1963). The increased disturbance in UU tests led foundation engineers to use CU tests in order to minimise the effect of sample disturbance.

3.2.2 Initial consolidation

Consolidated undrained (CU) triaxial tests are generally carried out to determine the undrained shear strength and deformation properties of cohesive soils. In CU tests, the effective vertical overburden pressure is used as the effective confining pressure. It was hypothesised by Skempton and Bishop (1954), that the effective angle of shearing resistance, ϕ' , and the pore pressure parameter at failure, A_f , are not affected by the effective consolidation ratio $K_c = \sigma'_{1c}/\sigma'_{3c}$, where, σ'_{1c} and σ'_{3c} are the effective vertical and lateral consolidation pressures, respectively in CU tests. However, evidence from studies by Ladd (1965), and Donaghe and Townsend (1978), show that anisotropic consolidation has little effect on the undrained shear strength, s_u , but the effective friction angle, ϕ' , and pore pressure parameter at failure, A_f , are lower than those obtained from isotropically consolidated samples. The value of Young's modulus depends on both the mean effective normal stress and the shear stress level (τ/τ_f). Accordingly, values for anisotropic consolidation are different from those of isotropic consolidation.

The state of stress of clay in the field is anisotropic, i.e., the horizontal and vertical stresses are not equal. Therefore, in order to obtain reasonable estimates of in situ soil properties, anisotropic consolidation, i.e., consolidation under K_0 conditions, has to be performed in the laboratory. It should be noted that performing K_0 consolidation on clay soils in the laboratory is a very complex and time consuming process. Thus a test

is needed which is viable, from the commercial testing standpoint, and whose results can be comparable to other tests. Wroth (1984), recommended isotropically consolidated undrained test as a standard reference to determine the soil properties. He showed a correlation by which the undrained shear strength of K_0 consolidation of normally consolidated clay can be predicted from the data of isotropic consolidation. From a large data base survey Mayne (1985) developed a relationship between the undrained shear strength of K_0 consolidated tests and that of isotropically consolidated tests. From the relationship it was indicated that the undrained shear strength of K_0 consolidated clay during undrained compression and extension tests can be determined from the data of isotropically consolidated undrained (CIU) tests. Most recently, Chen and Kulhawy (1993), reinforced the use of the CIU test as a 'test of reference' by obtaining correlations between CIU, UU, and UC tests. Two sets of data bases, which include the undrained shear strength from CIU and UU tests and from CIU and UC tests were used to develop correlations by which the undrained shear strength of UU and UC can be predicted from the data of CIU tests.

3.2.3 Effect of anisotropy

The anisotropy of cohesive soils was first predicted by Hansen and Gibson (1949) from theoretical considerations. Cohesive soils exhibit strength anisotropy essentially because of two reasons. First, the inherent anisotropy, which occurs during the formation of the clay deposit where the particles tend to orient in the horizontal direction due to one dimensional deposition and subsequent loading. It is this particle orientation which causes inherent anisotropy. It is very difficult to measure inherent anisotropy but the effects can be examined from UU or CU tests on samples cut at different inclinations. The second cause is stress induced anisotropy, caused by the rotation of principal stresses during shear and variations of the intermediate principal stress.

The undrained properties of a soil vary with the orientation of the failure surface, either as a result of inherent anisotropy or as a result of stress system induced anisotropy. Ladd et al (1977) summarised the combined effects of strength anisotropy from the data of six different normally consolidated soils which were taken from the work of Duncan and Dunlop (1969), Ladd and Edgers (1972), Vaid and Campanella (1974) and unpublished data from MIT & the University of British Columbia. The tests were carried out under anisotropic K_0 conditions similar to those in the field. The results from plane strain compression (PSC), direct simple shear (DSS) and plane strain extension (PSE) tests showed that the undrained shear strength, s_u , decreases progressively for five clays as the direction of the major principal stress, σ_{1f} , changes from the vertical to the horizontal direction. The decrease in shear strength of the five clays was attributed to stress induced anisotropy. Furthermore, the results for Varved Clay showed that the undrained strength from DSS tests is significantly lower than that of PSC and PSE tests, where the decrease of undrained shear strength is associated with inherent anisotropy of the clay. Anisotropy also has a significant effect on the deformation properties of cohesive soils. The undrained Young's modulus under vertical loading is generally higher than that under horizontal loading. The normalised secant modulus (E_u/σ'_{vc}) for Boston Blue Clay from PSC tests were 50% - 100% higher than those obtained from PSE tests (Ladd et al 1977). The change in the stress-strain behaviour due to anisotropy is accompanied by the development of pore pressure which will affect the effective cohesion, c' , effective friction angle, ϕ' , and pore pressure parameter at failure, A_f , of the soil.

3.2.4 Strain rate

The rate of testing affects the undrained properties of cohesive soils in CU and UU tests. Germaine and Ladd (1988), reported that in triaxial compression tests, a decrease in strain rate decreases the undrained shear strength of the soil. The results from UUC tests showed that the undrained shear strength at a strain rate of 1%/min is $20\% \pm 10\%$

higher for low OCR soils and 50% higher for heavily OCR soils than that of CU tests carried out at a strain rate of 1%/hour.

The decrease in shear strength at slower strain rates is governed by the plasticity and creep susceptibility of the soil (Ladd and Foott, 1974). The significance of undrained creep during shear is that it increases the pore pressure and hence decreases the effective stresses acting on the sample. Therefore a longer duration in triaxial compression (TC) causes more creep to occur, which reduces the shear strength significantly. Although the underlying mechanism is unclear, Germaine and Ladd (1988) reported that membrane leakage, structural viscosity, particle slippage or reorientation and redistribution of water, may lead to reduction of the undrained shear strength. Similarly the Young's modulus of elasticity is influenced to a great extent by the strain rate. At a small strain, ($\Delta\varepsilon =$ up to 0.5%), the Young's modulus of elasticity was found to double when the strain rate of 1% in 1 minute was used instead of 1% in 500 minutes (Richardson and Whitman, 1963).

3.3 Concept of normalised soil behaviour

3.3.1 Normalisation of soil parameters

Normalisation is an essential part in establishing correlations between soil properties. The correlations are used judiciously in a consistent and reproducible manner to evaluate the other soil properties. In most of the cases the soil properties are normalised with respect to the pre-consolidation pressure. Casagrande (1936) defined the pre-consolidation pressure, σ'_p , as the maximum overburden pressure that has been experienced by a soil deposit. The significance of σ'_p is that it represents the yield stress on the one-dimensional drained loading, and also the locus of stress states that separates the elastic behaviour from irrecoverable plastic deformation in undrained and

drained conditions. It should be noted, however, that different σ'_p mechanisms lead to different yield envelopes. Jamiolkowski et al (1985) presented the yield envelope of James B-6 Marine Clay under different consolidation pressures. The tests were carried out in undrained triaxial compression and extension at a consolidation pressure of $\sigma'_c = \sigma'_{vo}$ to measure the behaviour of 'intact' clay, at in situ OCR, consolidation to (σ'_c/σ'_p) between 0.6 and 1.0 to measure the effect of recompression on 'intact' clay and also $(\sigma'_c/\sigma'_p) = 1.3$ to 3 for destructured clay to examine the yield envelopes. From the results, Jamiolkowski et al (1985) found that the yield envelope of intact clay was different from those of destructured clay. Again the yield envelope of destructured clay was similar to those of Boston Blue Clay (Jamiolkowski et al 1985) which was also destructured by reconsolidating the clay to the virgin compression line.

From the above evidence one can conclude that the pre-consolidation pressure plays an important role in the basic behaviour of clays under both undrained and drained conditions. So, in order to establish dimensionless correlations for cohesive soils, the undrained shear strength and deformation properties are often normalised with respect to the pre-consolidation pressure. Sometimes, the undrained Young's modulus, E_u , is normalised with respect to the undrained shear strength, s_u , of the soil.

3.3.2 Normalised behaviour

Cohesive soils exhibit normalised behaviour which was first pointed out by Henkel (1960) and Parry (1960). In evaluating the shear strength characteristics of normally consolidated and overconsolidated samples of remoulded London Clay and Weald Clay at Imperial College, Parry (1960) found that samples with the same overconsolidation ratio, but different effective consolidation pressures, exhibit constant $(\sigma_1 - \sigma_3)/\sigma'_c$, when the deviator stress, $(\sigma_1 - \sigma_3)$, is normalised with respect to the effective consolidation pressure, σ'_c . It was also observed that the ratio of deviator stress at failure to effective

consolidation pressure shows an increase with overconsolidation ratio. Furthermore, from the analysis of test results carried out on the same clays, Henkel (1960) found identical effective stress Mohr failure envelopes when the ratio of the major to the minor principal effective stress and the ratio of the maximum consolidation pressure to the average effective stress at failure is used. It was further concluded that the ratio of principal effective stresses at failure, $(\sigma'_{1f}/\sigma'_{3f})$, depended upon the ratio of the maximum consolidation pressure to the average effective stresses at failure, (σ'_p/p'_f) , and was independent of the value of the maximum consolidation pressure.

Similar normalised behaviour of cohesive soils was also observed by Ladd (1964) when he examined the stress-strain behaviour of six different clays (undisturbed Amuay Clay, Boston Blue Clay, Kawasaki Clay, and Lagunillas Clay; and remoulded Boston Blue Clay and Vicksburg Buckshots Clay). Ladd found that the clay samples with the same overconsolidation ratio (OCR), but different effective consolidation stresses, and therefore different effective maximum past pressures, exhibited similar stress-strain characteristics when the deviator stress was normalised with respect to the effective consolidation pressure. Figure 3.1(a) shows the idealised stress-strain curves for isotropically consolidated clay at two different effective consolidation pressures of 200 kPa and 400 kPa respectively. When normalising the deviator stress, $(\sigma_1 - \sigma_3)$, with the effective consolidation pressure, σ'_c , i.e. $(\sigma_1 - \sigma_3)/\sigma'_c$, the two curves plot on the same line as shown in Figure 3.1(b).

Loudon (1967) summarised the normalised behaviour of reconstituted Kaolin from the critical state concept. Results obtained from a series of isotropically consolidated undrained triaxial compression tests showed that the effective stress paths for different effective consolidation pressures terminated at a single point, defined as the critical state point, when the stresses were normalised with respect to equivalent pressure, p'_e . From this it was concluded that normalised behaviour is also an integral part of the critical state soil mechanics (CSSM) concept.

In reality, the normalised behaviour which has been summarised in previous paragraphs, is not the ideal unique lines. The divergence of the normalised plot of Maine Organic Clay was attributed to sample heterogeneity and large differences in the vertical consolidation stresses used (Ladd and Foott, 1974). Furthermore, Ladd et al (1977) indicated, from the normalised plot of Boston Blue Clay, that the variability of normalised plots was mainly due to testing procedure. Nevertheless the variations are quite small and the normalised s_u values generally lie within 10% of the mean value. This is shown in Figure 3.2 where the normalised undrained shear strength of Boston Blue Clay is plotted against overconsolidation ratio. Thus, minor divergence observed in the normalised plots is due to the heterogeneity of the soil samples, different consolidation stresses and variations in procedure adopted from one test to another.

The advantage of the normalised plot is that it can be used widely to reproduce the stress-strain behaviour, undrained shear strength, Young's modulus of elasticity etc., of the same samples consolidated to any other effective stresses from the same type of test. Furthermore, the normalised stress-strain relationships for different clay soils can be compared, and the general trends used to determine variations in the clay's behavioural characteristics with the same or different effective consolidation pressure, σ'_c .

A design procedure known as the SHANSEP method has been developed for soils that exhibit normalised behaviour. It is used to determine the in situ soil properties from normalised soil parameters (NSP) obtained in the laboratory. The most widely used normalised soil parameter in soil mechanics is the undrained shear strength ratio (s_u/σ'_{v0}) where σ'_{v0} is the in situ vertical effective stress. Other common NSP variables are (E_u/σ'_{v0}) , and (E_u/s_u) .

3.4 The SHANSEP method

Apart from the fundamental geological controls, the properties of cohesive soils vary with depth of the deposit. This is because the moisture content, void ratio and stress history vary with depth of the deposit. Accordingly, evaluation of the shear strength and deformation properties must take into account the moisture content, void ratio, stress history, and depth of the deposit. The SHANSEP is a method which considers the effect of stress history and the field properties can be evaluated systematically over the depth of the deposit. The method assumes that the in situ soil exhibits normalised behaviour which can be simulated in the laboratory by mechanical overconsolidation. The typical stresses which are used in the SHANSEP method is described in Figure 3.3 with regard to stresses used in the in situ, UU tests and CK_0U compression tests.

Figure 3.3 shows the in situ, UU and laboratory K_0 compression curves for a slightly overconsolidated soil. The points 1 and 2 represent the effective stresses of in situ, and "undisturbed" soil samples in UU test, respectively. It can be seen by the points 1 and 2, that the major disturbance is caused by stress relief due to sampling. The UU compression test is particularly unreliable because shearing starts from a reduced effective stress compared to the in situ stress. Therefore, due to the limitations of UU triaxial testing, the CU test is used in the SHANSEP method to minimise the adverse effects of stress relief.

Davis and Poulos (1967) and Bjerrum (1973) suggested using K_0 consolidated undrained (CK_0U) tests on samples reconsolidated to the in situ effective overburden pressure, σ'_{v0} . This leads to a decrease in volume of the sample that varies typically between 2% and 8% for both normally consolidated and low overconsolidated clays which is represented by the point 3 in Figure 3.3. However, the decrease in volume due to consolidate the sample to the effective in situ overburden pressure, σ'_{v0} , causes an overestimate of the field properties.

Therefore, to obtain the soil properties more reasonably, Ladd and Foott (1974) recommended that, for a soil which exhibits normalised behaviour, the in situ soil properties can be determined by consolidating the samples to a consolidation pressure of 1.5 to 2 times the maximum in situ effective pressure, σ'_{vm} . The points A to D correspond to typical stresses used in the SHANSEP method.

3.4.1 Laboratory shear tests in the SHANSEP method

The laboratory shear strength test used in the SHANSEP method should be the most appropriate for the field conditions. Thus, where a plane strain active (PSA) failure is likely to occur, normalised data from PSC tests, or the similar value for triaxial compression (TC) tests, should be used in the design of foundation or stability problems. Similarly, for a design involving passive loading of the clay, strength data from plane strain extension (PSE), or triaxial extension (TE), tests should be used. Figure 3.4 shows the different shear strength tests necessary to duplicate the in situ modes of failure due to changes in major principal stress in various field situations. Thus, it is advisable to use PSC test for the long vertical cut and PSE test for the long loaded retaining wall. In order to analyse circular arc and wedge type stability problems, it was suggested by Koutsoftas and Ladd (1985) to consider the average shear strength from TC, DSS and TE tests.

In order to select the rate of shearing in the shear tests, Ladd and Foott (1974) recommended to use an axial strain rate between 0.5% and 1% per hour for K_0 consolidated undrained triaxial compression (CK_0UTC) tests, and 5% per hour for K_0 consolidated undrained direct simple shear (CK_0UDSS) tests for cohesive soils. It should be noted, however, that in order to duplicate the in situ failure behaviour of cohesive soils, there is no agreed framework for selecting the strain rate in undrained tests. The above strain rates have been used in different laboratories and from the case

studies it was concluded that they provide reasonable undrained shear strength data for cohesive soils (Germaine and Ladd, 1988).

3.4.2 Testing procedure for normalised soil parameters

In developing the normalised soil parameter of a soil, the testing procedure has been traditionally divided into two distinct phases. First, the normalised behaviour of the soil is examined. The normalised soil parameter is only applicable if the soil exhibits normalised behaviour. Once the soil shows normalised behaviour then the normalised soil parameters (s_u/σ'_{v0}) , (E_u/σ'_{v0}) , and (E_u/s_u) are determined for different overconsolidation ratios.

The testing procedure followed at MIT (Ladd and Foott, 1974) for developing NSP in the SHANSEP method is as follows:

- (1) In order to minimise the effects of sampling, the samples are reconsolidated back to the virgin compression line from A to B (Figure 3.3) at the normally consolidated state. Approximately 1.5, 2.5 or 4.0 times the in situ effective maximum past pressure, σ'_{vm} , are used in the reconsolidation procedure. Then, the compression tests are carried out, from which the undrained shear strength, s_u , is determined. A clay exhibiting normalised behaviour will yield constant values of normalised undrained shear strength, (s_u/σ'_{vc}) , at least for the two higher stresses. If (s_u/σ'_{vc}) varies consistently with stresses, the NSP concept does not apply for that soil.
- (2) To achieve a known OCR first the samples are reconsolidated back to the virgin compression line from A to B in Figure 3.3, followed by unloading to point D corresponding to the required OCR. In order to obtain the relationship between a normalised soil parameters and OCR it is necessary

to perform tests at OCR values of 2 ± 0.5 , 4 ± 1 , and 6 ± 2 . It is important to use a range of effective consolidation pressures, σ'_{vc} , over which normalised behaviour is valid. After performing the tests, the normalised soil parameters are plotted against OCR.

3.4.3 Representation of various NSP in the SHANSEP method

This section presents a discussion of representations of different normalised soil parameters in the SHANSEP method with regard to the overconsolidation ratio.

(a) Normalised undrained shear strength

The undrained shear strength, s_u , is one-half of the difference between the major and minor principal stresses at failure. In the SHANSEP method, the undrained shear strength is determined from a series of triaxial tests which are sheared under undrained conditions for both normally consolidated and overconsolidated soil samples. The undrained shear strengths are normalised with respect to the effective overburden pressure, σ'_{v0} , and correlated with different overconsolidation ratios.

The normalised undrained shear strength, (s_u/σ'_{v0}) , with overconsolidation ratios of different cohesive soils have been examined by a number of investigators (Parry, 1960; Ladd and Edgers, 1972; Ladd and Foott, 1974; Poulos, 1978; Andresen et al 1979). The relationship between the normalised undrained soil parameter, (c_u/σ'_{vc}) , (where c_u = undrained shear strength), and overconsolidation ratio, $(\sigma'_{vm}/\sigma'_{vc})$, on six clays (Maine Organic Clay, Bangkok Clay, Atchafalaya Clay, AGS CH Clay, Boston Blue Clay, and Conn. Valley Varved Clay) carried out by Ladd and Edgers (1972), from K_0 consolidated undrained direct-simple shear (DSS) tests, are shown in Figure 3.5. It can be seen from Figure 3.5 that the normalised undrained shear strength, (c_u/σ'_{vc}) , increases markedly with increasing OCR. The data points of these soils form a series

of smooth concave upward curves. It should be noted that despite differences between the soil types, the curves are all similar in shape. Thus, these normalised curves can be used to compare the soil characteristics of different clays. However, the increasing trend of normalised undrained shear strength with OCR has been explained by Ladd et al (1977), where it was pointed out that the decrease in the pore pressure parameter at failure, A_f , with increasing overconsolidation significantly increases the undrained shear strength.

The correlation between the normalised undrained shear strength and the overconsolidation ratio provides a format of presenting the undrained shear strength of overconsolidated soil. The results reported by Ladd and Edgers (1972) in Figure 3.5, were reinterpreted by Ladd et al (1977), who plotted the normalised undrained shear strength of overconsolidated soil divided by that of normally consolidated soil against OCR as shown in Figure 3.6. It can be seen that the data for all the soils fall in a very narrow band that can be described by the following equation:

$$\frac{\left(\frac{s_u}{\sigma'_{vc}}\right)_{o.c}}{\left(\frac{s_u}{\sigma'_{vc}}\right)_{n.c}} = (\text{OCR})^m \quad (3.2)$$

where

$$\left(\frac{s_u}{\sigma'_{vc}}\right)_{o.c} = \text{undrained shear strength ratio for overconsolidated}$$

clay,

$$\left(\frac{s_u}{\sigma'_{vc}}\right)_{n.c} = \text{undrained shear strength ratio for normally}$$

consolidated clay,

OCR = overconsolidation ratio and

$m \approx 0.80$.

From the above findings it was concluded that the undrained shear strength ratio of overconsolidated soil is dependent on the stress history of the deposit.

Similar results was obtained from Drammen Clay by Andresen et al (1979), in the Norwegian Geotechnical Institute. The tests were carried out up to an overconsolidation ratio of 40 in simple shear. Both normalised undrained strength ratio and OCR were plotted on logarithmic scales and yielded a straight line. The slope of the straight line was almost found to be 0.80 which further indicates that the undrained shear strength is dependent to the OCR of the deposit.

The theoretical format of expressing the normalised undrained shear strength of overconsolidated soil was examined further by Wroth (1984) in the context of critical state soil mechanics using isotropically consolidated undrained triaxial tests. A typical result from the isotropically consolidated undrained triaxial compression test for normally consolidated and overconsolidated soil is presented in Figure 3.7, where the effective mean normal stress, p' , is related to the shear stress, q , and the specific volume, v . In Figure 3.7 the effective stress path for normally consolidated soil during the shearing stage is represented by the path CD, whereas the overconsolidated sample at point R follows the path RS. It can be seen from Figure 3.7 that for the overconsolidated sample the maximum shear strength occurs above the critical state line which is shown by point T and if the test is continued, it reaches the critical state line at point S. Wroth (1984) further showed that the line joining the failure points in the p' - v curve, is approximately parallel to the normal consolidation line.

By definition, the undrained shear strength of an overconsolidated soil is

$$\begin{aligned} s_u &= \frac{1}{2} q_s \\ &= \frac{1}{2} M p'_s \end{aligned} \quad (3.3)$$

where

s_u = undrained shear strength in compression,

q_s = deviator stress at critical state,

M = slope of critical state line,

$$= \frac{6 \sin \phi_{tc}}{(3 - \sin \phi_{tc})}$$

p_s' = mean normal stress on critical state line.

ϕ_{tc} = effective friction angle and

Wroth (1984) reported that the ratio of effective stress at the beginning and at the end of the test are related by the following relationship:

$$\frac{p_s'}{p_r'} = \left(\frac{R}{r}\right)^\Lambda \quad (3.4)$$

where

R = overconsolidation ratio,

$$= (p_c'/p_r')$$

p_c' = maximum effective consolidation pressure,

p_r' = effective consolidation pressure of overconsolidated soil,

r = (p_c'/p_x') represents the spacing between the normal consolidation line and the critical state line and

p_x' = mean effective normal stress at critical state on swelling line.

The plastic volumetric strain ratio, Λ , is defined by

$$\Lambda = \frac{\lambda - K}{\lambda} \text{ or } \Lambda = \frac{C_c - C_s}{C_c} \quad (3.5)$$

where

- λ = slope of normal consolidation line and
- K = slope of the swelling line (isotropic condition).
- C_c = compression index and
- C_s = swelling index (one dimensional deposition)

Substituting the value of p'_s in Equation 3.3 then it becomes

$$\begin{aligned} \frac{s_u}{p_r} &= \frac{s_u}{\sigma'_{vo}} \\ &= \left(\frac{M}{2}\right)\left(\frac{R}{r}\right)^\Lambda \end{aligned} \quad (3.6)$$

In Equation 3.6, M , Λ and r are constant for a particular soil. Thus the undrained shear strength ratio of an overconsolidated soil depends on the overconsolidation ratio, R , raised to the power Λ . However, the above equation can be written in the form of normalised undrained shear strength ratio of overconsolidated clay to that of normally consolidated clay which is as follows:

$$\frac{\left(\frac{s_u}{\sigma'_{vc}}\right)_{o.c.}}{\left(\frac{s_u}{\sigma'_{vc}}\right)_{n.c.}} = R^\Lambda \quad (3.7)$$

So from Equation 3.7 it can be concluded that the normalisation of undrained shear strength parameters is an "outcome" of critical state soil mechanics.

(b) Normalised deformation parameters

In practice, the modulus of elasticity is calculated from the stress-strain diagram to obtain an initial tangent modulus, E_i , and Young's modulus corresponding to stress

levels equal to 25%, E_{25} , and 50%, E_{50} , of the peak deviator stress. In the SHANSEP method the normalised deformation parameters, (E_u/σ'_{v0}) , and (E_u/s_u) are plotted against the overconsolidation ratio.

In examining the normalised stress-strain modulus with overconsolidation ratio and stress level, Ladd (1964) found that the modulus of elasticity at different stress levels increases substantially with increasing OCR, although at higher OCR, the modulus sometimes decreases. He concluded that the modulus decreases with increasing stress level and the increase of modulus with OCR is more pronounced at lower stress levels. However, it was noticed that the increase in normalised Young's modulus of elasticity, (E_u/σ'_{v0}) , with OCR is not as pronounced as that for normalised undrained shear strength, (s_u/σ'_{v0}) . Ladd et al (1977) summarised the effect of the ratio of deformation parameters to undrained shear strength (E_u/s_u) with various stress levels and overconsolidation ratios. In this comparison, the data were taken from CK_0UDSS tests of six different soils which was reported by Ladd and Edgers (1972) and is shown in Figure 3.8. The investigation was carried out at stress levels of $(\tau_h/c_u) = 1/3$ and $(\tau_h/c_u) = 2/3$ and overconsolidation ratios up to $OCR = 10$. From Figure 3.8, they found that the normalised undrained modulus of elasticity, (E_u/s_u) , decreases with increasing stress level. It can also be seen from the figure that the ratio of E_u/c_u increases up to $OCR = 1.8$ and then decreases rapidly.

Poulos (1978) also investigated the normalised deformation parameters with different overconsolidation ratios from CK_0U triaxial compression tests for Sydney Kaolin. In Figure 3.9, the normalised undrained Young's modulus is plotted for three incremental stress levels, $(\Delta q/\Delta q_f) = 0, 1/3, 2/3$, which is defined as:

$$\frac{\Delta q}{\Delta q_f} = \frac{(\Delta \sigma_v - \Delta \sigma_h)}{(\Delta \sigma_v - \Delta \sigma_h)_f} \quad (3.8)$$

where

$\Delta\sigma_v$ = vertical stress increment (over and above the initial stress),

$\Delta\sigma_h$ = lateral stress increment (over and above the initial stress), and

$(\Delta\sigma_v - \Delta\sigma_h)_f$ = the difference between $\Delta\sigma_v$ and $\Delta\sigma_h$ required for failure.

Poulos found that the normalised undrained Young's modulus of elasticity, (E_u/σ'_{v0}) , increases with increasing OCR up to OCR = 2 to 4 and thereafter, remains constant, irrespective of increasing OCR. It can be seen also that, from this figure, the normalised deformation parameter decreases with increasing stress level.

(c) Pore pressure parameter at failure

The effective stress paths of both normally consolidated and overconsolidated soils are largely influenced by the excess pore pressures developed during the undrained test. In triaxial test, the excess pore pressure is expressed in terms of pore pressure parameter. The term pore pressure parameter, A, for triaxial compression test was first introduced by Skempton (1954), which is as follows:

$$A = \frac{(\Delta u - \Delta\sigma_3)}{(\Delta\sigma_1 - \Delta\sigma_3)} \quad (3.9)$$

where

Δu = change in pore pressure,

$\Delta\sigma_3$ = change in cell pressure and

$(\Delta\sigma_1 - \Delta\sigma_3)$ = deviator stress.

For overconsolidated clay negative pore pressure develops during undrained shearing and the tendency of developing negative pore pressure increases with increasing OCR. This can be related with pore pressure parameter at failure, A_f , and OCR.

Wroth (1984) investigated the relationship between the pore pressure parameter at failure, A_f , and the OCR from the critical state viewpoint. In Figure 3.7 the path RS represents the effective stress path for overconsolidated soil. In a triaxial compression test where the cell pressure is kept constant the total stress path is represented by a gradient of 3 i.e. $\Delta p = 1/3 \Delta q$. From Figure 3.7 the change in excess pore pressure can be written as,

$$\begin{aligned} \Delta u &= p_t - p'_s \\ &= p'_r + \Delta p - p'_s \\ &= p'_r + 1/3 q_s - p'_s \end{aligned} \quad (3.10)$$

where

$$p_t = \text{peak normal stress}$$

Substituting the value of p'_s from $q_s = Mp'_s$, and Δu into Equation 3.9, the pore pressure parameter at failure can be expressed as

$$A = \frac{\left(\frac{R}{r}\right)^{-\Lambda} + \frac{M}{3} - 1}{M} \quad (3.11)$$

where R, r and M have been defined earlier.

For a particular soil the parameters M and r are constant. So it can be concluded that the pore pressure parameter at failure varies only with overconsolidation ratio, R. This was examined by Wroth (1984) using experimental results on Weald Clay reported by Bishop and Henkel (1957). In Figure 3.10 both the experimental and theoretical pore pressure parameter at failure are plotted against different OCR. The theoretical curve

was obtained by substituting the values of the parameters $M = 0.95$, $r = 2$ and $\Lambda = 0.6237$ for Weald Clay in Equation 3.11. From Figure 3.10 it can be seen that the experimental results are closely matched with the theoretical curve.

(d) Normalised effective stress path

The response of a soil element to a particular test depends on the changes in effective stresses it undergoes. In the SHANSEP method the effective stress path from a series of normally consolidated and overconsolidated soils are expressed in the normalised form where the effective mean normal stress, $p' = \frac{(\sigma'_1 + 2\sigma'_3)}{3}$, and shear stress, $q = (\sigma'_1 - \sigma'_3)$, are normalised either with respect to the maximum consolidation pressure, σ'_p , or effective equivalent pressure, p'_e . Koutsoftas and Ladd (1985) investigated the strength parameter of a marine clay deposit and found that the normalised mean normal stress decreases for normally consolidated soil whereas the opposite occurs for heavily overconsolidated soil. This behaviour is shown in Figure 3.11, where the normalised shear stress, q/σ'_p , is plotted against the normalised effective mean normal stress, p'/σ'_p . The tests were carried out in plane strain compression (PSC), plane strain extension (PSE), triaxial compression (TC) and triaxial extension (TE). From the figure it can be concluded that the effective stress paths for heavily overconsolidated clay exhibit significant strength anisotropy.

3.4.4 Steps involved in the SHANSEP method to extend laboratory data to field conditions

The SHANSEP method is a convenient format for presenting variations of soil parameters with stress history from which the in situ undrained shear strength and deformation properties can be determined. In doing so, it requires the stress history of the soil deposit which can be determined by evaluating the effective overburden

pressure, σ'_{v0} , and maximum past pressure, σ'_{vm} , throughout the profile. Then the appropriate NSP values can be used to evaluate the soil properties. The basic steps of the SHANSEP method are summarised below.

- (a) Determine the variation of effective overburden pressure, σ'_{v0} , from a knowledge of the variation of total unit weight and pore water pressure throughout the deposit. Evaluate the variation of maximum effective pressure, σ'_{vm} , from oedometer tests using undisturbed soil samples.
- (b) Consolidate the soil sample to a consolidation pressure 1.5 to 2 times the maximum effective pressure, σ'_{vm} , followed by a reduction in effective stress to give the required OCR. The exact procedure has been described in Section 3.4.2.
- (c) Evaluate and express the results in normalised form, i.e. (s_u/σ'_{v0}) , (E_u/σ'_{v0}) , and (E_u/s_u) versus OCR.
- (d) Compute the variation of undrained shear strength and deformation properties throughout the soil deposit. Knowledge of the effective overburden pressure, σ'_{v0} , and maximum effective pressure, σ'_{vm} , of the soil profile enables calculation of the variation of OCR with depth which in turn enables calculation of the in situ undrained shear strength and deformation properties from NSP.

Using the steps involved in the SHANSEP method, the undrained shear strength throughout the profile corresponding to any type of failure for a uniform deposit can be determined. In order to do that, Ladd and Foott (1974) carried out a case study using the data of Ladd et al (1969) from a typical soil profile from Portland, Maine tidal area. The soil profile shown in Figure 3.12, is a comprehensive summary of undrained shear

strengths which include, field vane, unconfined compression and UU tests, along with the stress history of the deposit. It would appear from this figure that the maximum past pressure, σ'_{vm} , decreases whereas the effective overburden pressure, σ'_{vo} , increases linearly with depth. The values of σ'_{vm} and σ'_{vo} from Figure 3.12 were used to calculate the variation of OCR with depth. Using this OCR profile the normalised undrained shear strength, (s_u/σ'_{vc}) , of Maine Organic Clay was determined from Figure 3.5, which in turn provided the undrained shear strength with depth of the profile. The obtained undrained shear strength, s_u , was found almost constant with depth of the profile. This is attributed to the variations of OCR which is found to be greatest near the ground surface and decreases with depth. A summary of effective overburden pressure, σ'_{vo} , maximum past pressure, σ'_{vm} , OCR, (s_u/σ'_{vc}) , and s_u , with depth is presented in Table 3.1.

3.4.5 Assessment of the SHANSEP method in practice

From the previous discussion it can be seen that SHANSEP is a design method which has introduced an improved testing technique with an associated framework for calculating the in situ soil properties from laboratory test results. Recent research which reveals the factors that affect the properties of cohesive soil have been considered in the testing procedure of this method. Thus, it can be said that the properties obtained from the SHANSEP method can be used more reasonably to determine the in situ soil properties compared to UU test. The only assumption involved in this method is that it can only be applied to a fairly regular deposit where the in situ overconsolidation can be simulated in the laboratory by the reconsolidation procedure. However, one might raise the question, like Mesri (1975), that the procedure which has been adopted in the SHANSEP method can be misleading because the natural structure of the soil in this method might be disturbed by reconsolidation rather than overcoming the effects of sample disturbance. While this may be true for a cemented clay, where the structure can be destroyed by reconsolidation, for natural

non-cemented deposits it is not valid. It should be noted that the structure of a natural deposit of overconsolidated clay that was formed during geological history cannot be precisely duplicated in the laboratory by the reconsolidation procedure but the extent to which the soil structure is altered and the appropriateness of soil properties obtained from the SHANSEP reconsolidation procedure are more acceptable compared to other methods commonly used in practice (Ladd and Foott, 1980).

In view of the above considerations, it can be concluded that the properties obtained from this method are more appropriate for solving geotechnical engineering problems. This has been reinforced from a number of case studies carried out by Ladd and Foott (1974), which include an embankment on Organic Clay, an embankment on Boston Blue Clay, etc., where subsequent data were taken from the studies of Ladd et al (1969), D' Appolonia et al (1971), which indicated that the factor of safety obtained from the SHANSEP method is more suitable compared to field vane (FV), unconfined (U), and UU tests for stability problems.

3.5 Summary

The available literature presented in this chapter has focussed on some of the results of recent research which affect the properties of cohesive soils. Considering these effects, a detailed method of determination of in situ soil properties from normalised soil parameters, called SHANSEP, has been briefly outlined. In this chapter the following points have been highlighted:

- (a) Among the factors that affect the properties of cohesive soils, (such as, sample disturbance, initial consolidation, strength anisotropy and strain rate), sample disturbance tends to be the most significant factor which affects the properties of soils. The undrained shear strength can be reduced

up to 50% in some cases, and the undrained Young's modulus is affected to a greater extent.

- (b) The normalised behaviour concept for cohesive soils has indicated that the normalised plot can be used widely to determine the undrained shear strength and deformation properties of clay consolidated to any other effective consolidation pressure.
- (c) A discussion of the SHANSEP method has revealed an improved testing procedure to determine the soil properties in the laboratory. The principal factors that affect the soil properties have been considered in the testing technique so that it simulates the in situ conditions.
- (d) The increase of the normalised undrained shear strength, (s_u/σ'_{v0}) , with OCR has been expressed by an empirical formula. The existence of such empirical formula has also been found from the critical state soil mechanics concept.
- (e) In general the normalised deformation parameter (E_u/σ'_{v0}) , increases up to OCR = 2 to 4 while the pore pressure parameter at failure, A_f , decreases as the OCR increases.
- (f) Following the steps of the SHANSEP method, the in situ undrained shear strength of a typical soil profile has been determined from the normalised soil parameter, indicating the method's applicability to real life situations.

The procedures described in this chapter are used with little modification in Chapter 4, to develop the normalised soil parameters, and to determine the normalised undrained shear strength and deformation properties of remoulded Keswick Clay.

Table 3.1 Computation of in situ undrained shear strength, s_u , from Figure 3.5 (after Ladd and Foott, 1974)

Depth (m) (Figure 3.12) (1)	Effective overburden pressure, σ'_{vo} , (kPa) (Figure 3.12) (2)	Maximum past pressure, σ'_{vm} , (kPa) (Figure 3.12) (3)	OCR (3)/(2) (4)	(s_u/σ'_{vc}) (Figure 3.5) (5)	s_u (kPa) (6)
2.0	9.0	48.0	5.4	1.14	10.0
3.5	15.0	38.0	2.55	0.65	9.80
5.0	22.0	36.0	1.65	0.45	9.60
6.5	28.0	36.0	1.25	0.35	9.80
8.0	35.0	37	1.05	0.30	10.30

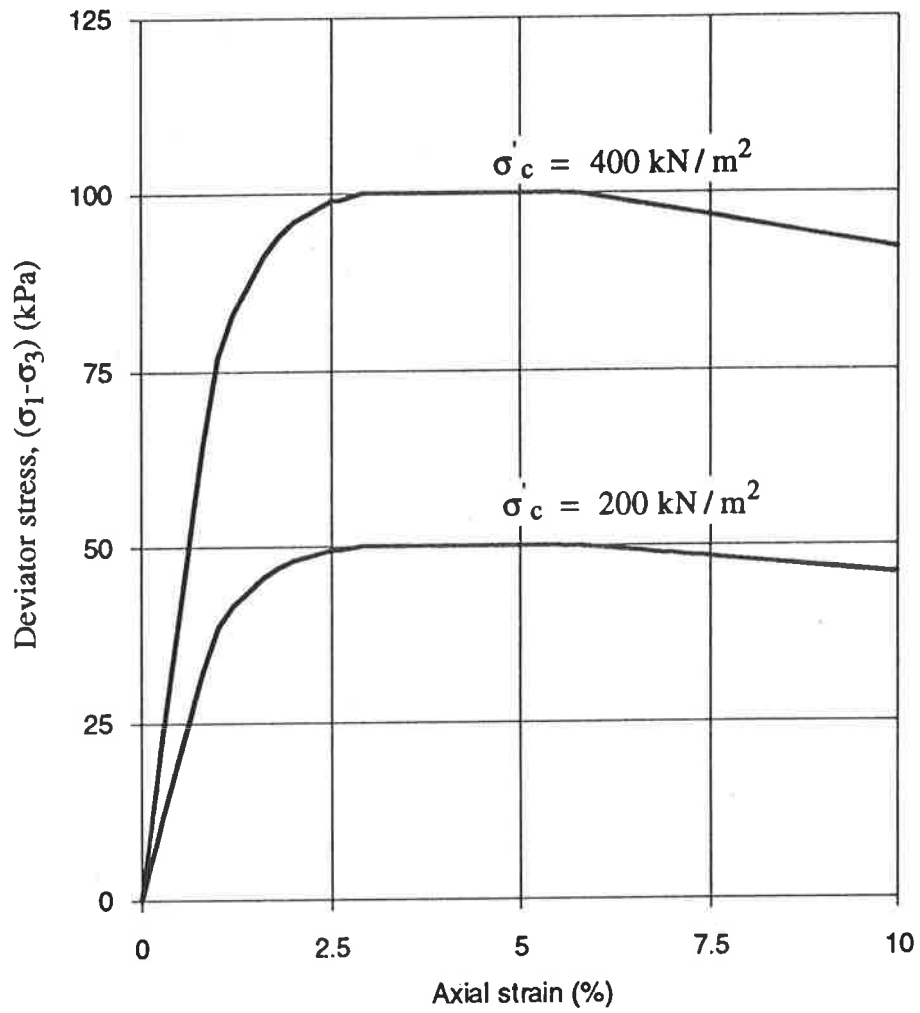


Figure 3.1(a) Triaxial compression test data for $\sigma'_c = 200$ and 400 kN/m^2
(after Ladd and Foott, 1974)

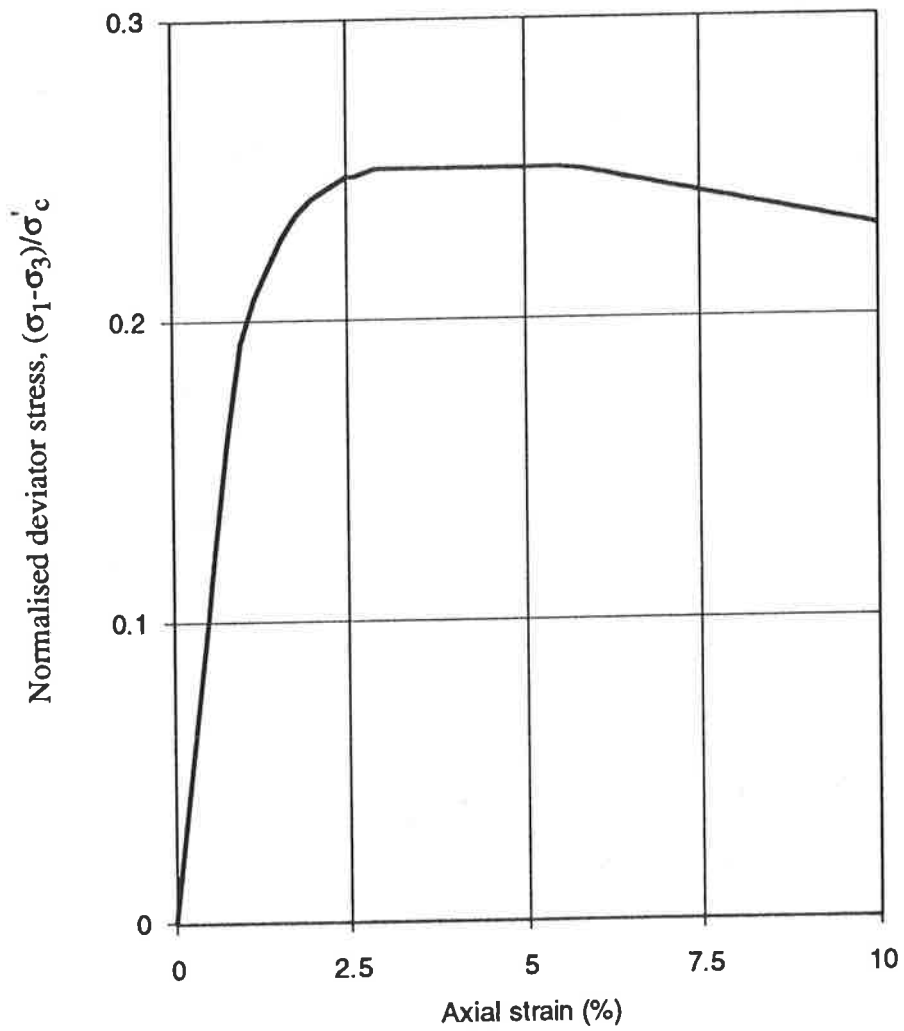


Figure 3.1(b) Normalised plot of triaxial test data (after Ladd and Foott, 1974)

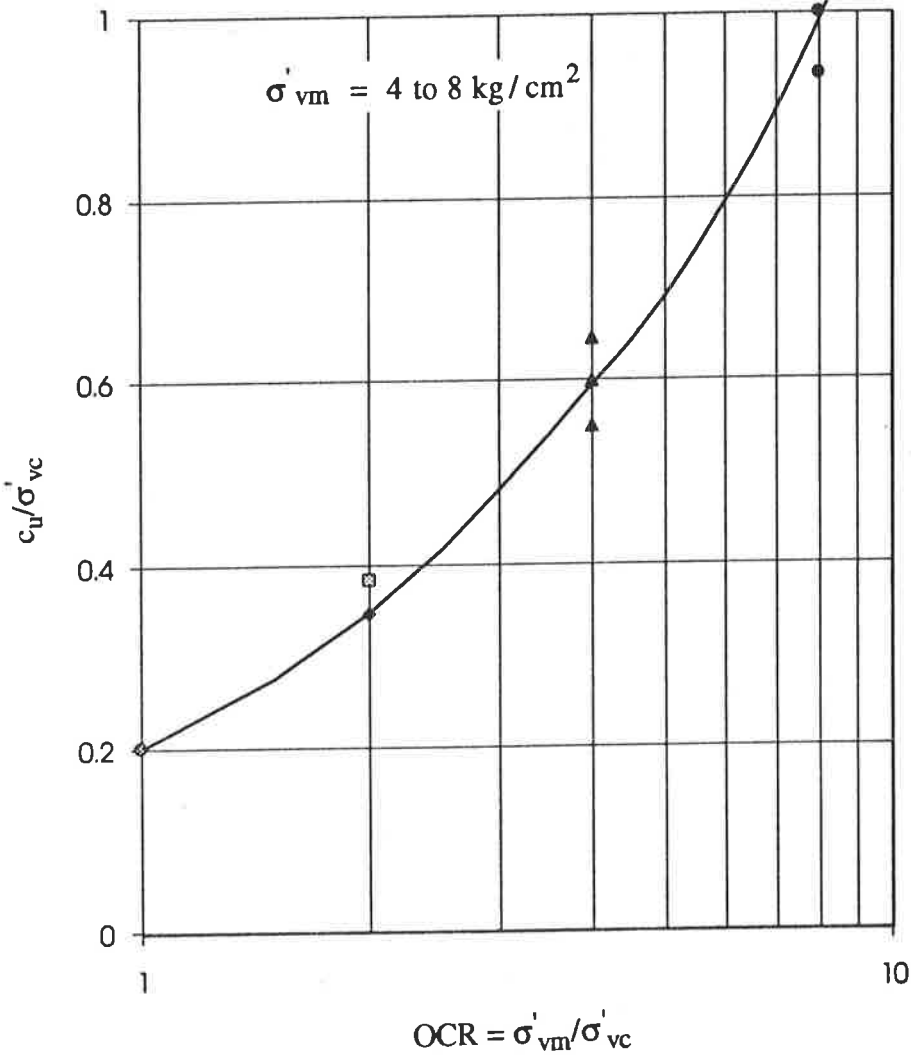


Figure 3.2 Normalised undrained shear strength for overconsolidated Boston Blue Clay (after Ladd and Foott, 1974)

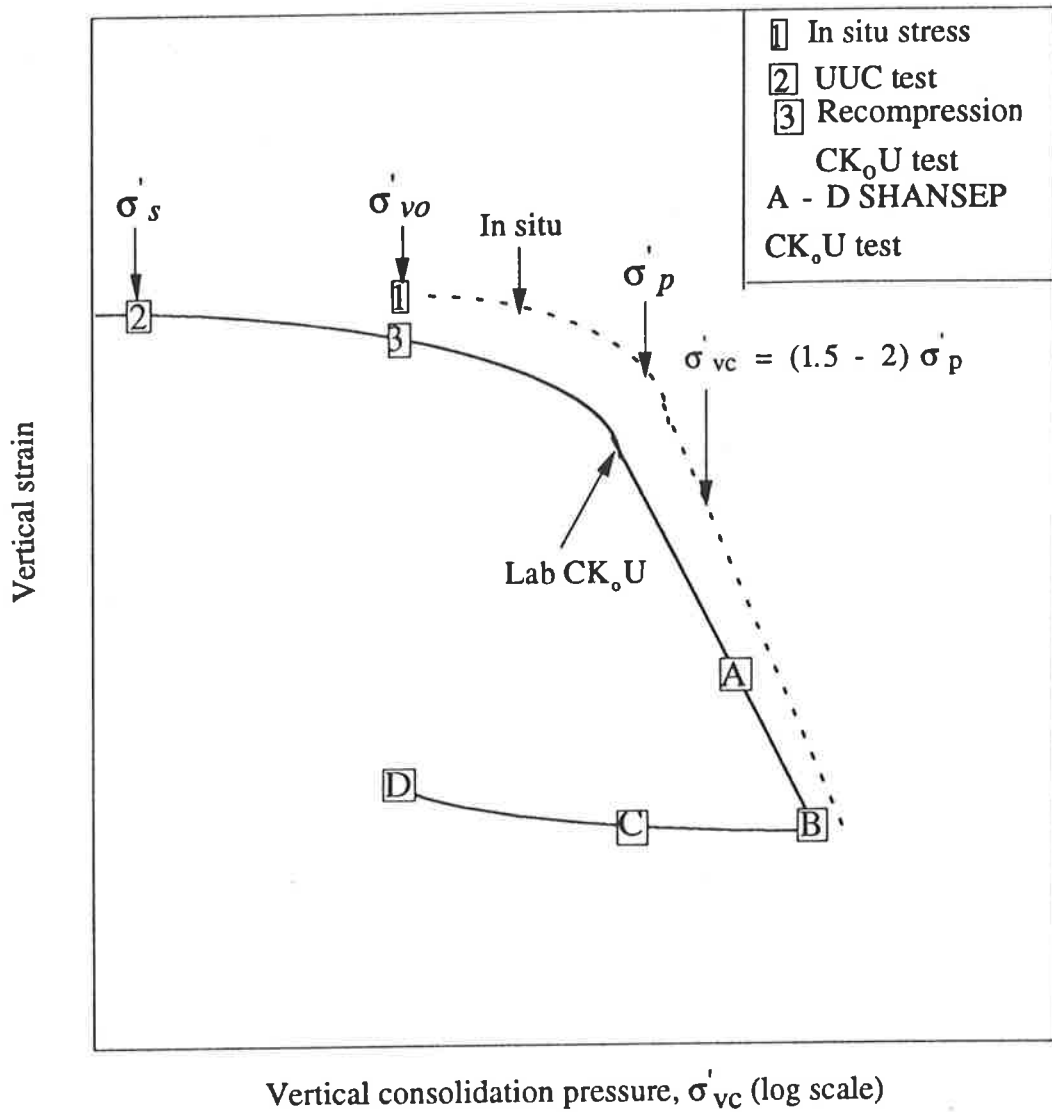
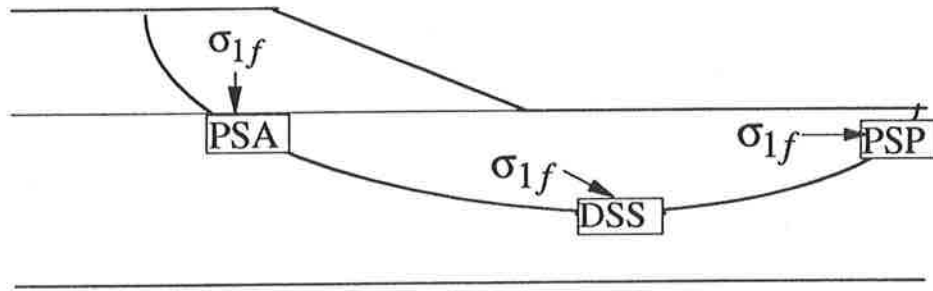
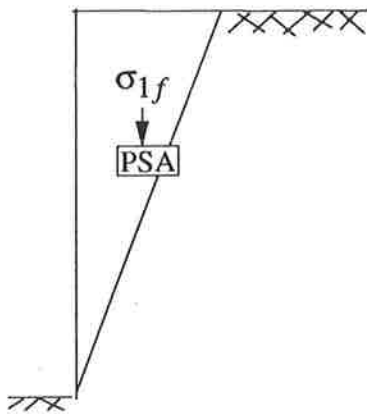


Figure 3.3 Consolidation procedure in the laboratory (after Germaine and Ladd, 1988)

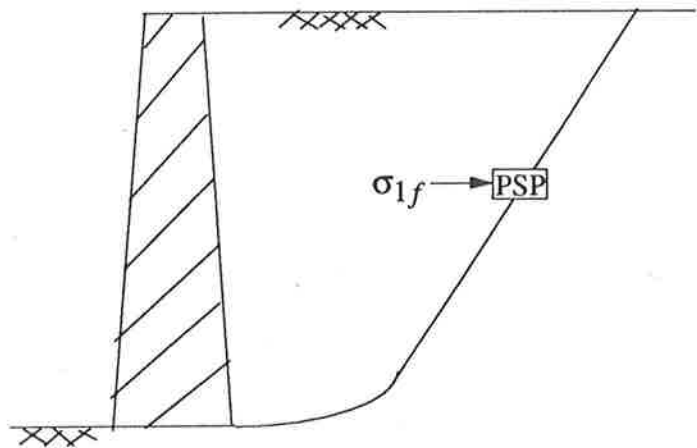


Long embankment

PSA= Plane strain active
 PSP= Plane strain passive
 DSS= Direct simple shear



Long vertical cut



Long loaded retaining wall

Figure 3.4 Stress system for in situ modes of failure
 (after Ladd and Foott, 1974)

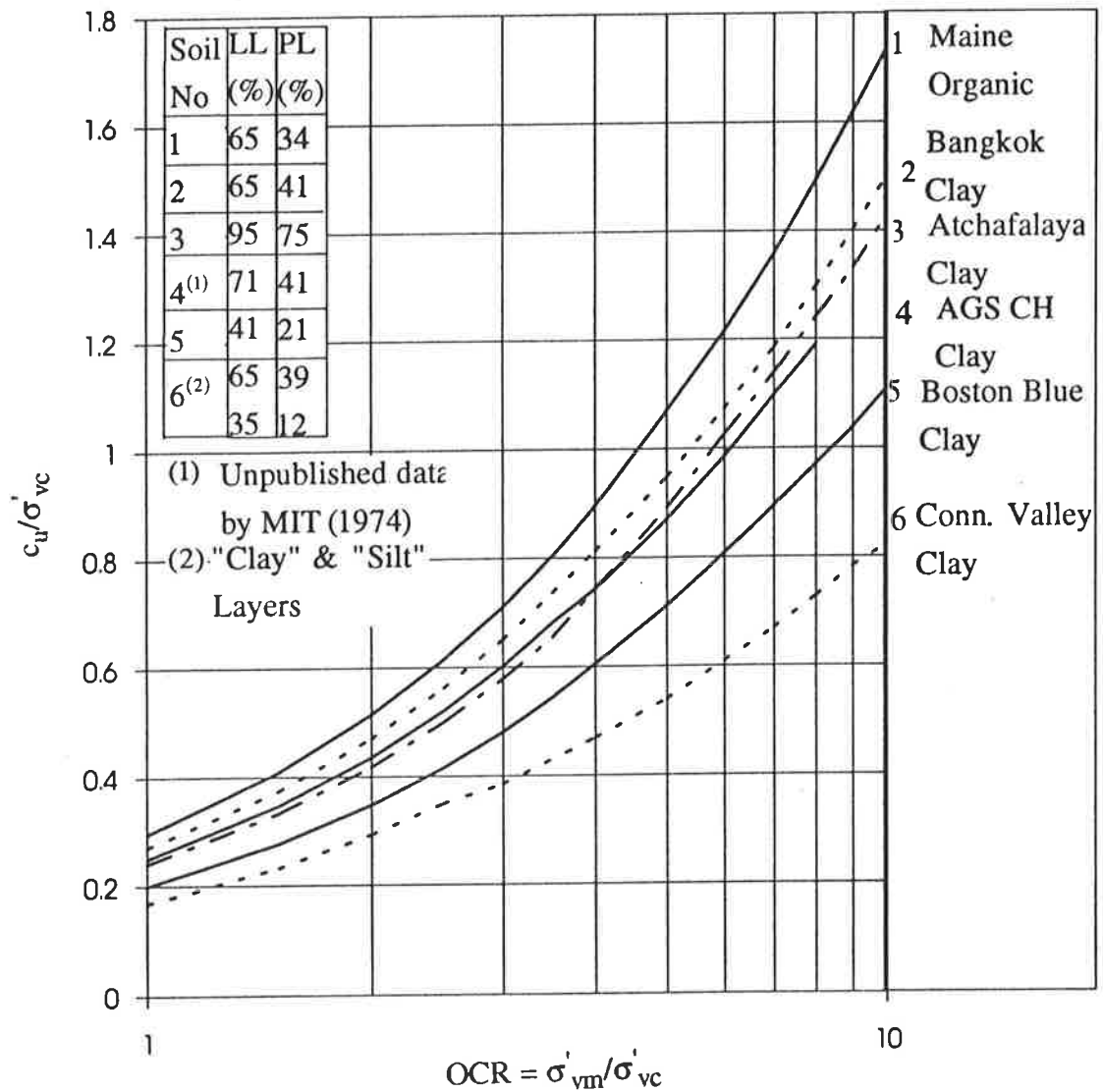


Figure 3.5 Variations of normalised undrained shear strength with OCR
 (after Ladd and Edgers, 1972)

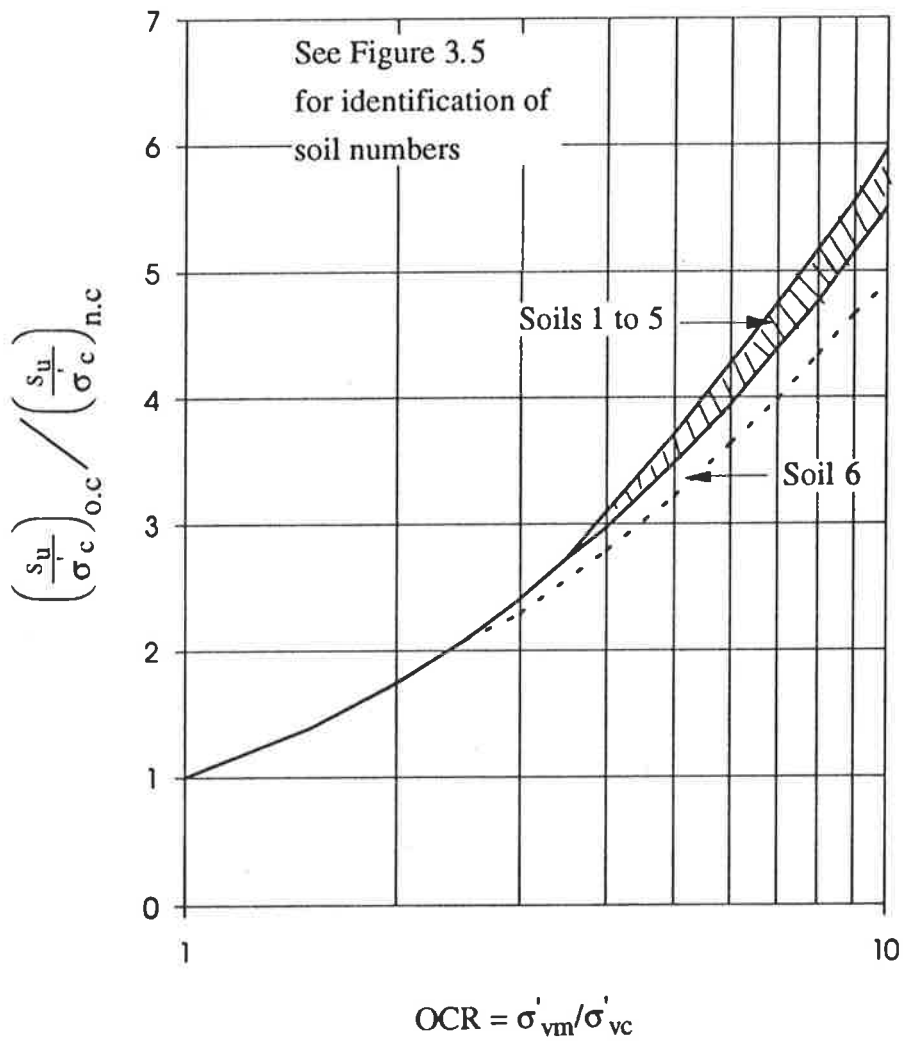
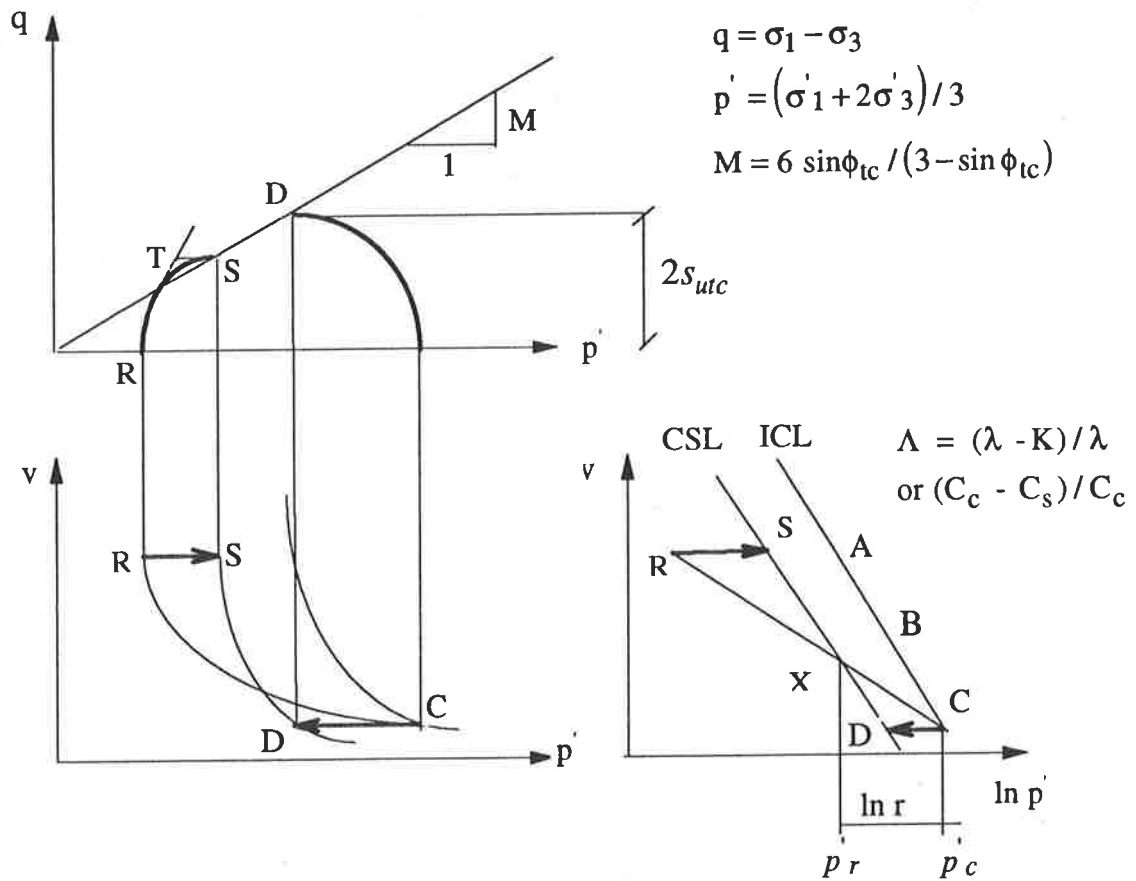


Figure 3.6 Relative increase in undrained strength ratio with OCR from CK_0U DSS tests (after Ladd et al 1977)



- Overconsolidation ratio : $R = p'_c / p'_r$
- Spacing ratio of ICL and CSL : $r = p'_c / p'_x$
- Undrained strength ratio : $s_{utc} / p' = \frac{M}{2} \left(\frac{R}{r}\right)^\Lambda$
- Normalised strength ratio : $(s_{utc} / p') / (s_{utc} / p')_{nc} = R^\Lambda$

Figure 3.7 Idealised undrained behaviour in triaxial compression test
(after Wroth, 1984)

See Figure 3.5 for identification of soil

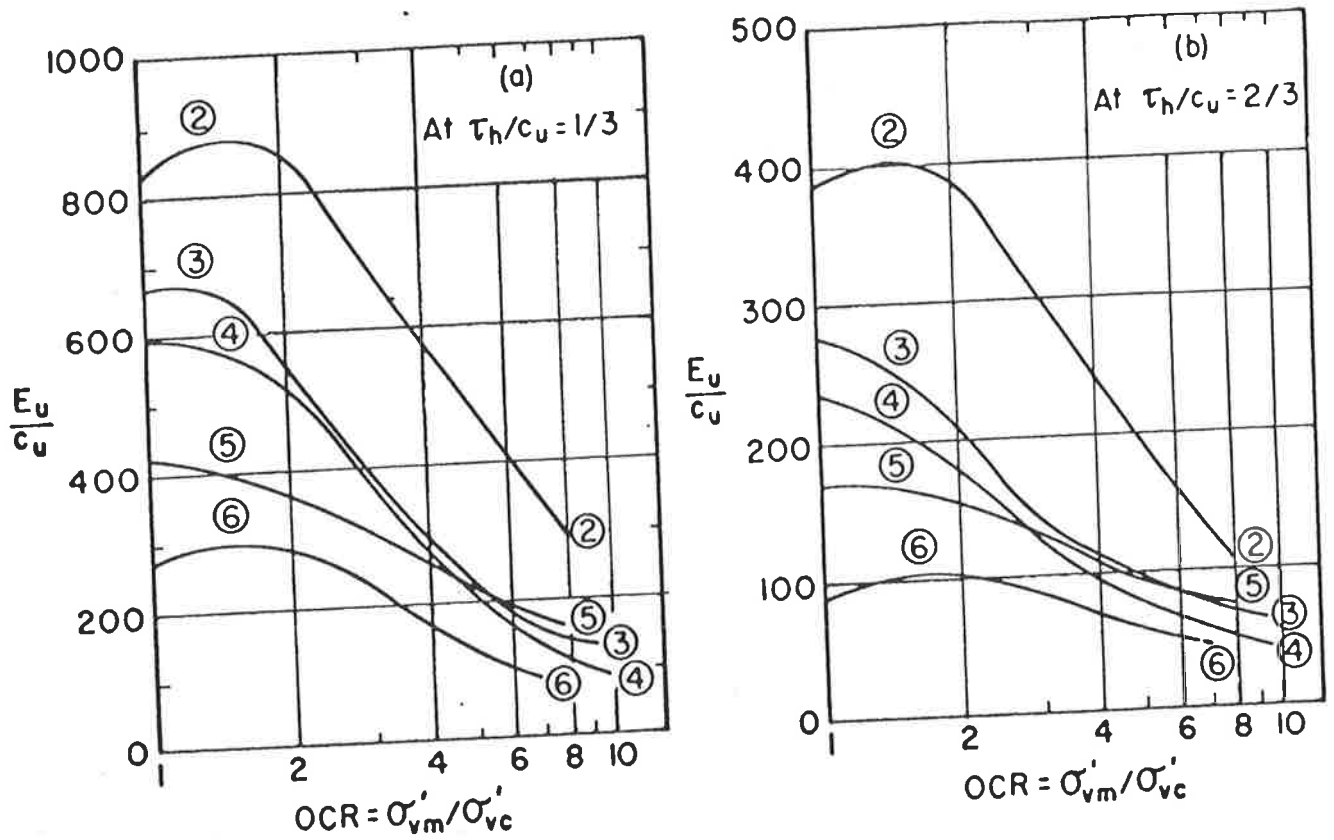


Figure 3.8 Normalised undrained modulus versus OCR
(after Ladd and Edgers, 1972)

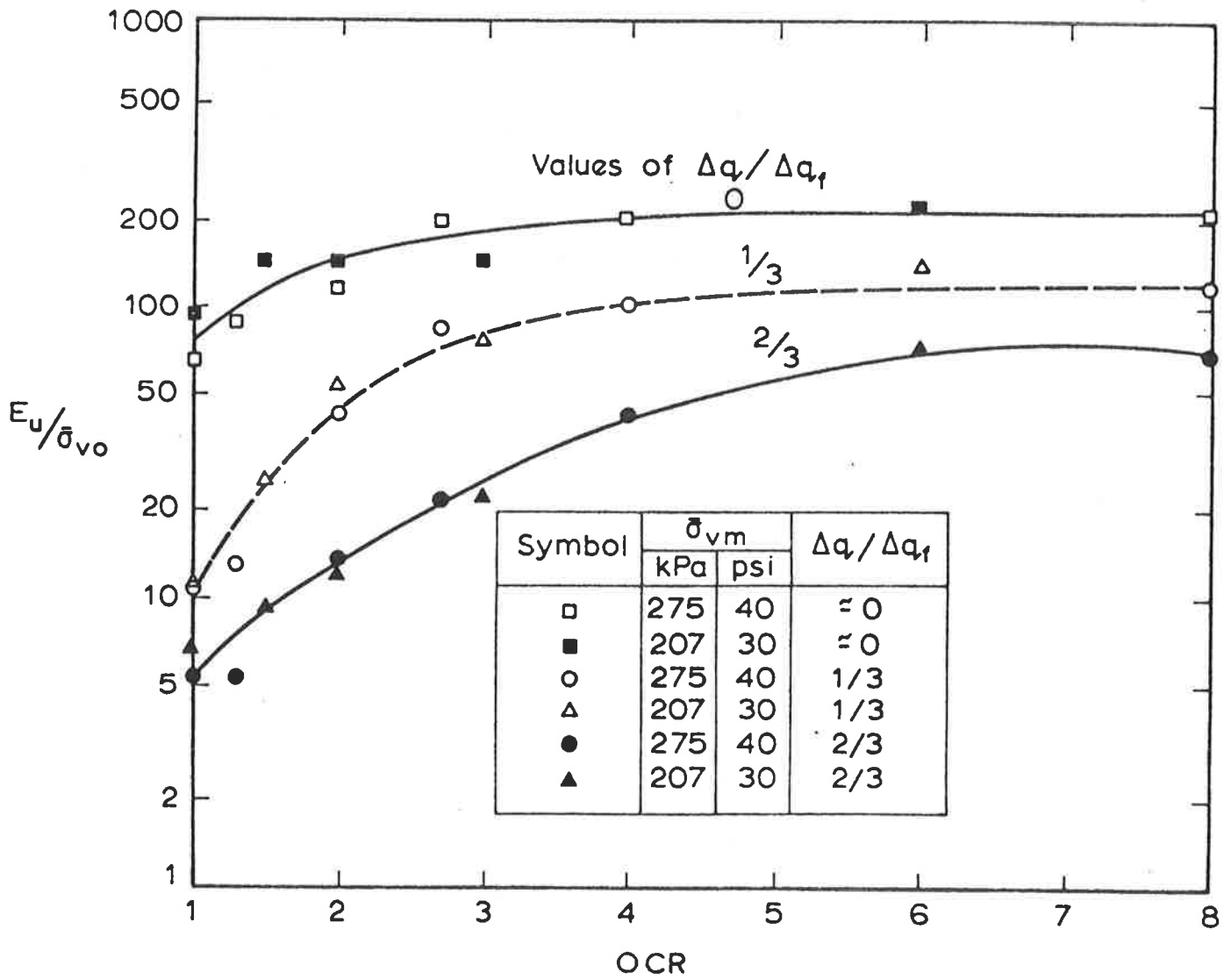


Figure 3.9 Normalised undrained modulus for Sydney Kaolin
(after Poulos, 1978)

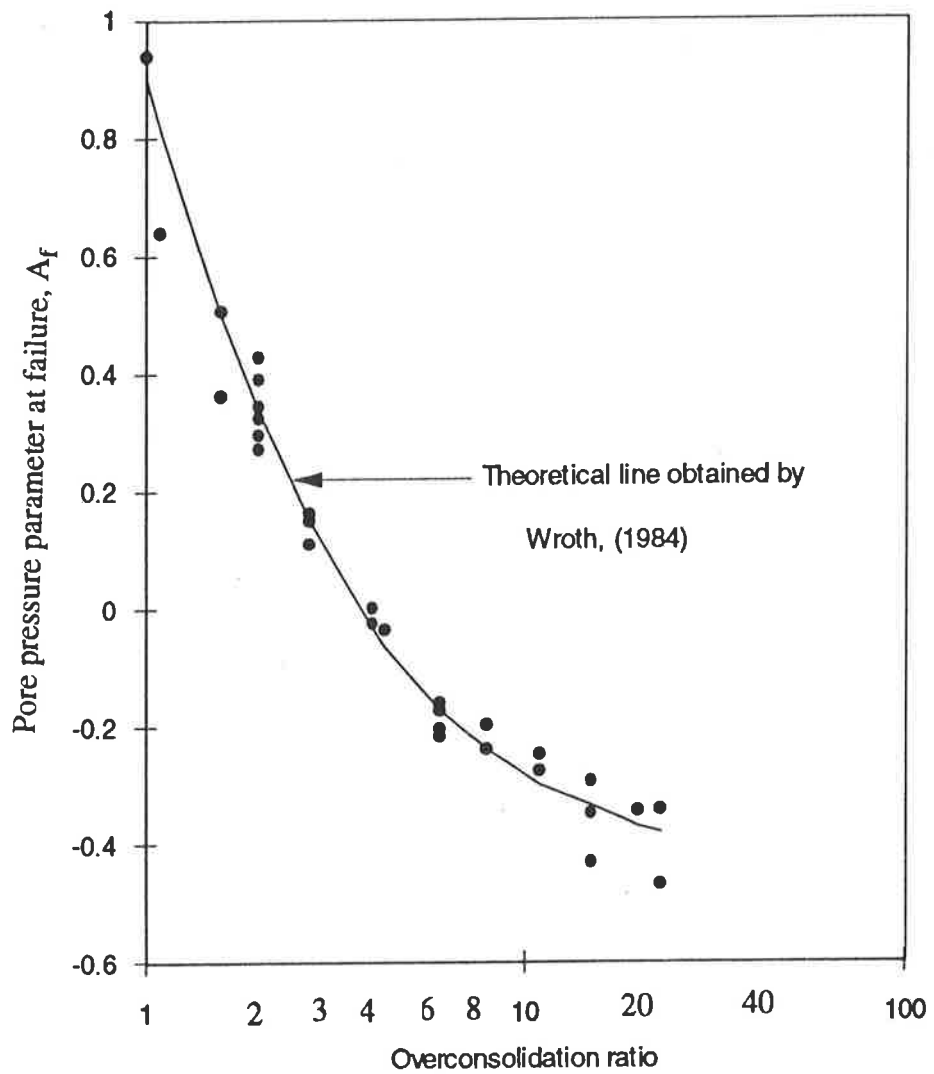


Figure 3.10 The variation of the pore pressure parameter at failure with OCR
(after Bishop and Henkel, 1957)

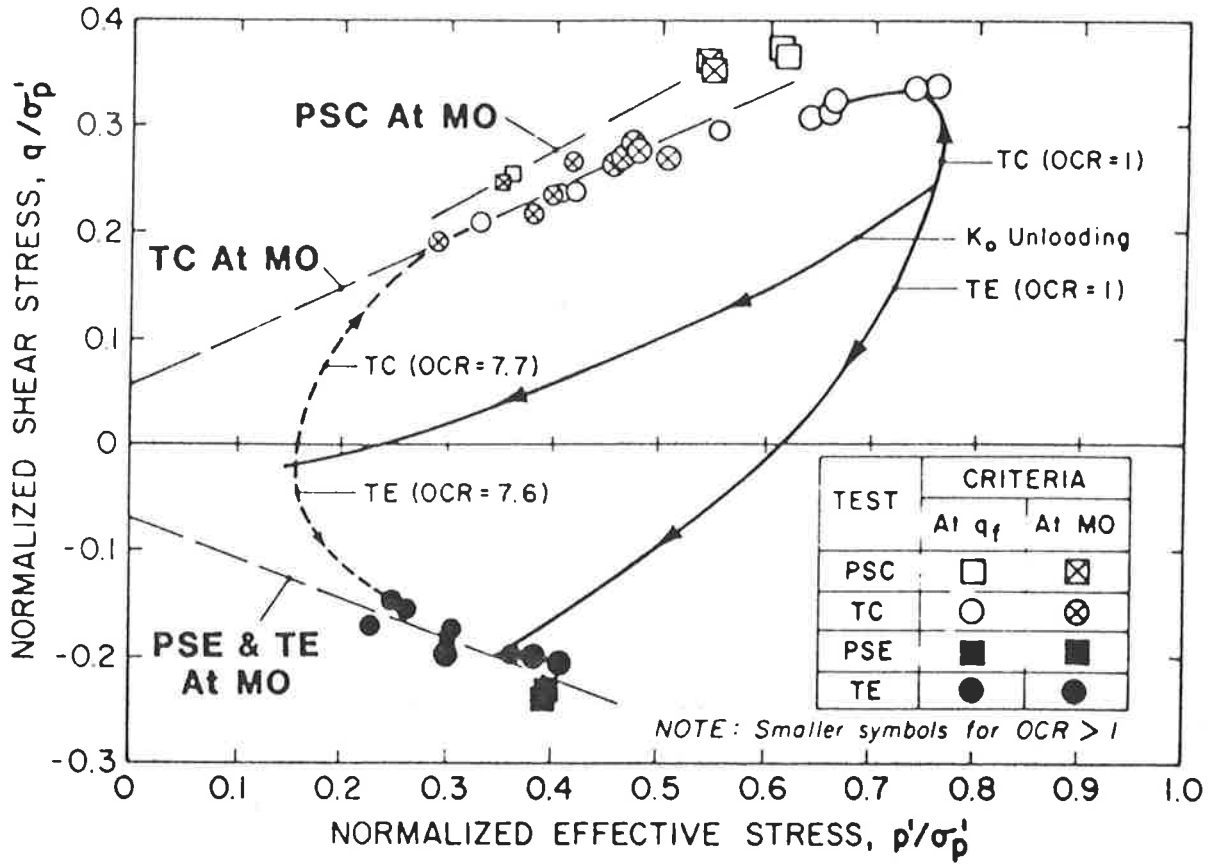


Figure 3.11 Effective stress path for Marine Clay
(after Koutsoftas and Ladd, 1985)

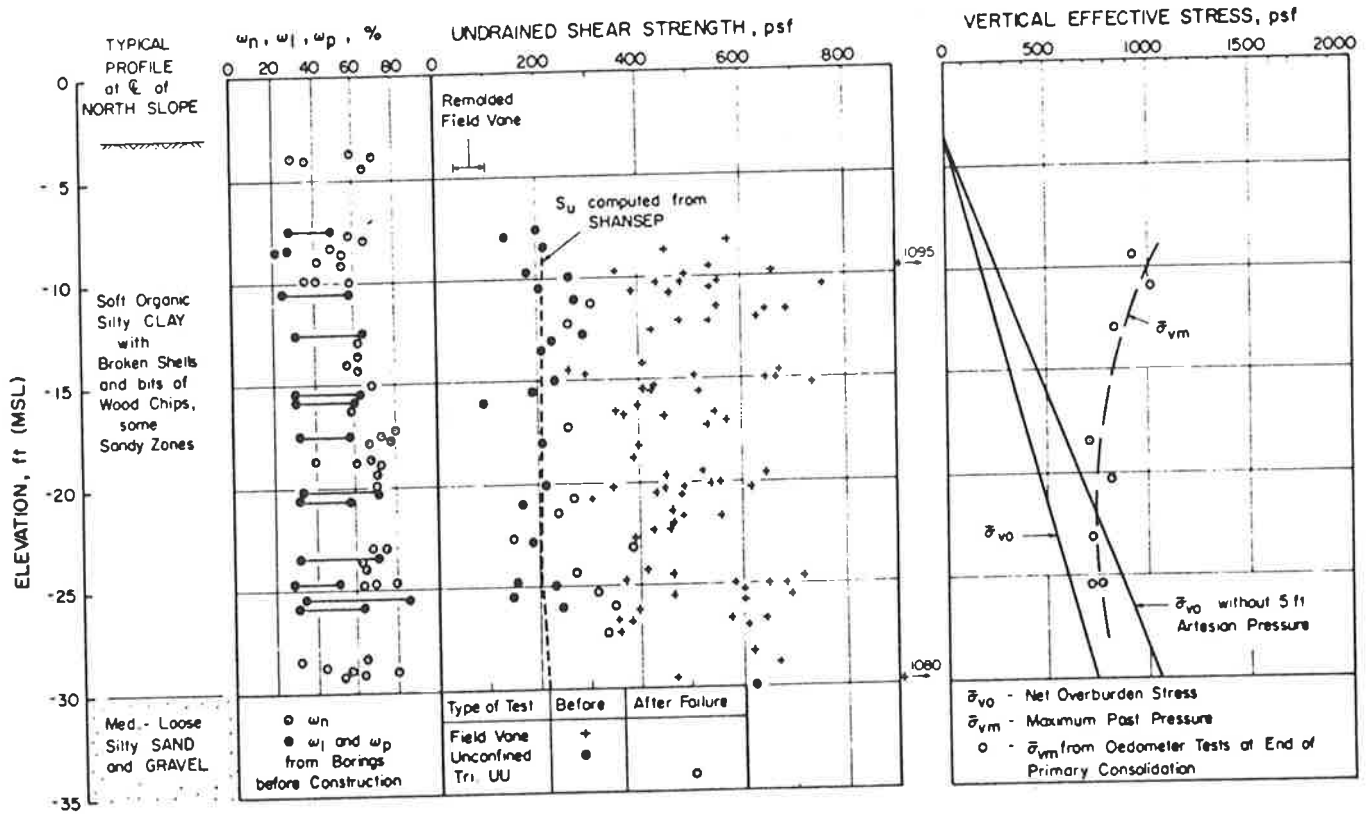


Figure 3.12 Soil conditions of a soil profile at Portland (after Ladd and Foott, 1974)

Chapter 4

Description of soil used and experimental program

4.1 Introduction

This chapter describes the results of preliminary tests used to determine the index properties of a clay soil (the Keswick Clay) from the Adelaide metropolitan area, as well as a detailed testing program for quantifying the normalised behaviour of the clay under undrained conditions. The preliminary tests include particle size distribution, Atterberg limits, specific gravity, permeability and oedometer tests. Results of these tests are used to characterise and describe the soil. The laboratory testing program involved isotropically consolidated undrained triaxial compression (CIUTC) tests. In these tests the soil samples were consolidated to an all-round effective stress and then either sheared or unloaded to achieve an overconsolidated stress state, with overconsolidation ratios varying between 1

to 13. These tests were performed to develop correlations between the normalised shear strength and deformation parameters with stress history.

The following sections review the soil profile which underlies the metropolitan area of Adelaide and describe the properties of Keswick Clay from the available literature. Collection and preparation of remoulded Keswick Clay are summarised. The results obtained from the preliminary tests are then presented, followed by a description of the procedures used in the testing program.

4.2 Soil profile within the Adelaide metropolitan area

Until recently it was considered that the Adelaide metropolitan area was underlain by recent surface deposits, followed by a very expansive clay formation of three layers known as Hindmarsh Clay (Cox, 1970). The upper and lower clay layers are very similar in nature. The upper clay soil is described as a grey, stiff to very stiff clay, which is heavily fissured and has high plasticity. The intermediate layer is grey and brown in colour and the soil is generally a clayey sand known as the middle sand layer. It was thought that the Hindmarsh Clay layer was formed during the Pleistocene period and the layer extends up to a depth of 20 m (Cox, 1970). Sheard and Bowman (1987, a and b) found that there exists a disconformity between the upper clay layer and the underlying middle sand layer. Thus the upper layer has been renamed the Keswick Clay, with the middle and lower layers known as the Hindmarsh Clay formation.

A typical soil profile under the Adelaide city area that surrounds the central business district of Adelaide and the suburb of North Adelaide (Cox, 1970) is shown in Figure 4.1. It consists of recent deposits which extend up to a depth of 2 m followed by the upper clay

layer of expansive clay, Keswick Clay. The thickness of this layer varies between 0 to 15 m (Jaksa et al 1994). The sand layer that lies underneath the Keswick Clay is generally less than 4 m in thickness followed by the lower expansive clay, Hindmarsh Clay (generally less than 5 m) (Cox, 1970; Kaggwa, 1992). This layer is underlain by Hallett Cove Sandstone.

4.3 Description and properties of Keswick Clay from available literature

It is customary in geotechnical engineering practice to refer to a soil by its locality e.g. London Clay, Bangkok Clay. Accordingly, Cox (1970), referred to the upper clay layer as the 'Adelaide City Clay' which has since been referred to as the Keswick Clay, as stated in Section 4.2.

Keswick Clay has been described as being highly plastic, reactive and overconsolidated with a classification CH, based on the Unified Soil Classification System. The data published by Cox (1970) indicated that the average percentages of clay, silt and sand within the layer is 65%, 20% and 15% respectively. X-ray diffraction tests performed on the clay fraction pointed out that the dominant clay minerals in the Keswick Clay are "greater than 50% illite, greater than 20% kaolin and generally less than 20% montmorillonite". From three tests in the upper clay layer, Cox (1970) found an average specific gravity of 2.70. However, Jaksa and Kaggwa (1992) re-examined the specific gravity of Keswick Clay using sensitivity and statistical analyses and suggested a more appropriate value of the mean specific gravity, G_s , of between 2.73 and 2.77. From their analysis it was further added that the majority of the Keswick Clay within the Adelaide City area is saturated or very close to saturation.

The Keswick Clay is subjected to cycles of wetting and drying due to the arid climate. During drying, large negative pore pressures develop which lead to high normal effective stresses whereas during wetting, the negative pore pressure dissipate leading to lower normal effective stresses. This is the main reason for overconsolidation of Keswick Clay (Kaggwa and Jaksa, 1992). The properties like, dry density, moisture content and total soil suction vary markedly for a given depth below the ground surface. The variations can be attributed to the natural variability of geological materials, the highly fissured nature of the clay, sampling disturbance, the effect of seasonal variation on the sample, and the stress history of the clay. These factors affect the soil properties like the shear strength and compressibility characteristics of the clay.

To avoid large scatter, the measurements of soil properties like, shear strength and compressibility characteristics of Keswick Clay are usually based on field tests. However, due to the fissured nature of the clay laboratory tests have been used to confirm the results of field tests. From the detailed study by Kaggwa and Jaksa (1992), which included a data base of field tests and laboratory tests, the following points emerged with respect to the undrained shear strength and compressibility characteristics of Keswick Clay.

- From field tests which include self-boring pressuremeter (SBPM) tests, cone penetration tests and screw plate load tests (SPLT), the ratio ($s_u/\gamma z$) was found to lie in the range 1.8-5.0 (where γ is the bulk unit weight and z is the depth below the ground surface).
- The large scatter in undrained Young's modulus of elasticity from SBPM and SPLT tests resulted in the ratio ($E_{ui}/\gamma z$) varying significantly between 300 and 2000 (where E_{ui} is the initial undrained Young's modulus of elasticity).

- The maximum undrained shear strength, s_u , of "undisturbed" Keswick Clay from UU test in the laboratory triaxial test was reported as being approximately 300 kPa. The tests also gave values of the effective strength parameter, $c' = 0$, and effective friction angle $\phi' = 18^\circ$ to 21° , which is within the range of values reported by Richards and Kurzeme (1973).
- The Young's modulus of elasticity corresponding to 50% of the failure deviator stress increased significantly with increasing effective confining pressure, σ'_c , and the ratio (E_{u50}/σ'_c) varied between 75 and 200.

The properties of Keswick Clay were found to be remarkably similar to those of London Clay (Cox, 1970). A summary of results of tests reported by Cox (1970) on, what is now named Keswick Clay, are presented and compared with London Clay in Table 4.1. It shows that, among the index properties, the moisture content, liquidity index and void ratio were found to decrease with depth, while the density increases with depth. The shear strength data give an apparent cohesion at the surface of 18 kPa and at depth, 192 kPa, which indicates that the strength of Keswick Clay increases substantially as the depth of the clay increases. The angle of shearing resistance with respect to total stresses falls between 2° and 8° . The volume compressibility, m_{vc} , of Keswick Clay indicates that it decreases with depth of the clay and the pre-consolidation pressure increases with depth.

4.4 Source of Keswick Clay used in testing program

The Keswick Clay used for both preliminary and isotropically consolidated undrained triaxial tests (CIUTC) was collected in 1989 from a depth of approximately 6.0 m below

the ground surface at the site of the Myer Building¹, Adelaide (Figure 4.2). Since the collection of soil, samples of the Keswick Clay have been stored in the laboratory and dried out into clay lumps.

4.4.1 Preparation of remoulded clay

In the preliminary tests and CIUTC tests, remoulded soil was used rather than the undisturbed soil. In the case of undisturbed soil, variations in individual samples lead to variable undrained shear strength and deformation properties which are often difficult to interpret, beyond getting overall trends. To overcome these variations and obtain homogeneous soil samples it is desirable to use large batches of thoroughly mixed and remoulded soil. Though there are differences between remoulded clays and natural deposits, Henkel (1960) asserted that the results from remoulded soil samples give reasonable guidance to the behaviour of natural soil deposits, provided the clay does not have high sensitivity, where the sensitivity is defined as the ratio of undisturbed to remoulded undrained shear strength of soil.

In order to obtain remoulded Keswick Clay, the dried clay lumps were reconstituted by soaking in distilled water for three months followed by thorough mixing into a homogeneous paste. The moisture content of the paste was in the range 95%-100% which is higher than the liquid limit of the soil. The clay was then stored in desiccator bowls for subsequent use.

¹Myer Building is one of the biggest shopping centre in Adelaide city which is located in the heart of the city as shown in Figure 4.2.

4.5 Preliminary tests on Keswick Clay

Preliminary tests were carried out to check whether comparable results would be obtained to those reported in the literature (Section 4.3 and Table 4.1). These tests included soil classification tests (particle size distribution, Atterberg limit and specific gravity tests) permeability and oedometer tests.

(a) Particle size distribution

The percentages of different particle sizes present in the Keswick Clay was determined by sieve analysis, AS 1289.C6.1 (Standards Association of Australia, 1977) and pipette method. The results of particle size distribution are presented in Figure 4.3. From the grain size distribution curve shown in Figure 4.3, the percentages of clay, silt and sand were determined as 71% clay, 19.5% silt and 9.5% sand. The clay content was found to be slightly higher than that reported by Cox (1970). Selby and Lindsay also (1982) reported a comprehensive data of particle distribution of 14 samples where the clay content of most of the samples were found higher than Cox's investigation and about one-third were found even higher than the present investigation.

(b) Atterberg limit tests

The Atterberg limit tests included liquid limit, plastic limit and shrinkage limit which are the water contents at which soil changes from liquid to plastic, plastic to semi-solid and semi-solid to solid states respectively. The Atterberg limits for Keswick Clay were determined following AS 1289.C1.1, AS 1289.C2.1, and AS 1289.C4.1 (Standards Association of Australia, 1977) and are shown in Table 4.2.

The plasticity index is determined from the difference between the liquid limit and the plastic limit following AS 1289.C3.1 (Standards Association of Australia, 1977). The significance of plasticity is the ability of soil to undergo irrecoverable deformation at constant volume without cracking. The plasticity chart of the Unified Soil Classification System (USCS) is shown in Figure 4.4. This classification system, which was developed by the United States' Bureau of Reclamation and the Corps of Engineers, provides a general indication of the permeability, strength and compressibility of various soil groups. Although these correlations may result in misleading predictions of field stability, flow magnitudes and displacements, it is often used as a basis to classify the soils in groups. From the Atterberg limits of Keswick Clay, it can be seen that it lies above the A-line of the plasticity chart. The USCS symbol for Keswick Clay is accordingly CH, which was also reported by Cox (1970) and Kagawa and Jaksa(1992). On the basis of the CH classification (Lambe and Whitman, 1979), the following characteristics of Keswick Clay would be expected.

- (i) The permeability of Keswick clay is expected to be very low and the shear strength increases with decreasing moisture content.
 - (ii) It is very difficult to compact the soil when wet and impossible to drain by ordinary means.
 - (iii) It is susceptible to expansion and contraction with changes in moisture content.
- (c) **Specific gravity of Keswick clay**

The specific gravity of solids is defined as the ratio of the mass density of solids, γ_s , to the mass density of water, γ_w , at 4°C. In the case of soil grains the specific gravity, G_s , which

typically varies between 2.60 and 2.75, can be obtained in the laboratory by the following equation:

$$\begin{aligned} G_s &= \frac{W_s}{V_s \times \gamma_w} \\ &= \frac{\gamma_s}{\gamma_w} \end{aligned} \quad (4.1)$$

where

W_s = weight of solids and

V_s = volume of solids.

For Keswick Clay the specific gravity was determined following the standard procedure and from 3 tests, the average specific gravity was found to be 2.73. This value is consistent with the statistical investigation reported by Jaksa and Kaggwa (1992) but slightly higher ($G_s = 2.70$) than the results reported by Cox (1970) and Atchison et al (1977).

(d) Compressibility

The one-dimensional compressibility of a soil is expressed either by the compression index for normally consolidated clay or the swelling index for overconsolidated clay. An oedometer test was carried out to determine the compressibility characteristics of Keswick Clay, and the result of which is shown in Figure 4.5. From the curve, the compression index and swelling index can be determined. The respective values are 0.62 and 0.25. The volume compressibility decreased with increasing effective stress and was found to be in the range between $m_{vc} = 4.8$ to $0.09 \text{ m}^2/\text{MN}$ as the effective stresses varied between 25 kPa and 6400 kPa.

(e) Permeability

According to Darcy's law, the rate of flow of water, Q , is proportional to the hydraulic gradient of the soil mass, which can be written as:

$$Q = kiA \quad (4.2)$$

where

Q = flow rate (m^3/sec),

k = coefficient of permeability (m/sec),

i = hydraulic gradient and

A = cross-sectional area of sample (m^2).

From Equation 4.2 it can be seen that the flow rate of water through a soil mass is a function of k , i , and A . For Keswick Clay the coefficient of permeability was found to be equal to 1.7×10^{-10} m/sec using the falling head method. Although the coefficient of permeability of Keswick Clay is absent in Cox's publication, the result of this investigation lies between the values near the surface and at depth of London Clay (Table 4.1).

4.6 Laboratory testing program

Undrained shear tests were carried out in this investigation to examine the normalised behaviour and to establish the relationship between the normalised soil parameter and different stress histories of Keswick Clay. The testing procedures followed were similar to those of the SHANSEP method, as proposed by Ladd and Foott (1974) and described in Chapter 3. The laboratory testing program included a series of isotropically consolidated undrained triaxial tests (CIUTC) aimed at investigating the normalised behaviour of Keswick Clay. The normally consolidated samples were consolidated isotropically to

consolidation pressures of 100 kPa, 200 kPa, 300 kPa and 400 kPa and then loaded to failure under undrained compression. Provided the soil exhibits normalised behaviour, the ratio (s_u/σ'_c) would be constant. All overconsolidated samples were consolidated to a maximum consolidation pressure of 400 kPa which was then reduced to give an overconsolidation ratio of either 2, 4, 8, 10 or 13. After full consolidation the samples were monotonically loaded under undrained conditions. The normalised soil parameters, (s_u/σ'_c) , and (E_u/σ'_c) were then determined from these tests. The series of tests performed in the testing program are summarised in Table 4.3.

4.7 Testing procedure

The testing procedure followed in the CIUTC tests is described below, including the choice of sample size, the sample preparation and set up, the methods of sample saturation, consolidation, and shearing.

4.7.1 Choice of sample size

In standard triaxial tests cylindrical samples are used to investigate the soil properties. In selecting sample size in this investigation, emphasis has been given to the maximum particle size present in the sample and the effects of sample size on the stress-strain properties of the soil. Generally the higher the particle size the larger will be the required sample size. The maximum particle size with nominal sample size, suggested by Head (1988), are summarised in Table 4.4. Table 4.4 indicates that the height/diameter (h/d) ratio for all samples is 2:1 and the sample size increases with increasing the maximum size of the particles present in the sample.

The effects of sample size and end friction on the undrained stress-strain properties, particularly, for overconsolidated clay samples, have been examined by various authors (Jacobson, 1967; Berre, 1977; Berre, 1978; and Lacasse and Berre, 1989). In their investigation on the effects of (h/d) ratio and end friction on Drammen Clay with an overconsolidation ratio of 40, Lacasse and Berre (1989) highlighted the following points:

- (a) The use of smooth² ends and (h/d) ratio of 1 instead of rough³ ends with (h/d) ratio of 2 exhibits similar strength up to 10% axial strains but, beyond that, it showed higher strength.
- (b) The initial part of the stress-strain curve for both smooth and rough ends showed that false deformations are more pronounced in smooth-end tests than the rough end tests. It was further added that the determination of the Young's modulus at low strain is more reliable with high sample and rough ends.

In view of the above considerations a sample size of 76 mm × 38 mm (h/d = 2) and rough-end plates were chosen in this investigation.

4.7.2 Preparation of the sample and set up

A cylindrical mould of internal diameter 38 mm and 100 mm high was used to prepare remoulded samples. Initially the moisture content of the remoulded Keswick Clay was in the range of 95%-100%, as mentioned previously. In order to form a cylindrical sample, the soft clay was placed in the cylindrical mould under a known hanger load for initial

²The term 'smooth' means polished metal plates with silicone grease and rubber sheets used in between the ends.

³The term 'rough' means that the filter paper having same diameter with the sample and placed between the sample ends and the pedestal and top cap.

consolidation. First, the soil was kneaded carefully to remove any air voids. Then it was carefully placed into the mould using a small spatula. Two porous disks with filter papers were placed at the top and bottom of the cylinder to drain out the water during initial consolidation. A hanger load of 65 N (corresponding to an axial stress of 57 kPa) was applied for a period of at least 14 days. After this initial one-dimensional consolidation, the samples were typically 38 mm in diameter and 70-78 mm high.

Before setting up the sample in the triaxial apparatus the pore pressure line was flushed with de-aired water. Then a small volume of water was allowed to flow from the volume change cylinder to cover the pedestal of the cell. A saturated porous disk was placed on the top of the pedestal and the sample quickly mounted on the pedestal. Another saturated porous disk was placed on top of the sample, followed by the top cap. A rubber membrane was then, placed around the sample using a membrane stretcher. Finally, o-rings were put in position in order to seal the sample. A small negative pore pressure was applied to ensure that the sample was sitting firmly on the pedestal while the perspex cylinder was put in position.

4.7.3 Sample saturation stage

To avoid errors due to volume changes during the CIUTC test, full saturation of the sample is necessary to ensure the simulation of no volume change during the undrained shearing stage. In remoulded soil samples, lack of saturation may be caused by any of the following factors:

- (a) Air may be introduced into the soil during the preparation of the sample in the mould.

- (b) During assemblage in the triaxial cell, air may be trapped between the membrane and soil sample.
- (c) Air may be trapped between the membrane and porous disk, between the porous disk and top cap, or between the porous disk and the pedestal.

Accordingly, care was taken to minimise the entry of air at every stage of the test procedure.

The pore pressure response of a soil is largely affected by any lack of saturation because the compressibility of water and air are different. During the shearing stage, the tendency for volume change of the soil skeleton would not be fully resisted by the pore fluid because of the compressibility of free air. Thus, some volume change would occur and the pore pressure change would be less, affecting the stress-strain relationship, undrained shear strength, and effective stress path. In the laboratory the degree of saturation is checked by measuring the pore pressure coefficient B (Skempton, 1954) and can be written as follows:

$$B = \frac{\Delta u}{\Delta \sigma_3} \quad (4.3)$$

where

Δu = change in pore pressure and

$\Delta \sigma_3$ = change in all-around pressure.

B value of 1 indicates complete saturation of soft clays.

In the past, four methods have been employed to increase the degree of saturation in laboratory tests. These are: percolation with water; the carbon dioxide (CO₂) method; the

application of back pressure; and the vacuum procedure (Lade, 1986). The back pressure method was employed in the testing program to saturate the samples. The main purpose of applying the back pressure is to dissolve any air bubbles present in the pore water. The process is based on the compressibility (Boyle's law) and solubility (Henry's law) properties of gases. The pressure required for saturation depends on the initial degree of saturation, the nature of the gas and the duration of time. In the present series of tests, a back pressure of 100 kPa was applied. The process involves simultaneously increasing the cell pressure and back pressure. After 24 hours of applying the cell pressure and back pressure, the Skempton's B parameter was checked by closing the drainage line of the sample, increasing the cell pressure, and recording the increase in the pore pressure.

4.7.4 Consolidation stage

The purpose of consolidation is to achieve the desired pre-shear effective stress state condition. The effective stress state for most soft soils in the field is anisotropic with the horizontal and vertical stresses being unequal. Thus, it is desirable to perform anisotropic consolidation rather than the usual isotropic consolidation. However, performing anisotropic consolidation, particularly K_0 consolidation, is more complicated and far more time consuming. The permeability of Keswick Clay is very low and it takes more than 12 days to consolidate a standard 38 mm diameter, 76 mm high triaxial test sample. As mentioned in chapter 3, it should be noted that isotropically consolidated undrained test can be used as a 'reference' test where the obtained results can be interpreted for K_0 condition. Therefore, isotropic consolidation was chosen over K_0 consolidation which also allows completion of consolidation in a shorter period. This represents a deviation from the procedures detailed in Chapter 3. In the present testing program the consolidation procedure was divided into two phases, namely normal consolidation and overconsolidation.

(a) Normally consolidated clay samples

The clay samples were kept for 24 hours at an initial effective stress of 50 kPa in order to achieve saturation of the sample using a back pressure of 100 kPa. Then, to obtain the behaviour of normally consolidated soil, samples were consolidated isotropically using effective consolidation pressures of 100 kPa, 200 kPa, 300 kPa and 400 kPa, with the consolidation pressure of 400 kPa being applied in two stages. First, 200 kPa consolidation pressure was applied and after consolidating the sample fully, final consolidation pressure, 400 kPa, was applied.

(b) Overconsolidated samples

The overconsolidated soil samples were consolidated isotropically to a consolidation pressure of 400 kPa following the standard procedure for normally consolidated soil described above. The samples were then allowed to swell under reduced effective consolidation pressures of either 200 kPa, 100 kPa, 50 kPa, 40 kPa or 30 kPa. In this way overconsolidation ratios, OCR of 2, 4, 8, 10, 13 were achieved.

4.7.5 Compression stage

Particulars of the triaxial compression test are summarised below.

(a) Strain rate

The strain rate plays an important role in determining the undrained shear strength of soil as discussed in Chapters 2 and 3. Considering the effect of the strain rate on the undrained shear strength, Ladd and Foott (1974) recommended a rate of 0.01 %/minute to 0.02

%/minute in the SHANSEP testing program. However, Nakese and Kamei (1988), Mitachi and Kitago (1979) and Hanzawa and Tanaka (1992) used strain rates of 0.07 %/minute, 0.04 %/minute and 0.1 %/minute, respectively, in determining the normalised soil parameters of reconstituted Kawasaki Marine Clay, a remoulded clay near Sapporo in Japan, as well as 7 clays from the Arabian Gulf, Indonesia and Japan. From the study of Hanzawa and Tanaka (1992) it was observed that the strain rate has very little effect on undrained shear strength if it lies between 0.02 %/minute and 0.05 %/minute. In order to examine the effect of strain rate upon undrained shear strength, a series of preliminary tests on Keswick Clay were carried out at different strain rates. From the results, the normalised undrained shear strengths are plotted against strain rate which is shown in Figure 4.6. From figure it can be seen that there is no significant change in the normalised undrained shear strength if the strain rate remains within 0.05 %/min. Accordingly, a strain rate of 0.05 %/minute was chosen which enabled completion of the shearing stage in 4 hours.

(b) Shearing of the sample

The loading platform and proving ring were brought into contact with the loading piston. The shearing of the samples were then carried out by increasing the axial strain at a constant strain rate of 0.05%/minute. During the shearing stage, the axial load, deformation and changes in pore pressure were recorded and later used to determine the normalised undrained shear strength and deformation properties of Keswick Clay. The results are described in Chapter 5.

After testing, the sample was removed from the triaxial cell, weighed, and placed in the oven to determine its moisture content.

4.8 Summary

In this chapter the properties of remoulded Keswick Clay from the preliminary tests have been presented, and then followed by a description of the laboratory testing program used to determine the normalised undrained shear strength and deformation properties of Keswick Clay. Results of these preliminary tests and other published data indicate that the properties of Keswick Clay are comparable to those of the London Clay. However, the clay content of Keswick Clay from this investigation has been found to be higher than that for London Clay.

The testing program and procedure for developing the normalised undrained properties of remoulded Keswick Clay includes preparation of the sample, saturation, consolidation and shearing stages. Isotropic consolidation was chosen rather than K_0 consolidation which is a variation from the testing procedure recommended by Ladd and Foott (1974) described in Chapter 3. Finally the sample was sheared in compression using a strain rate of 0.05%/min.

Published data on the Keswick Clay concentrate on undrained shear strength and undrained deformation properties. Although overconsolidation plays a significant role in determining the undrained shear strength, most of the previous researchers concentrated on the strength of undisturbed soil in a normally consolidated state (Cox, 1970; Kaggwa, 1992; and Kaggwa and Jaksa, 1992). Therefore in Chapter 5, the isotropically consolidated undrained triaxial test results of remoulded Keswick Clay are examined by relating the normalised undrained shear strength, (s_u/σ'_{v0}) , and normalised undrained deformation properties (E_u/σ'_{v0}) , to the overconsolidation ratio.

Table 4.1 Comparison between Keswick Clay and London Clay (after Cox,1970)

Soil Property		Adelaide City Clay (Keswick Clay)		London Clay	
		At surface	At depth	At surface	At depth
Description		Grey-green, firm to stiff, Clay		Grey-blue, firm to very stiff, Clay	
Geologic Age		Pleistocene		Tertiary-Eocene	
Depth of deposit		9.15m-18.30m		30.5m-61m	
Mineralogy		Illite with some Kaolinite and Montmorillonite		Illite with some Kaolinite and Montmorillonite	
Index Properties:					
Clay content		65%		50%	
Specific gravity	G	2.70		2.74	
Moisture content	w	34%	30%	30%	26%
Liquidity Index	I _L	0.18	0	0.10	-0.10
Density		1.84 gm/cc	1.92 gm/cc	1.92 gm/cc	2.00 gm/cc
Void ratio	e	0.90	0.80	0.80	0.70
Liquid limit	w _L	75 to 115% (increases to south)		75%	
Plasticity index	I _p	55 to 80% (increases to south)		50%	
Activity		0.75 to 1.20 (increases to south)		0.75 to 0.90 (increases to east)	
Shear strength Characteristics:					
Apparent cohesion	c	48 kPa	192 kPa	48 kPa	383 kPa
Angle of shearing resistance	φ	2° to 8° (above overburden pressure)		0° (above overburden pressure)	
Apparent cohesion	c'	-		0 to 24 kPa	
Angle of shearing resistance	φ'	-		21°	
Sensitivity	S	1.00 but sensitive to structural disturbance		1.00 but sensitive to structural disturbance	
Consolidation Characteristics:					
Volume compressibility	m _{vc}	0.10×10 ⁻³ m ² /kN	0.05×10 ⁻³ m ² /kN	0.20×10 ⁻³ m ² /kN	0.10×10 ⁻³ m ² /kN
Volume expansibility	m _{vs}	0.01×10 ⁻³ m ² /kN (in lower layer)		0.06×10 ⁻³ m ² /kN	0.01×10 ⁻³ m ² /kN
Pre-consolidation pressure	c _e	479 to 1436 kN/m ²		2155 kN/m ² to 3591 kN/m ²	
Consolidation coefficient ratio 1/m _{vc}	C _v	-		0.37m ² /year	
		150 to 200		100 (75 for block samples)	
Others:					
Elastic modulus	E	6894 kN/m ²	41366 kN/m ²	11031 kN/m ²	55154 kN/m ²
Ratio E/c		150		140	
Permeability	k	-		7×10 ⁻⁷ cm/sec(field)	5×10 ⁻⁹ cm/sec(field)
Swelling pressure on samples		192 to 862 kN/m ²		96 kN/m ²	383 kN/m ² (approximates overburden pressure)

Table 4.2: Results of Atterberg limit tests

Characteristics	Average
(a) Liquid limit %	76.5
(b) Plastic limit %	27.0
(c) Linear shrinkage %	17.6
(d) Plasticity index	49.5

Table 4.3: Summary of testing program

TEST NO	OCR	σ'_c (kPa)
1	1	100
2	1	200
3	1	300
4	1	400
5	2	200
6	4	100
7	8	50
8	10	40
9	13	33

**Table 4.4. Suggested maximum particle size for triaxial samples
(after Head, 1988)**

Nominal sample size height \times diameter (mm \times mm)	Suggested maximum size of particles (mm)
76 \times 38	3.35
100 \times 50	6.3
140 \times 70	10
200 \times 100	20
300 \times 150	37.5

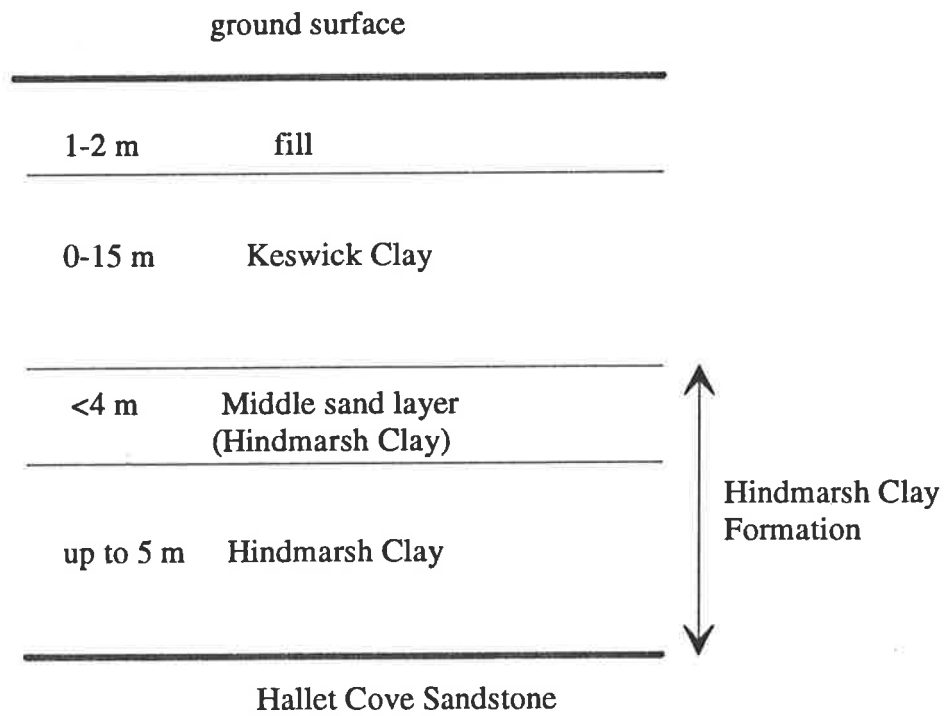


Figure 4.1 Typical soil profile beneath Adelaide Metropolitan area

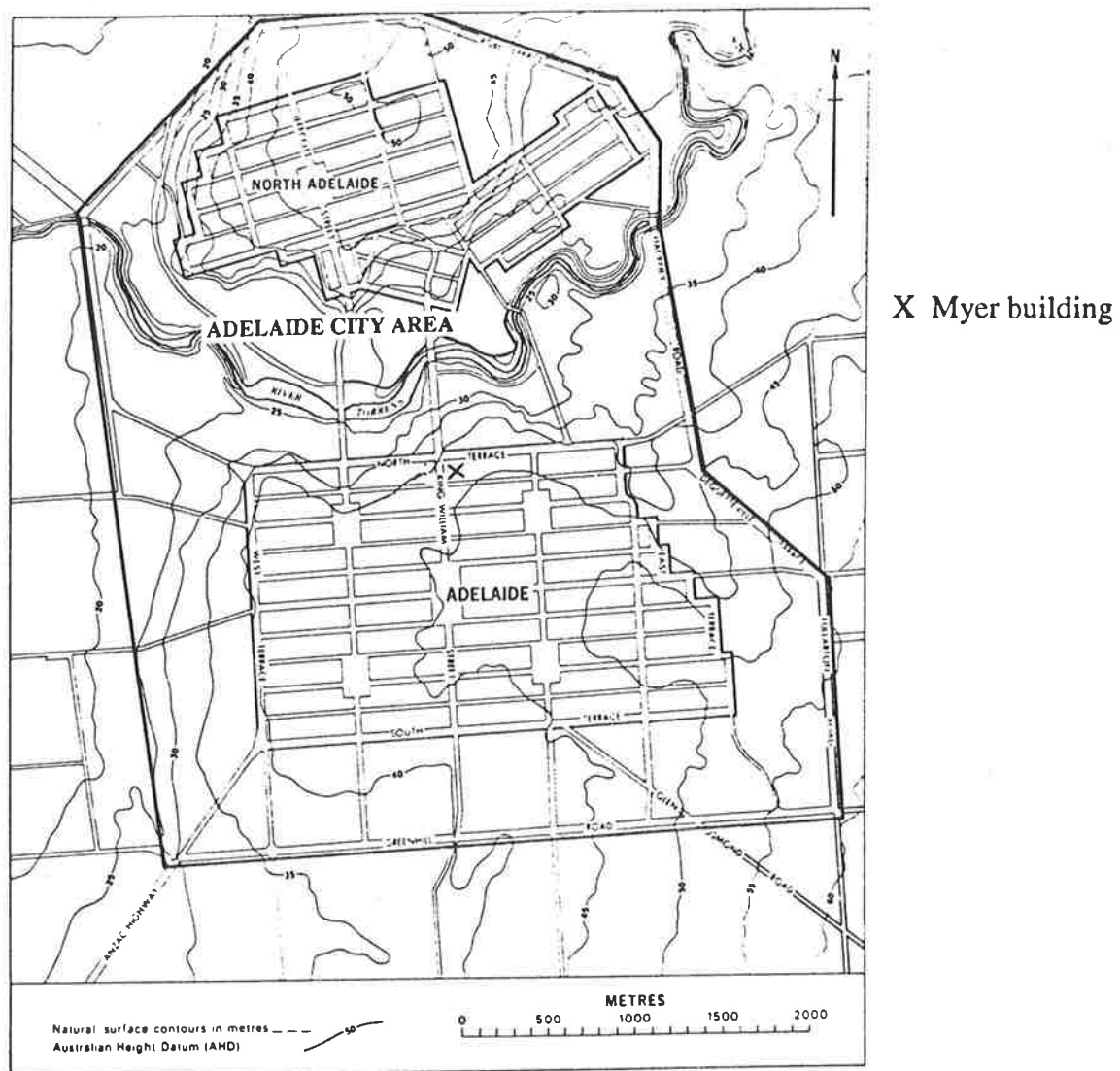


Figure 4.2 Map of Adelaide city area showing the location of Myer Building

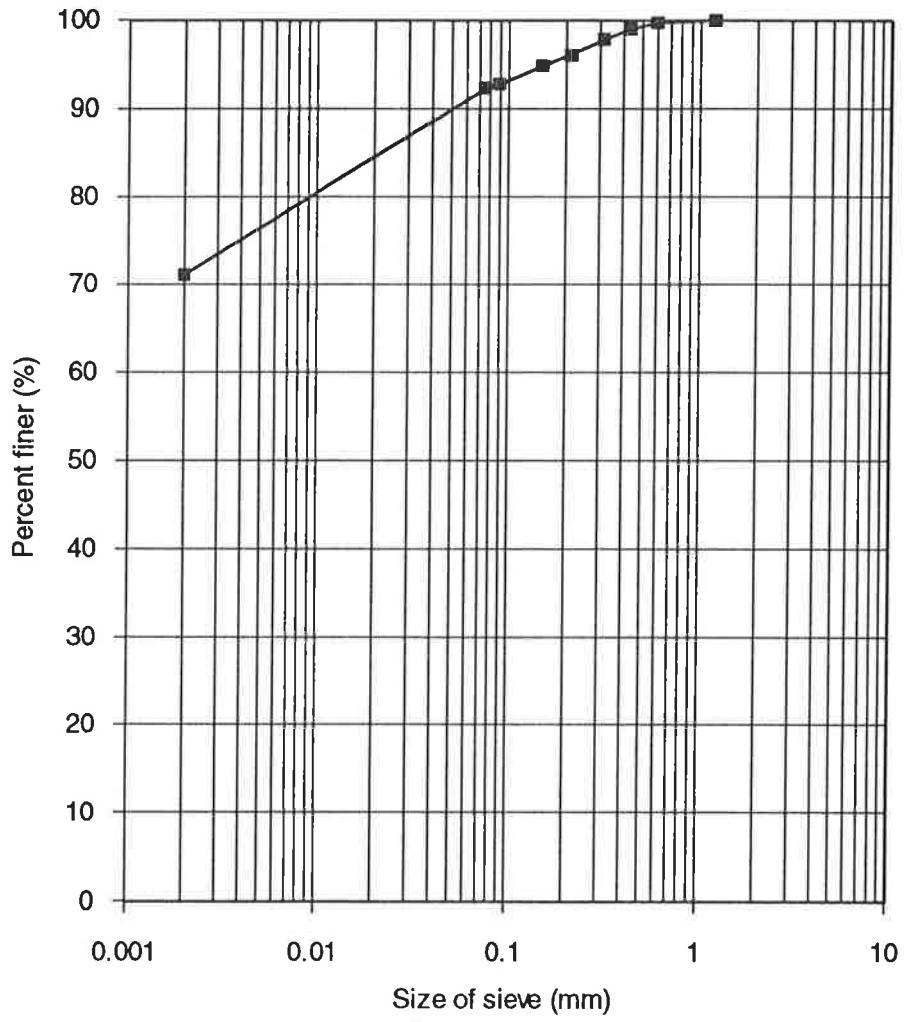


Figure 4.3 Particle size distribution for Keswick Clay sample.

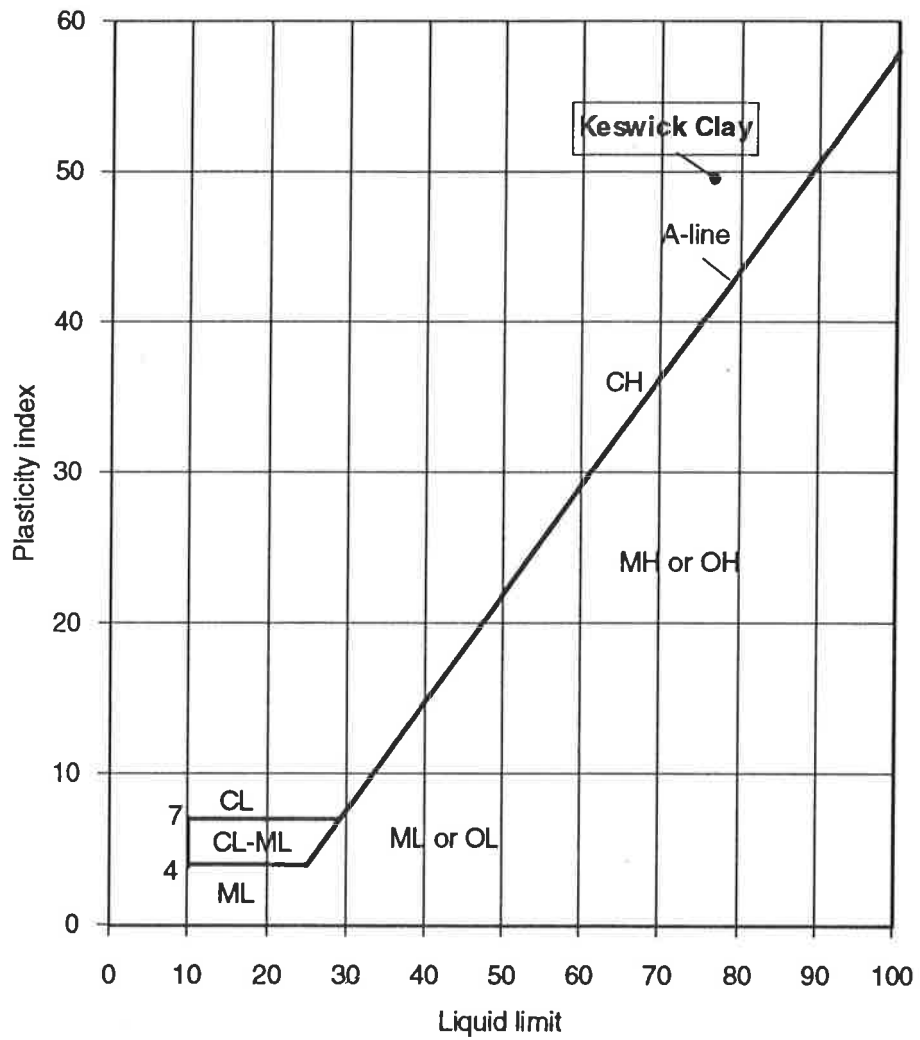


Figure 4.4 Plasticity chart for Keswick Clay sample

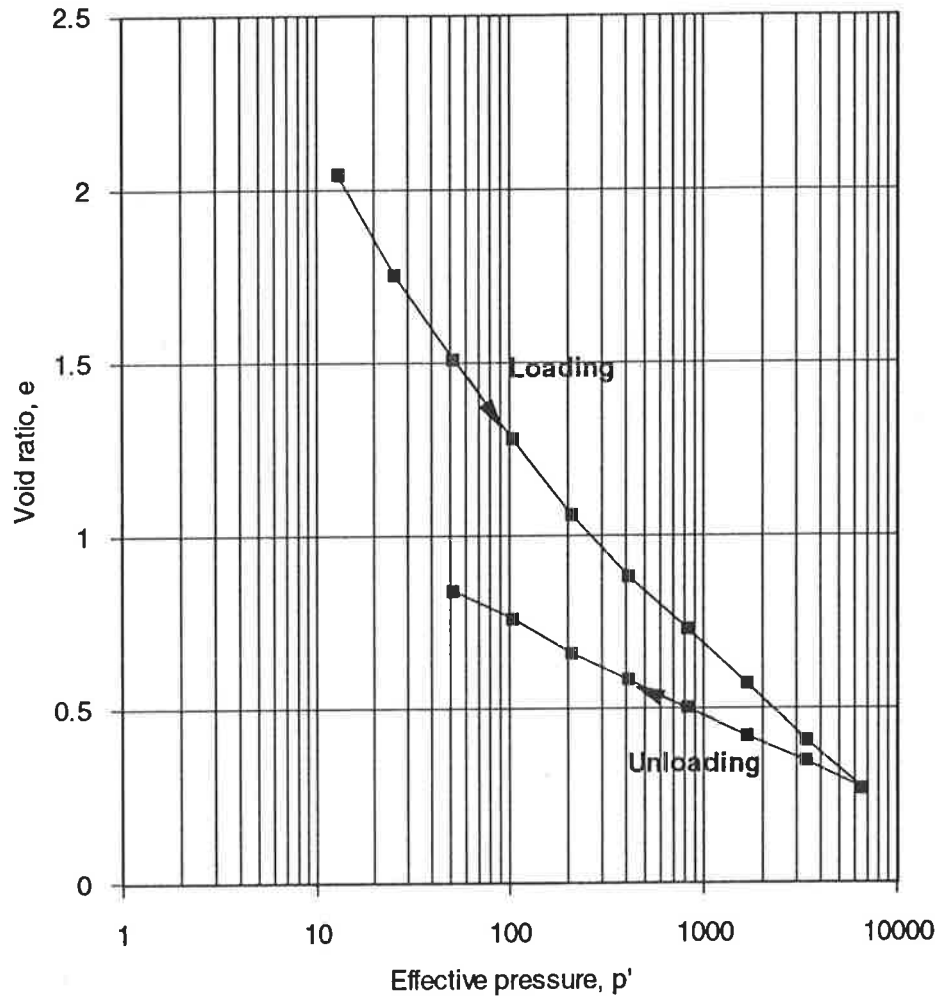


Figure 4.5 Consolidation curve for Keswick Clay sample.

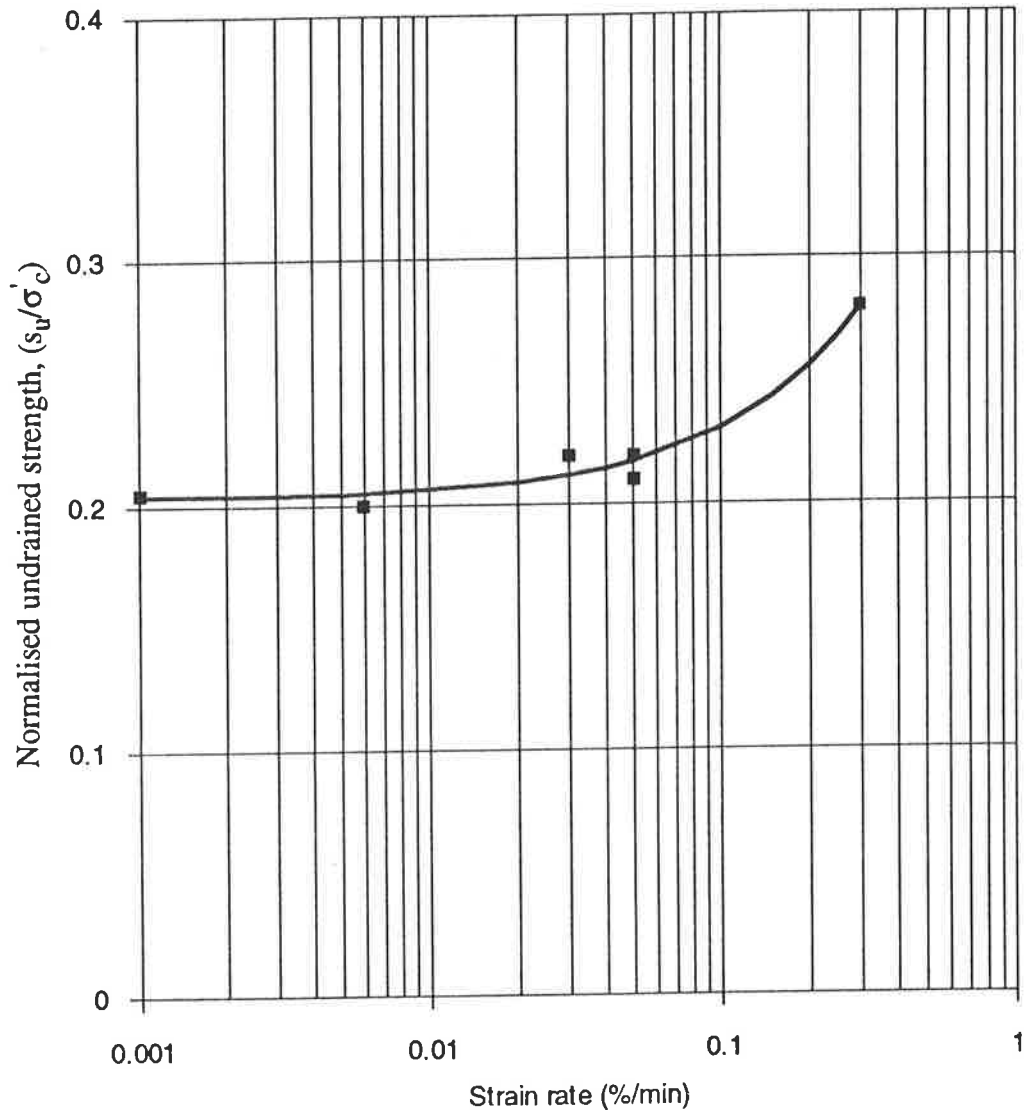


Figure 4.6 Relationship between the normalised undrained shear strength and strain rate.

Chapter 5

Triaxial test results and analyses

5.1 Introduction

This chapter examines and analyses the results obtained from the CIUTC of remoulded Keswick Clay. The undrained triaxial compression tests consist of a series of tests that were carried out on normally consolidated and overconsolidated clay. In analysing the results, the undrained shear strength, s_u , specific volume at residual strength, $(1+e_f)$, effective strength parameters, (c', ϕ') , undrained Young's modulus, E_u , and pore pressure parameter at failure, A_f , are examined. The normalised behaviour is validated from the test results obtained from the normally consolidated clay samples. From the analysed results the normalised undrained shear strength, normalised undrained Young's modulus, and pore pressure parameters at failure are correlated with overconsolidation ratio, which is the basis of the SHANSEP design procedure described in Chapter 3.

In the following sections the undrained triaxial compression test results are summarised. The results are analysed in detail, to determine the undrained shear strength, s_u , undrained Young's modulus of elasticity, E_u , effective strength parameters, (c', ϕ') , and also to check the validity of normalised behaviour. As the clay exhibited normalised behaviour, the undrained shear strength, s_u , and undrained Young's modulus of elasticity, E_u , are normalised with respect to the effective consolidation pressure, σ'_c , and correlated against overconsolidation ratio. Finally, the normalised soil parameters with OCR obtained from the remoulded Keswick Clay are then compared with those results that were reported by various investigators.

5.2 Consolidated undrained triaxial test results

Results of isotropically consolidated undrained triaxial tests (CIUTC) performed on normally consolidated and overconsolidated remoulded Keswick Clay are presented in this section. A summary of the pre-shear conditions of test samples and the final water content is given in Table 5.1. The axial load, axial displacement and excess pore water pressure were recorded during shearing of each sample. Shearing of the samples continued up to axial strain ranging between 10% and 14%, where there were strong indications (such as constant load with increasing axial strain) that residual conditions had been reached. These data from each test are presented in the form of stress-strain and excess pore water pressure-strain diagrams. In establishing the relationships between stress-strain and excess pore pressure-strain response the following procedures were adopted.

- (1) The axial strain was calculated from the following equation:

$$\varepsilon = \frac{\Delta l}{L} 100 \% \quad (5.1)$$

where

ϵ = axial strain expressed as percentage,

Δl = change in length and

L = original length of the sample.

- (2) The corrected areas of the samples during undrained shearing were calculated using the following equation given by Bishop and Henkel (1962).

$$A = \frac{A_0}{1 - \epsilon} \quad (5.2)$$

where

A = modified area,

A_0 = initial area and

ϵ = axial strain.

From the corrected modified area axial stresses were determined and plotted against axial strains. In some cases the results have been corrected due to the seating error.

- (3) The induced pore pressures that were developed during shearing of the samples were recorded and plotted against axial strains.

The stress-strain and excess pore water pressure-strain characteristics of remoulded Keswick Clay are discussed below.

5.2.1 Deviator stress and excess pore water pressure versus axial strain

The general trends of the variation of deviator stress, $(\sigma_1 - \sigma_3)$, and pore water pressure with axial strain are summarised below:

- (a) The deviator stress, $(\sigma_1 - \sigma_3)$, versus axial strain for normally consolidated clay samples are presented in Figure 5.1(a). It can be seen from this figure that the deviator stress, $(\sigma_1 - \sigma_3)$, for each test sample increases rapidly to a peak value, and then decreases until the residual strength was reached. The peak deviator stresses increases with effective consolidation pressure for normally consolidated clay samples. Figure 5.1(a) also indicates that the failure strain increases with effective consolidation pressure, except for 300 kPa. This is attributed to the heterogeneity of the sample.
- (b) The excess pore water pressure versus axial strain curves for normally consolidated samples are shown in Figure 5.1(b). It can be seen that the excess pore water pressure also increases sharply with the increase in the axial strain up to a strain corresponding to the peak deviator stress. Thereafter, only slight increases occur up to the residual strengths. Figure 5.1 indicates positive correlation between the excess pore water pressure and the effective consolidation pressure.
- (c) The stress-strain response of overconsolidated clay samples is shown in Figure 5.2(a). The deviator stress, $(\sigma_1 - \sigma_3)$, increases with increasing axial strain, followed by a substantial strength loss with further shearing, i.e., significant strain softening occurs. From the same figure one may observe an inverse relationship between the peak deviator stress and

overconsolidation ratio (OCR). Failure strains did not vary significantly as the overconsolidation ratio increases. The axial strain at peak deviator stress was in the range of 2% to 3%.

- (d) For overconsolidated clay samples, the general trends of the curves indicate that the excess pore pressure increases with an increase in the axial strain although significant discrepancy was observed for one of the OCR = 2 tests. The excess pore water pressure at peak deviator stress, $(\sigma_1 - \sigma_3)_{\max}$, decreases with increasing OCR.

A summary of axial loading data which includes deviator stress, $(\sigma_1 - \sigma_3)$, excess pore water pressure, Δu , Skempton's pore pressure parameter, A , and axial strain, ϵ , with OCR obtained from the stress-strain and excess pore water pressure-strain curves are presented in Table 5.2. These data were calculated at peak deviator stress, $(\sigma_1 - \sigma_3)_{\max}$, and at the residual strength. In Table 5.2 the pore pressure parameters were determined from the ratio of change in pore pressure and the increase in deviator stress. The results presented in Table 5.2, together with the stress-strain and excess pore pressure-strain diagrams, are used for further analysis, which is treated below.

5.3 Analysis of test results

In this section the test results that were summarised in Section 5.2.1 are analysed to establish the relationships between the normalised soil parameters, $(s_u/\sigma'_c, E_u/\sigma'_c, E_u/s_u)$, and OCR. Using the stress-strain and excess pore water pressure-strain curves, the undrained shear strength, s_u , undrained Young's modulus, E_u , and effective strength

parameters, (c', ϕ') , were determined. In evaluating the soil properties and establishing the normalised soil parameters the following procedures were used.

- (1) The undrained Young's modulus is calculated from an initial tangent, at 25% and 50% stress levels, from the stress-strain diagram of each test.
- (2) In order to determine the effective strength parameters, (c', ϕ') , the successive states of stress of the test samples are represented by a Cambridge p' - q diagram where the shear stress, $q = (\sigma_1 - \sigma_3)$ is plotted against the effective mean normal stress, $p' = \left(\frac{\sigma_1 + 2\sigma_3}{3} \right)$.
- (3) The undrained shear strength, s_u , undrained initial modulus, E_{ui} , undrained modulus at 25% stress level, E_{u25} , and 50% stress level, E_{u50} , for each test are normalised with respect to the effective consolidation pressure σ'_c . The undrained Young's modulus, E_u , is also normalised with respect to the undrained shear strength, s_u .

Detailed analysis of the test results are presented below.

5.3.1 Undrained shear strength

The undrained shear strength, s_u , can be readily determined from the peak deviator stress which is related to the following equation:

$$s_u = \frac{(\sigma_1 - \sigma_3)_{\max}}{2} \quad (5.3)$$

where

$$(\sigma_1 - \sigma_3)_{\max} = \text{peak deviator stress.}$$

A detailed summary of the undrained shear strengths for different overconsolidation ratios together with the effective consolidation pressures, σ'_c , are presented in Table 5.3. The results show that for OCR = 1, the undrained shear strength, s_u , increases significantly as the effective consolidation pressure increases. The undrained shear strength increases from $s_u = 21$ kPa for $\sigma'_c = 100$ kPa, to $s_u = 76$ kPa for $\sigma'_c = 400$ kPa. It should be noted, however, that the ratio (s_u/σ'_c) , is relatively constant. For same effective consolidation pressure, σ'_c , overconsolidated samples show higher (s_u/σ'_c) which varies between 0.33 and 0.76 as the overconsolidation ratio (OCR) varies between 1 and 13.

The undrained residual shear strength, s_{ur} , can be determined from the following equation:

$$s_{ur} = c'_r + \sigma'_r \tan \phi'_r \quad (5.4)$$

where

c'_r = residual effective cohesion,

σ'_r = residual mean effective normal stress and

ϕ'_r = residual effective shearing angle.

In order to obtain the undrained residual shear strength parameters (c'_r, ϕ'_r) , the residual mean normal stress, p'_r , is plotted against the residual shear stress, q_r , in Figure 5.3. It can be seen that there exists a relationship between the data points of the residual state for normally consolidated clay which can be represented by a straight line. But for overconsolidated clay most of the data points fall above the line evaluated for the normally consolidated clay. It is possible that these data points would have reached the residual state line if the tests were continued to a larger strain. From the straight line, the

undrained residual shear strength of normally consolidated clay was determined. The ratio $(s_{ur}/\sigma'_c) = 0.14$, was found to be constant for the normally consolidated clay.

- **Undrained shear strength versus effective consolidation pressures**

In Figure 5.4 the undrained shear strength is plotted against the effective consolidation pressure. As can be seen from this figure, the undrained shear strength obtained from normally consolidated clay samples form a straight line passing through the origin. It can therefore be concluded that, for remoulded Keswick Clay in a normally consolidated state, there exists a linear relationship between the undrained shear strength, s_u , and the effective consolidation pressure, σ'_c . On the other hand, the results from overconsolidated clay samples show a non-linear relationship. Figure 5.4 clearly indicates that the undrained shear strength, s_u , of an overconsolidated clay sample is higher than that of a normally consolidated clay sample with the same effective consolidation pressure.

5.3.2 Undrained stress-strain modulus

The undrained Young's modulus of elasticity can be determined by assuming that the soil mass is an isotropic linear elastic material, having a unique Young's modulus. From the stress-strain diagrams, the undrained Young's modulus, $E_{u(j)}$, at stress level j , was evaluated using the following equation:

$$E_{u(j)} = \frac{(\sigma_1 - \sigma_3)_j}{\epsilon_u(j)} \quad (5.5)$$

where

$(\sigma_1 - \sigma_3)_j$ = deviator stress at stress level j , and

$\epsilon_u(j)$ = axial strain corresponding to the stress level.

(a) Initial undrained modulus, E_{ui}

Using Equation 5.5, the initial tangent modulus, E_{ui} , was determined from the initial slope of the stress-strain curves. The results of these calculations are presented in Table 5.4. For normally consolidated clay samples, E_{ui} , increases sharply as the effective consolidation pressure increases from 100 kPa to 400 kPa. Except for effective consolidation pressure, $\sigma'_c = 100$ kPa, the ratio of (E_{ui}/σ'_c) , from three tests indicate that for normally consolidated clay it remains constant. For overconsolidated clay samples, the initial tangent modulus, E_{ui} , is basically constant except for OCR = 8, and 13. On the other hand, the normalised initial tangent modulus, (E_{ui}/σ'_c) , increases as the overconsolidation ratio increases from 2 to 10 except for OCR = 13, which decreases.

(b) Undrained modulus at 25% stress level, E_{u25}

The undrained Young's modulus at 25% stress level, E_{u25} , has been calculated from the slope of the line that passes through the origin and 25% of peak deviator stress of the stress-strain curves. For overconsolidated clay the ratio, (E_{u25}/σ'_c) , increases for OCR 2 and 10 except for OCR = 4, 8, and 13, where it remains almost constant.

(c) Undrained modulus at 50% stress level, E_{u50}

The value of undrained Young's modulus corresponding to 50% of peak deviator stress, E_{u50} , has been computed as the secant modulus. The undrained modulus for normally consolidated clay samples increases substantially as the effective consolidation pressure increases from 100 kPa to 400 kPa. The undrained moduli for overconsolidated clay samples are decreased from 19.2 MPa to 3.1 MPa as the overconsolidation ratios vary between 2 and 13. The results indicate that the undrained modulus, E_{u50} , decreases with

increasing overconsolidation ratio. The ratio of (E_{u50}/σ'_c) , show that it increases slightly as the overconsolidation increases from 2 to 10.

A summary of the undrained Young's modulus, E_u , at different stress levels, undrained Young's modulus ratio, (E_u/σ'_c) , together with OCR are presented in Table 5.4. It would appear from the results presented in this table that the undrained moduli are dependent on the stress level, effective consolidation pressure and stress history. For normally consolidated clay samples, the modulus increases with increasing effective consolidation pressure but the ratio (E_u/σ'_c) remains constant. For OCR = 2, and 10, the ratio (E_u/σ'_c) increases but for OCR = 4, 8 and 13 the ratio (E_u/σ'_c) remains almost constant but increases with stress level.

5.3.3 Effective stress paths during undrained loading

The relationship between the effective mean normal stress, p' , and shear stress, q , from the series of samples consolidated to effective consolidation pressures of 100 kPa, 200 kPa, 300 kPa and 400 kPa, at normally consolidated states of the clay are shown in Figure 5.5. This figure shows that for each test, the mean normal effective stress, p' , increases and then decreases, as the magnitude of excess pore pressure increases. The shear stress, q , for each test increases until failure and then decreases to a value equal to residual strength. The best fit straight line drawn through the peak shear stress of the stress paths, passes through the origin. It indicates that the effective cohesion, c' , for normally consolidated clay is essentially zero. This line is also denoted as the critical state line. The effective friction angle at failure, ϕ' , can be determined from the slope of the critical state line, M , which is related to the following equation:

$$\phi' = \sin^{-1}\left(\frac{3M}{6+M}\right) \quad (5.6)$$



Figure 5.5 shows that the slope of the critical state line $M = 0.46$ corresponds to effective friction angle at failure, $\phi' = 12^\circ$, for normally consolidated clay. Figure 5.5 also shows that there is a relationship between the effective mean normal stress, p' , and shear stress, q , at the residual state. The best fit straight line drawn through the residual points also passes through the origin indicating that the effective residual shear strength parameter, c'_r , is zero. The slope of the straight line passing through the residual points, $M = 0.32$, corresponds to residual friction angle, $\phi'_r = 9^\circ$.

Figure 5.6 highlights the stress paths of the overconsolidated clay samples. The effective stress paths for $OCR = 2$, $\sigma'_c = 200$ kPa, indicate that the mean normal stress, p' , increases throughout the test but the others show that the effective mean normal stress, p' , decreases because the pore water pressure increases. It is very difficult to establish a linear relationship between the effective mean normal stress and shear stress at peak deviator stress and residual state of the stress paths. It would appear from Figure 5.6 that there exists a non-linear relationships between the two at residual state, which indicates that effective residual cohesion, c'_r , is zero as the line pass through the origin.

- **Relationship between effective normal stress, shear stress and specific volume**

The relationships between the specific volume at residual state, $(1+e_f)$, peak shear stress, q_f , and peak effective normal stress, p'_f , for normally consolidated and overconsolidated clay are shown in Figures 5.7 and 5.8. It can be seen from Figure 5.7 that for normally consolidated clay, there exists linear relationships between p'_f and $(1+e_f)$, and q_f and $(1+e_f)$ which are almost parallel to each other. It would appear from Figure 5.7 that both peak effective mean normal stress, p'_f , and peak shear stress, q_f , increases as the specific volume decreases. It should be noted that the increasing trends are the same for both parameters with decreasing specific volume.

From the best fit lines between p'_f and $(1+e_f)$, and q_f and $(1+e_f)$, Figure 5.8 reveals the existence of relationships between p'_f , q_f , and $(1+e_f)$ for overconsolidated state of the clay. It can be seen from Figure 5.8 that, for overconsolidated clay, the increasing trend of peak effective mean normal stress with decreasing specific volume is higher than that of peak shear stress, q_f , and specific volume, $(1+e_f)$.

Figure 5.9 shows the relationships between the specific volume in the residual state, $(1+e_f)$, and the normalised effective peak normal stress and peak shear stress for both normally consolidated and overconsolidated clay samples. In this case, the parameters, are normalised with respect to the effective equivalent pressure, p'_e . From the line of best fit in Figure 5.9 indicates that there exists a linear relationship between the specific volume in the residual state and the normalised shear stress and the mean normal effective stress. It should be noted that the normalised parameters, $\left(\frac{q_f}{p'_e}\right)$, and $\left(\frac{p'_f}{p'_e}\right)$, increase with increasing the specific volume however the trend is higher for the latter than the former.

A detailed summary of the specific volume in the residual state, $(1+e_f)$, peak shear stress, q_f , peak mean normal effective stress, p'_f , (p'_f/p'_e) , and (q_f/p'_e) with OCR is presented in Table 5.5. Figures 5.7 to 5.9, suggest that the three quantities p'_f , q_f , and $(1+e_f)$ are closely interrelated which implies that changes in either p'_f or $(1+e_f)$ will affect the shear strength and each other.

5.3.4 Validity of normalised behaviour

A soil that exhibits normalised behaviour with the same overconsolidation ratio but different effective consolidation pressures will produce identical stress-strain curve when individual stress-strain curves are normalised with respect to the effective consolidation

pressure. From Figure 5.1, the stress-strain curves were replotted using $\left(\frac{\sigma_1 - \sigma_3}{\sigma_c} \right)$ against axial strain. The normalised data points are shown in Figure 5.10. Some discrepancy in the normalised plot can be attributed to the sample heterogeneity and slight fluctuation of the effective consolidation pressures that occur in the apparatus but the overall data indicates that normalised behaviour is valid.

5.3.5 Normalised soil parameters with different OCR

(a) Normalised undrained shear strength

The undrained shear strength, s_u , obtained from the undrained triaxial tests for normally consolidated and overconsolidated clay samples are summarised in Table 5.3. These results were normalised with respect to the effective consolidation pressures and plotted against the overconsolidation ratios as shown in Figure 5.11. It can be seen from Figure 5.11, that the normalised undrained shear strength increases significantly with increasing overconsolidation ratio, although this trend is not valid for overconsolidation ratios 10 and 13. For OCR = 10 and 13, the normalised undrained shear strength was found lower than OCR = 8. This was attributed to the fluctuation of the effective consolidation pressure of the apparatus. It should be noted that at higher OCR, a small variation of effective consolidation pressure substantially affects the OCR.

(b) Normalised undrained Young's modulus

The results of undrained Young's modulus at three incremental stress levels (Section 5.3.2) are presented in Table 5.4. These values have been normalised with respect to the effective consolidation pressure, σ'_c , and plotted against different overconsolidation ratios

which are shown in Figure 5.12. This figure and Table 5.4 indicate that the normalised undrained initial Young's modulus, (E_{ui}/σ'_c) , remains almost constant for $OCR = 1$ and increases substantially as the overconsolidation ratio increases from 1 to 2. The slightly increasing trend continues to $OCR = 8$. The normalised undrained Young's modulus, (E_{u25}/σ'_c) , and (E_{u50}/σ'_c) , also exhibit constant values for normally consolidated clay. The moduli for both cases show an increasing trend with OCR, similar to that for the initial modulus. It should be noted that although the moduli were calculated at different stress levels, the results only vary slightly. Figure 5.12 indicates some scatter in the normalised undrained modulus data for the same overconsolidation ratio. This could be due to the heterogeneity of the samples which affect the stress-strain characteristics for same OCR.

The undrained moduli at different stress levels are normalised with respect to the undrained shear strength, s_u , of the soil and summarised in Table 5.6. These values are plotted against overconsolidation ratio in Figure 5.13. The normalised undrained moduli at different stress levels, decrease steadily as the overconsolidation ratio increases. It can be seen from Figure 5.13 that the normalised undrained Young's modulus, (E_u/s_u) , does not vary substantially although the stress levels are different.

(c) Pore pressure parameter at failure

The pore pressure parameter, A , at peak deviator stress, $(\sigma_1 - \sigma_3)_{max}$, and in the residual state for normally consolidated and overconsolidated clay samples are presented in Table 5.2. As can be seen from Table 5.2, the pore pressure parameters at failure i.e. $(\sigma_1 - \sigma_3)_{max}$, for normally consolidated clay samples, were highly inconsistent with large variations, whereas in the residual state, they vary between 0.65 and 1.0. The inconsistency of these parameters is likely to be due to homogeneity of the samples. The

parameters at failure and in the residual state are plotted against OCR in Figure 5.14. Besides the scatter of parameters at failure, A_f , the best fit curve drawn through the data points exhibits that parameters at failure, A_f , slightly decreases with OCR. On the other hand, the best fit curve drawn through parameters in the residual state, decreases substantially with OCR.

(d) Normalised p' and q diagram

The effective stress paths for normally consolidated and overconsolidated clay samples have been shown in Figure 5.5 and Figure 5.6. The effective mean normal stress, p' , and shear stress, q , from all the tests are normalised with respect to the effective equivalent pressure, p'_e , where p'_e is the mean normal stress on the normal consolidation line corresponding to the specific volume of interest. The normalised mean normal stress, p'/p'_e , is plotted against normalised shear stress, q/p'_e , and is shown in Figure 5.15. This figure shows that the normalised effective stress paths for normally consolidated clay samples almost coincide along a single failure envelope, indicating normalised behaviour of Keswick Clay. In addition, this curve also forms the Roscoe surface (Atkinson and Bransby, 1978). As the overconsolidation ratio increases, the normalised stress paths also move away from the peak points but fall in a straight surface, which is known as Hvorslev surface (Atkinson and Bransby, 1978).

5.4 Comparison of test results with available literature

In order to compare the results, emphasis is given to normalised undrained shear strengths, normalised deformation properties and pore pressure parameters with OCR. These are as follows.

5.4.1 Normalised undrained shear strength with OCR

The normalised undrained shear strength, (s_u/σ'_c) , for Keswick Clay has been compared with the results of those clays that were investigated by Ladd and Edgers (1972) and the generalised expression developed from the critical state soil mechanics concept. In order to compare the results the relationship of expressing the normalised undrained shear strength of overconsolidated clay, established by Ladd et al (1977), was chosen. This relationship was described in Equation 3.2 in Chapter 3. It should be noted that the equation was developed empirically from the results of (s_u/σ'_{vo}) , with OCR which were carried out on different soils by Ladd and Edgers (1972). Using Equation 3.2, the theoretical variation of the normalised undrained shear strength ratio of overconsolidated clay and normally consolidated clay, $\left(\frac{s_u}{\sigma'_c}\right)_{o.c} / \left(\frac{s_u}{\sigma'_c}\right)_{n.c}$, with OCR was determined for remoulded Keswick Clay.

These data points are plotted in Figure 5.16 against different overconsolidation ratios, together with the experimental shear strength ratios obtained from the undrained triaxial tests. Figure 5.16 indicates that the undrained shear strength ratios based on $m = 0.80$ form a smooth concave upward curve which varies between 1 and 7.80. On the other hand, the experimental undrained shear strength ratios vary between 1 and 3.70 and fall in a narrow band which is further represented by two curves based on $m = 0.72$, and 0.48.

Clearly, Figure 5.16 shows that the increasing trend for theoretical and experimental shear strength ratios with OCR are almost the same up to OCR = 4, but as the OCR increases beyond 4 the theoretical values increase much more than to the experimental values. Hence, from the comparison of experimental results with that of the theoretical, it can be concluded that remoulded Keswick Clay shows lower normalised undrained strength for OCR greater than 4, than those of Maine Organic, Bangkok Clay, Boston Blue Clay, Atchafalaya Clay, AGS CH Clay and Conn. Valey Varved Clay which form the basis of the theoretical expression.

It has been observed that the values of m obtained from experiments, decreases as the overconsolidation ratio increases. A value of $m = 0.60$ best fits the measurements obtained for Keswick Clay. For Keswick Clay Equation 3.2 can be written as:

$$\frac{\left(\frac{s_u}{\sigma'_c}\right)_{o.c.}}{\left(\frac{s_u}{\sigma'_c}\right)_{n.c.}} = (\text{OCR})^{0.60} \quad (5.7)$$

The normalised undrained shear strength ratio of overconsolidated clay to that of normally consolidated clay has also been obtained from the critical state soil mechanics concept. The relationship that was established by Wroth (1984), and presented in Equation 3.7, showed that the normalised undrained shear strength ratio, $\left(\frac{s_u}{\sigma'_c}\right)_{o.c.} / \left(\frac{s_u}{\sigma'_c}\right)_{n.c.}$, is dependent on the overconsolidation ratio, R , and the volumetric strain ratio, Λ . In this investigation the one dimensional normal consolidation line and swelling line drawn through the points between the void ratio, e , and effective mean normal stress, p' , from the oedometer test in Figure 4.5 gives the value $C_c = 0.62$, $C_s = 0.25$ and $\Lambda = 0.60$.

Therefore, substituting the values of $\Lambda = 0.60$ into Equation 3.6 gives the following equation:

$$\frac{\left(\frac{s_u}{\sigma'_c}\right)_{\text{o.c.}}}{\left(\frac{s_u}{\sigma'_c}\right)_{\text{n.c}}} = (\text{OCR})^{0.60} \quad (5.8)$$

From the above equation, the normalised undrained shear strength ratios can be determined. The results obtained from Equation 5.8 are plotted in Figure 5.17 against OCR in conjunction with the experimental values. Figure 5.17 shows that the theoretical curve which is based on $\Lambda = 0.60$, is matched with the experimental data. A value of $\Lambda = 0.66$ for Sydney Kaolin was found to be lower than the theoretical value of 0.80 (Mayne, 1979). This suggests that the lower value of Λ is not unreasonable.

A detailed summary of the normalised undrained shear strength ratios obtained from the experimental data, and the theoretical undrained shear strength ratios from Equation 3.2, with OCR is presented in Table 5.7. From this table it can be seen that the normalised undrained shear strength of remoulded Keswick Clay is lower than that obtained for the clays from which the theoretical relationship was established.

5.4.2 Normalised deformation parameter with OCR

The normalised undrained modulus of elasticity (E_u/σ'_c , E_u/s_u) with OCR has been summarised in Section 5.3.5. These results are compared with the results presented in Chapter 3 of different soils (namely, Maine Organic, Bangkok Clay, Boston Blue Clay, Atchafalaya Clay, AGS CH Clay and Conn. Valey Varved Clay) investigated by Ladd and Edgers (1972) and with Sydney Kaolin which was examined by Poulos (1978). As can be

seen from Figure 5.12 and Figure 3.9, that the normalised undrained modulus (E_u/σ'_c) at different stress levels to that for remoulded Keswick Clay shows similar trends to that of Sydney Kaolin, with some exceptions. Firstly, the ratio, (E_{ui}/σ'_c), for remoulded Keswick Clay was found to be lower than that of Sydney Kaolin. Secondly, the normalised undrained Young's modulus, (E_u/σ'_c), at different stress levels varied slightly for remoulded Keswick Clay while for Sydney Kaolin it varied significantly. Thirdly, the ratio, (E_u/σ'_c), for Keswick Clay increased up to OCR = 8, on the other hand, for the Sydney Kaolin, it increased up to OCR = 4.

From Figure 5.13 and Figure 3.8, the ratio of (E_u/s_u) can be compared. It would appear from these figures, that the ratio, (E_u/s_u), for remoulded Keswick Clay, was found to be lower than most of the clays that have been presented. It should be noted that the ratio, (E_u/s_u), did not vary greatly due to different stress level for the Keswick Clay but it varied substantially for the soils that were reported by Ladd and Edgers (1972).

5.4.3 Pore pressure parameter with OCR

Pore pressure parameters at failure with OCR obtained from the triaxial tests are compared with the results of Boston Blue clay reported by Wroth (1984) in Figure 3.10. It would appear from Figure 5.14 that the pore pressure parameters for remoulded Keswick Clay decreased slightly as the OCR increases while for Boston Blue Clay it decreased substantially. It should be noted that at higher OCR, Boston Blue Clay showed negative values of the pore pressure parameter at failure, A_f (Figure 3.10).

5.5 Summary

The results of undrained triaxial tests of normally consolidated and overconsolidated clay described in this chapter show that the deviator stress, $(\sigma_1 - \sigma_3)$, and the excess pore water pressure increases with increasing axial strain. The increase in excess pore water pressure decreases as the OCR increases from 1 to 13.

Analysis of the test results showed an increase in undrained shear strength, s_u , for normally consolidated clay as the effective consolidation pressure, σ'_c , increases. At constant effective consolidation pressure, but increasing OCR, the undrained shear strength rose. From the results, it was observed that the modulus of elasticity, E_u , was affected by the OCR. The ratio (E_u/σ'_c) at different stress levels was almost constant for normally consolidated clay and it increases with OCR. On the other hand, the ratio (E_u/s_u) decreases gradually with increasing OCR.

The stress paths during undrained shearing showed that there exist relationships between the mean normal stress, $\left(\frac{\sigma'_1 + 2\sigma'_3}{3}\right)$, and the shear stress, $(\sigma_1 - \sigma_3)$, at both the peak and residual strength for the normally consolidated clay. From the relationship the effective cohesion, $c' = 0$, the effective peak shearing angle, $\phi' = 12^\circ$, the effective residual cohesion, $c'_r = 0$, and the effective residual shearing angle, $\phi'_r = 9^\circ$, were found. The stress paths for overconsolidated clay showed a non-linear relationship between the effective mean normal stress and shear stress at both the peak deviator stress and residual strength. The effective cohesion, c' , and effective residual cohesion, ϕ'_r , were zero as the paths passed through the origin.

From the stress-strain diagrams of normally consolidated clay, it was concluded that the remoulded Keswick Clay exhibits normalised behaviour. A discussion of normalised soil parameters with respect to the OCR revealed that the undrained soil properties are largely dependent on the stress history of the deposit. The normalised undrained shear strength, (s_u/σ'_c) , showed significant increases with increasing OCR. A relationship was established to relate the normalised undrained shear strength and OCR. The normalised deformation properties at different stress level, slightly increases as the OCR increases from 1 to 10.

Comparisons of normalised soil parameters obtained from the analysis of remoulded Keswick Clay indicated that the normalised undrained shear strength and normalised deformation properties of remoulded Keswick Clay are lower than those found for other cohesive soils.

In the next chapter the results obtained from this study are applied to a soil deposit (with or without surcharge) to determine the variations of in situ undrained shear strength, s_u , and Young's modulus of elasticity, E_u , which are then used to determine settlement and bearing capacity of a circular footing.

Table 5.3 Undrained shear strengths and undrained shear strength ratios from CIUTC tests of remoulded Keswick Clay.

Test No	Effective consolidation pressure σ'_c (kPa)	OCR	Peak deviator stress, $(\sigma_1 - \sigma_3)_{\max}$ (kPa)	undrained shear strength $s_u = \frac{(\sigma_1 - \sigma_3)_{\max}}{2}$ (kPa)	$\frac{s_u}{\sigma'_c}$
1	100	1	42.75	21.40	0.21
2	200	1	83.90	41.95	0.21
3	300	1	120.24	60.10	0.20
4	400	1	151.20	75.60	0.19
5	200	2	135.75	67.90	0.34
6	200	2	132.35	66.20	0.33
7	100	4	100.15	50.10	0.50
8	100	4	105.80	52.95	0.53
9	50	8	75.75	37.90	0.76
10	40	10	57.15	28.60	0.72
11	30	13	42.40	21.20	0.70

Table 5.4 Undrained Young's modulus at different stress level from CIUTC tests.

Effective consolidation pressure σ'_c (kPa)	OCR	Initial modulus, E_{ui} (MPa)	$\frac{E_{ui}}{\sigma'_c}$	Modulus at 25% stress level, E_{u25} (MPa)	$\frac{E_{u25}}{\sigma'_c}$	Modulus at 50% stress level, E_{u50} (MPa)	$\frac{E_{u50}}{\sigma'_c}$
100	1	10.00	100	9.00	90	8.80	88
200	1	10.20	51	10.00	50	11.20	56
300	1	15.00	50	15.00	50	15.00	50
400	1	20.60	51	19.90	50	20.00	50
200	2	19.20	96	15.70	79	19.40	97
200	2	13.90	70	12.30	62	13.20	66
100	4	12.60	126	11.60	115	11.50	115
100	4	11.70	117	11.00	110	11.20	112
50	8	6.80	137	5.00	100	5.80	117
40	10	11.60	290	15.70	390	8.90	220
30	13	3.30	111	2.70	90	3.10	102

Table 5.5 Data of specific volume at residual state, $(1+e_f)$, peak shear stress, q_f , peak normal stress, p'_f , normalised shear stress, q_f/p'_e , and normalised effective mean normal stress, p'_f/p'_e , from CIUTC tests.

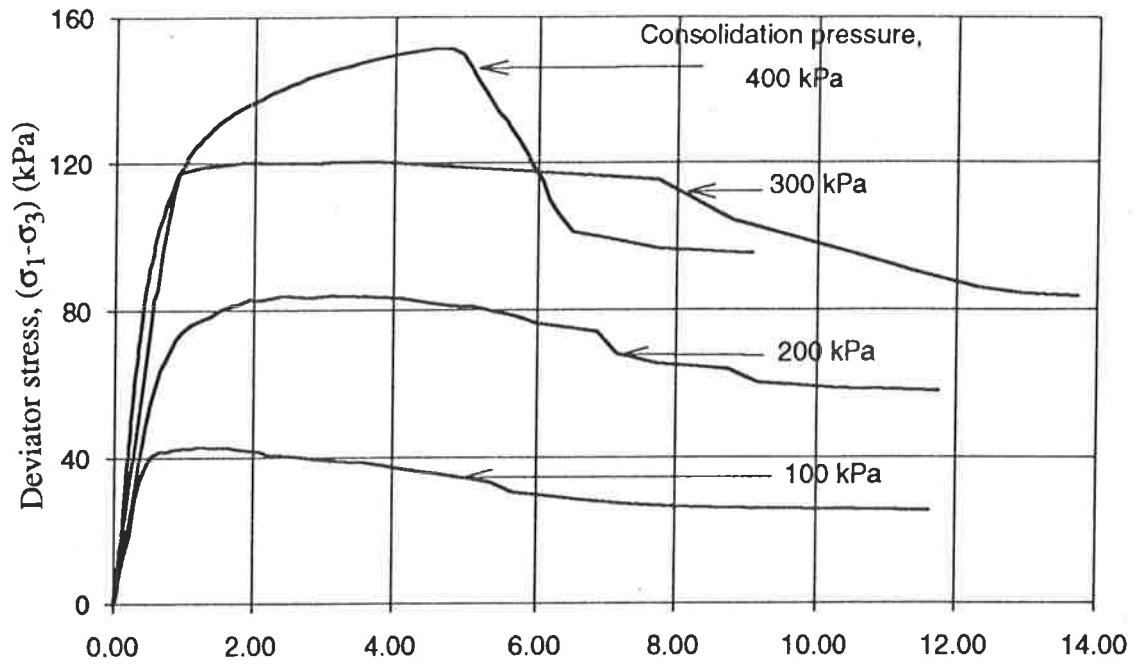
Effective consolidation pressure σ'_{vc} (kPa)	OCR	specific volume, $(1+e_f)$	Peak normal stress, p'_f (kPa)	Peak shear stress, q_f (kPa)	$\frac{p'_f}{p'_e}$	$\frac{q_f}{p'_e}$
100	1	2.50	99.50	42.75	1.00	0.40
200	1	2.30	191.50	71.20	0.96	0.35
300	1	2.15	259.7	120.20	0.90	0.40
400	1	2.10	373.50	151.20	0.95	0.40
200	2	2.20	211.70	135.75	0.65	0.40
200	2	2.15	211.70	132.35	0.70	0.45
100	4	2.20	88.70	100.15	0.30	0.30
100	4	2.25	90.25	105.80	0.30	0.30
50	8	2.30	48.35	75.75	0.20	0.30
40	10	2.35	49.75	57.15	0.23	0.26
30	13	2.45	31.30	42.40	0.20	0.25

Table 5.6 Variation of normalised undrained Young's modulus (E_u/s_u) with OCR from CIUTC tests.

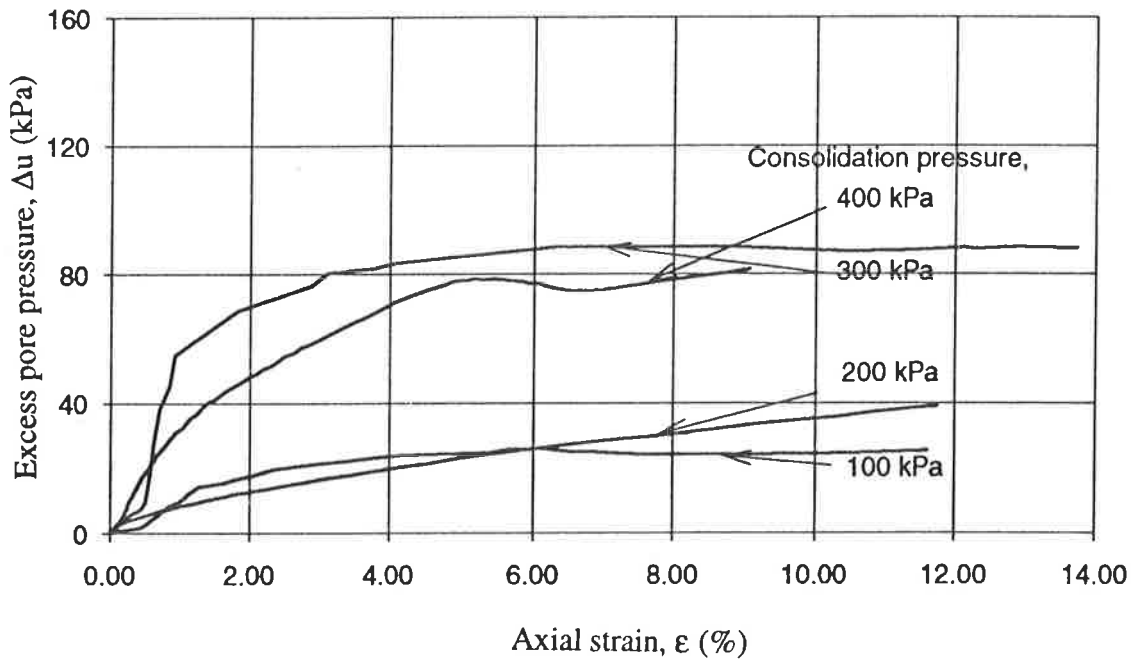
Effective consolidation pressure σ'_{vc} (kPa)	OCR	$\frac{E_{ui}}{s_u}$	$\frac{E_{u25}}{s_u}$	$\frac{E_{u50}}{s_u}$
100	1	470	420	410
200	1	245	240	265
300	1	250	250	250
400	1	270	265	265
200	2	285	230	285
200	2	210	185	200
100	4	250	230	230
100	4	220	210	210
50	8	180	135	155
40	10	400	780	310
30	13	160	125	145.

Table 5.7 Variation of experimental undrained shear strength ratio with theoretical undrained shear strength ratio.

Effective consolidation pressure σ'_c (kPa)	OCR	Experimental shear strength ratio $\frac{\left(\frac{s_u}{\sigma_c}\right)_{o.c.}}{\left(\frac{s_u}{\sigma_c}\right)_{n.c.}}$	Theoretical shear strength ratio = $\frac{\left(\frac{s_u}{\sigma_c}\right)_{o.c.}}{\left(\frac{s_u}{\sigma_c}\right)_{n.c.}} = (\text{OCR})^{0.8}$
100	1	1	1
200	1	1	1
300	1	1	1
400	1	0.90	1
200	2	1.65	1.75
200	2	1.65	1.75
100	4	2.45	3.0
100	4	2.45	3.0
50	8	3.70	5.30
40	10	3.45	6.30
30	13	3.40	7.80

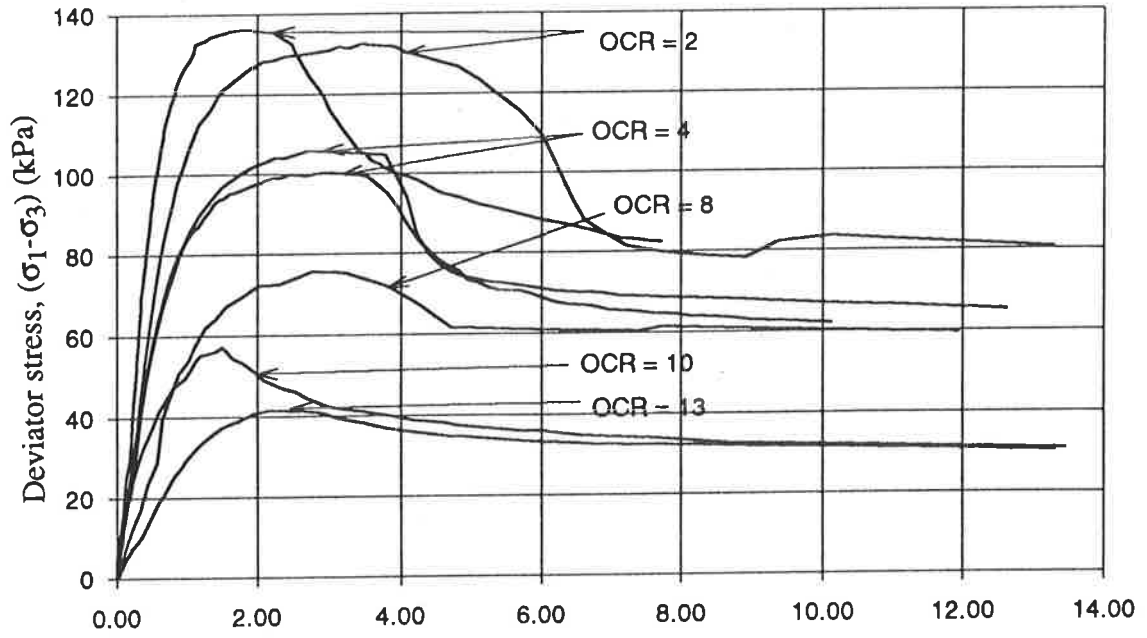


(a)



(b)

Figure 5.1 Stress-strain and excess pore water pressure-strain curves for remoulded normally consolidated Keswick Clay.



(a)

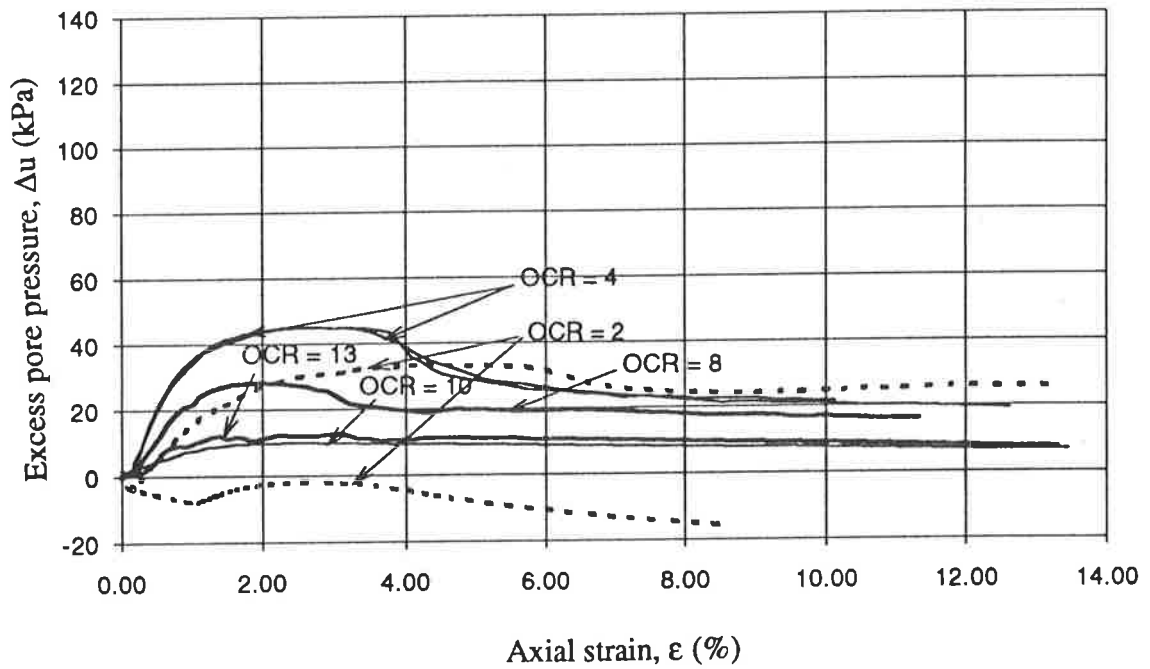


Figure 5.2 Stress-strain and excess pore pressure-strain curves for remoulded overconsolidated Keswick Clay.

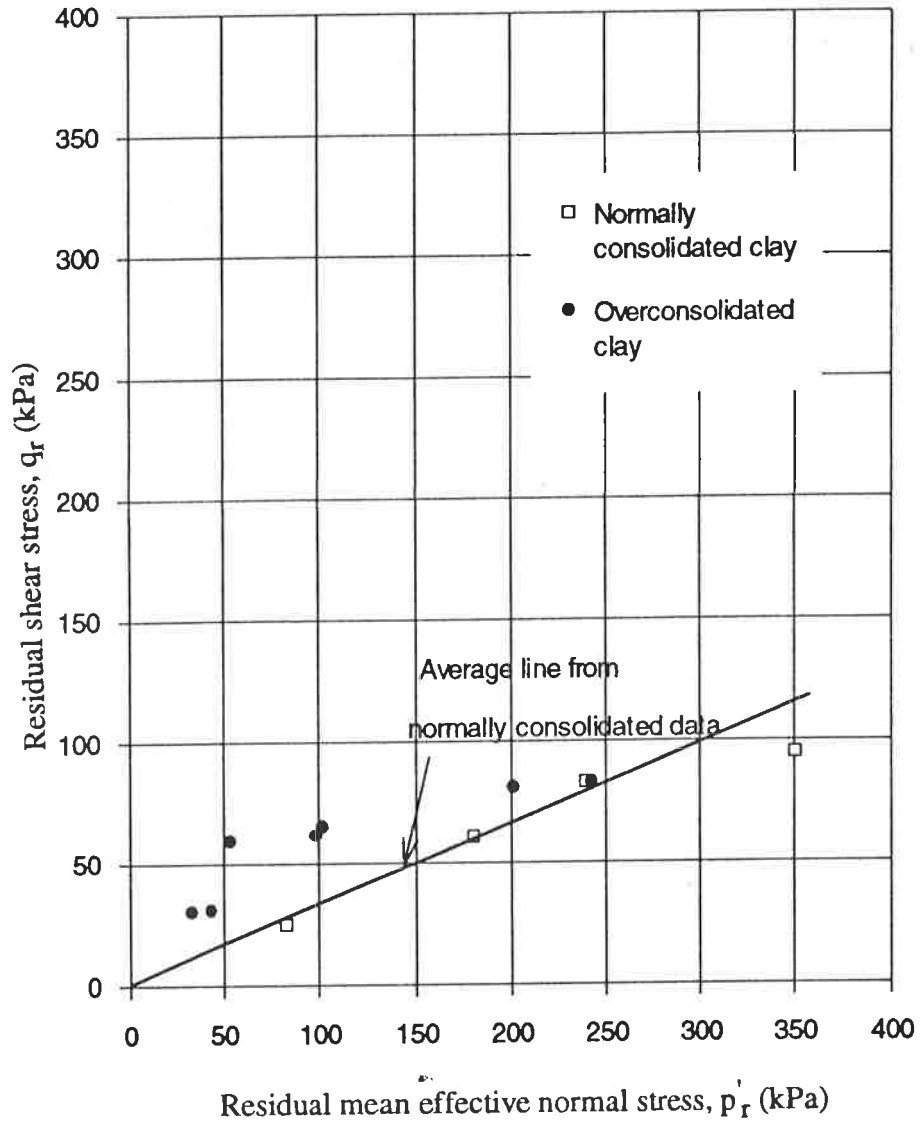


Figure 5.3 Relationship between effective residual mean normal stress and residual shear stress.

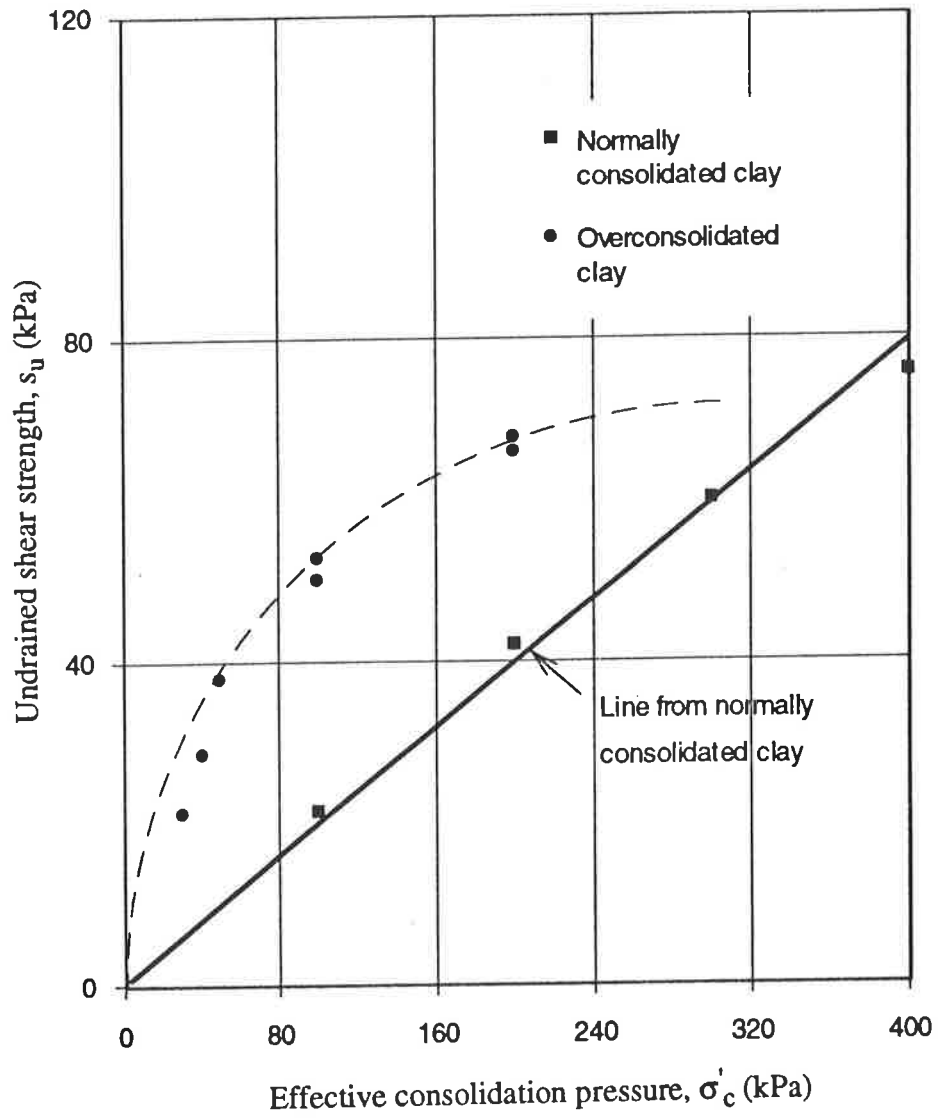


Figure 5.4 Relationship between undrained shear strength of Keswick Clay and effective consolidation pressure

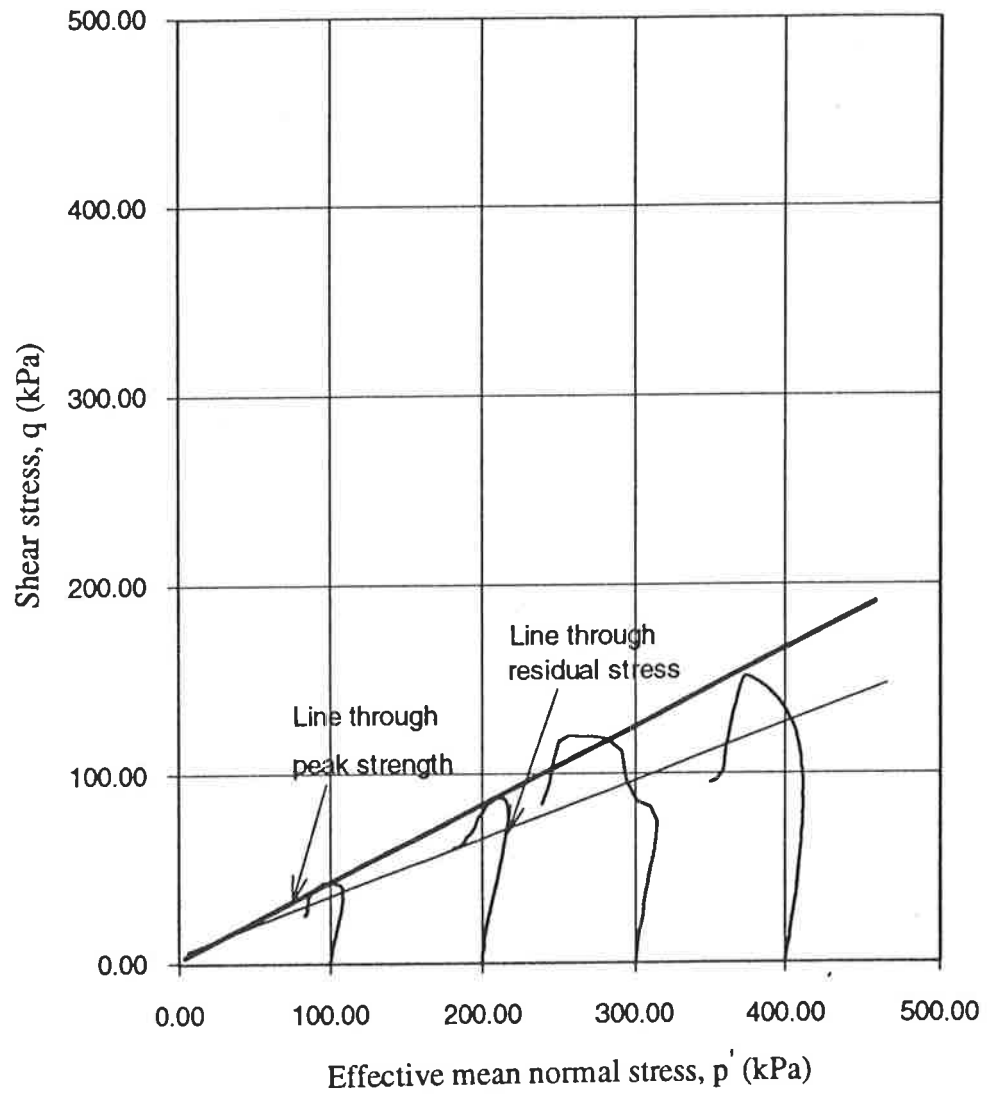


Figure 5.5 Effective stress path for normally consolidated remoulded Keswick Clay

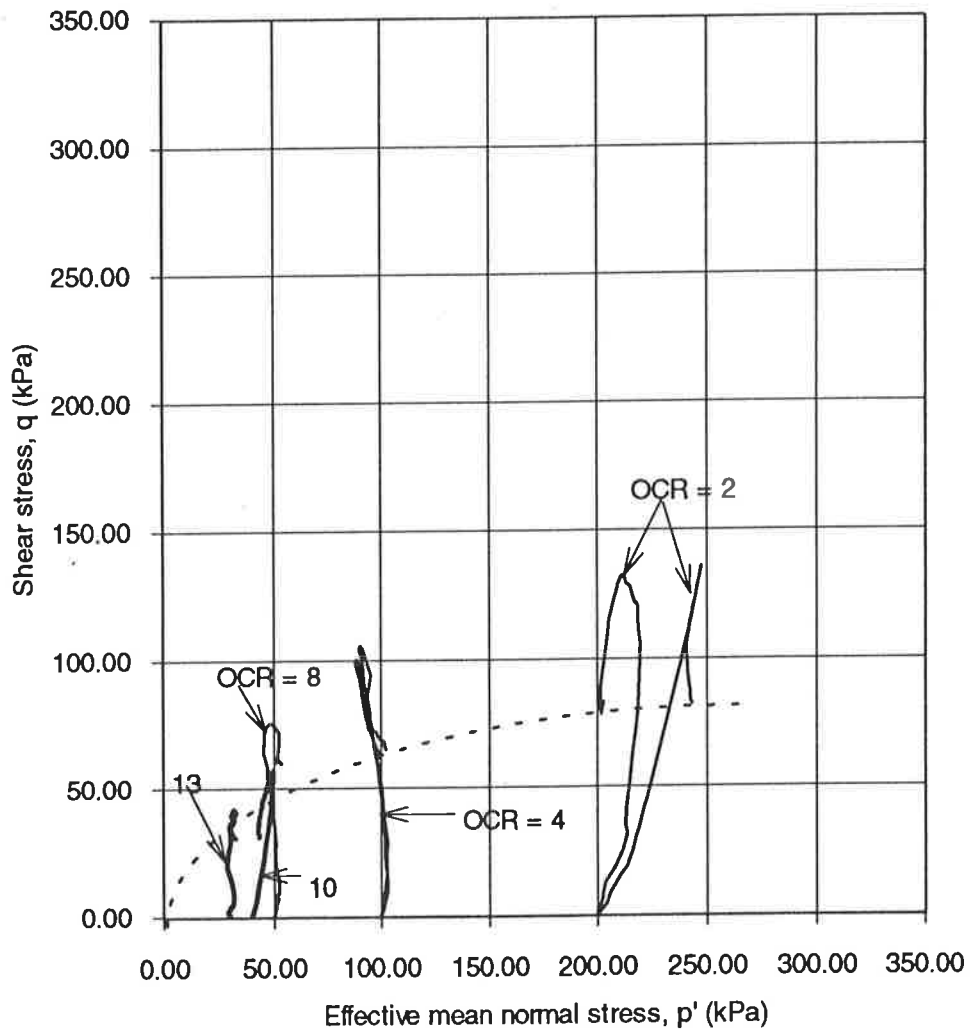


Figure 5.6 Effective stress path for overconsolidated remoulded Keswick Clay

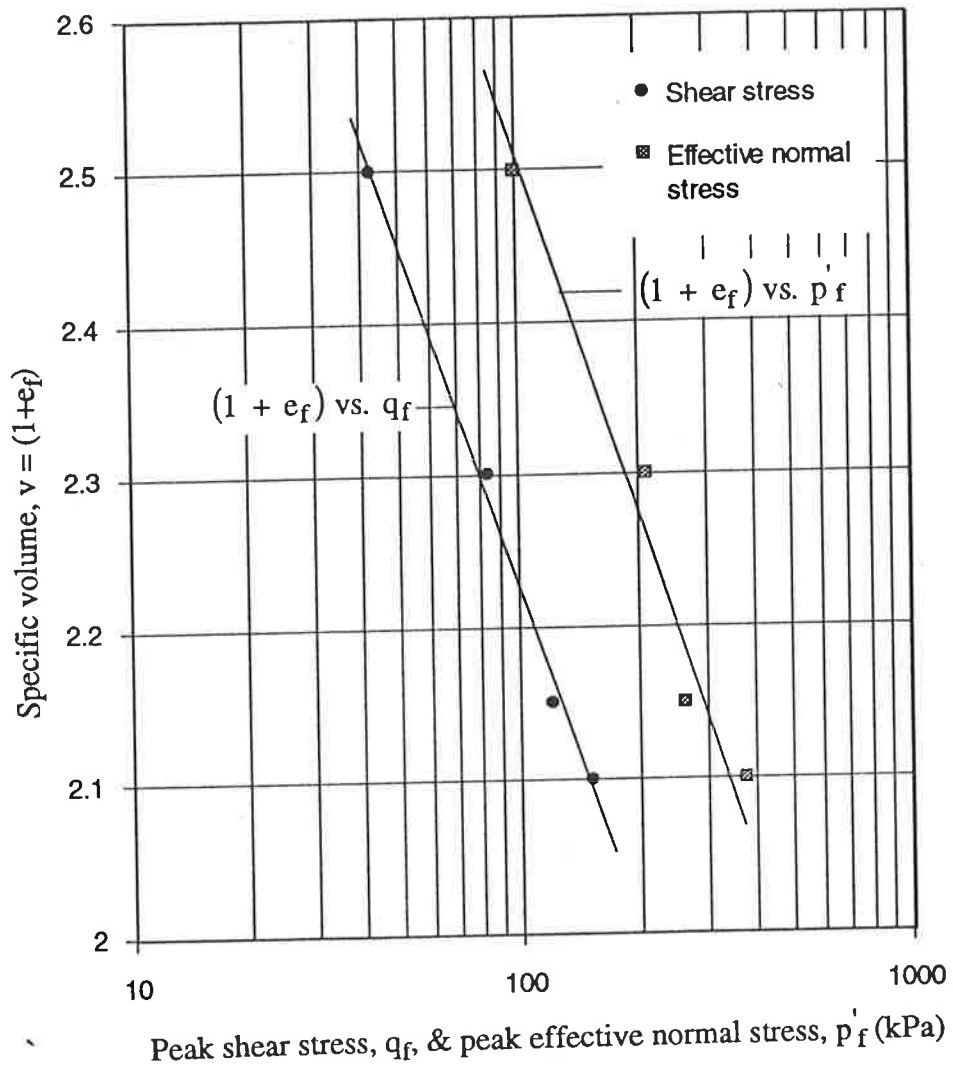


Figure 5.7 Relationships between $(1 + e_f)$, p'_f , and q_f for normally consolidated clay.

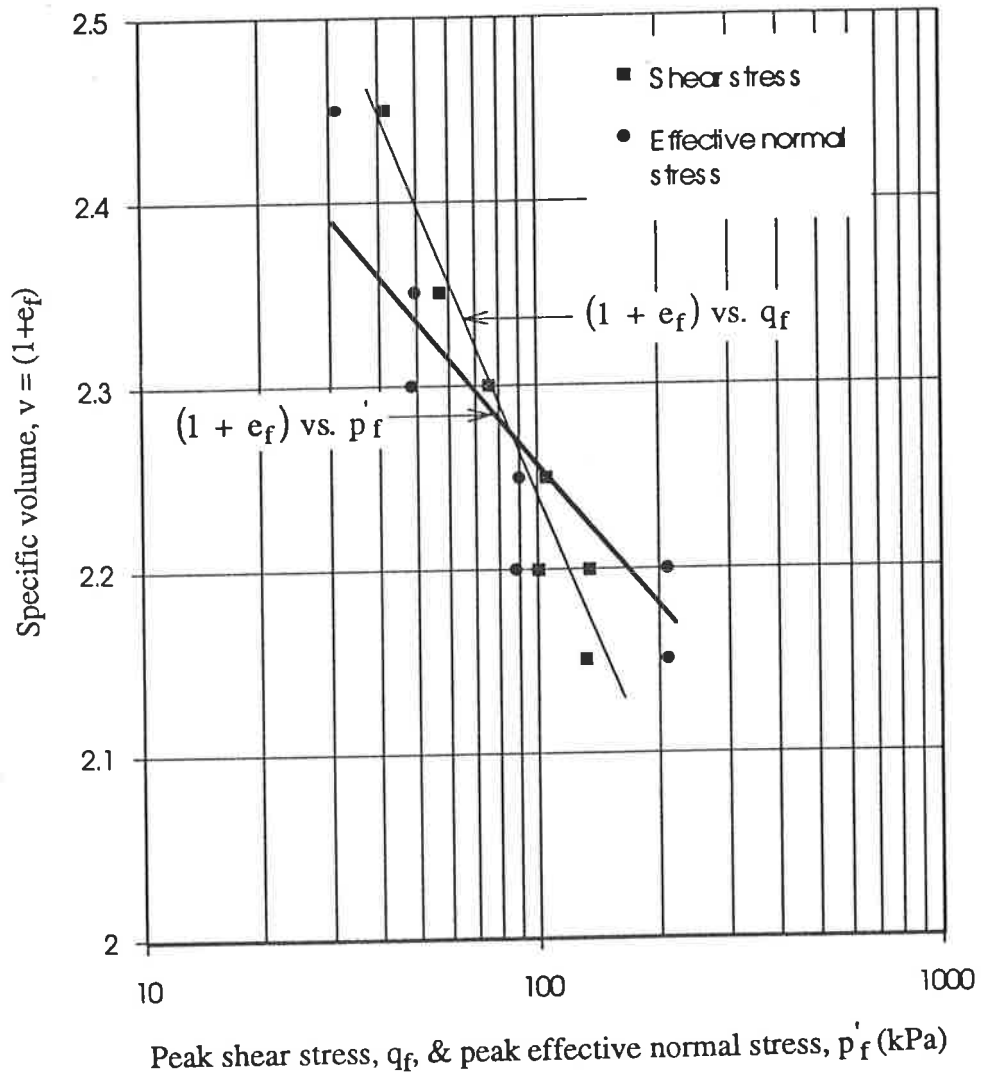


Figure 5.8 Relationships between $(1 + e_f)$, p'_f , and q_f , for overconsolidated clay.

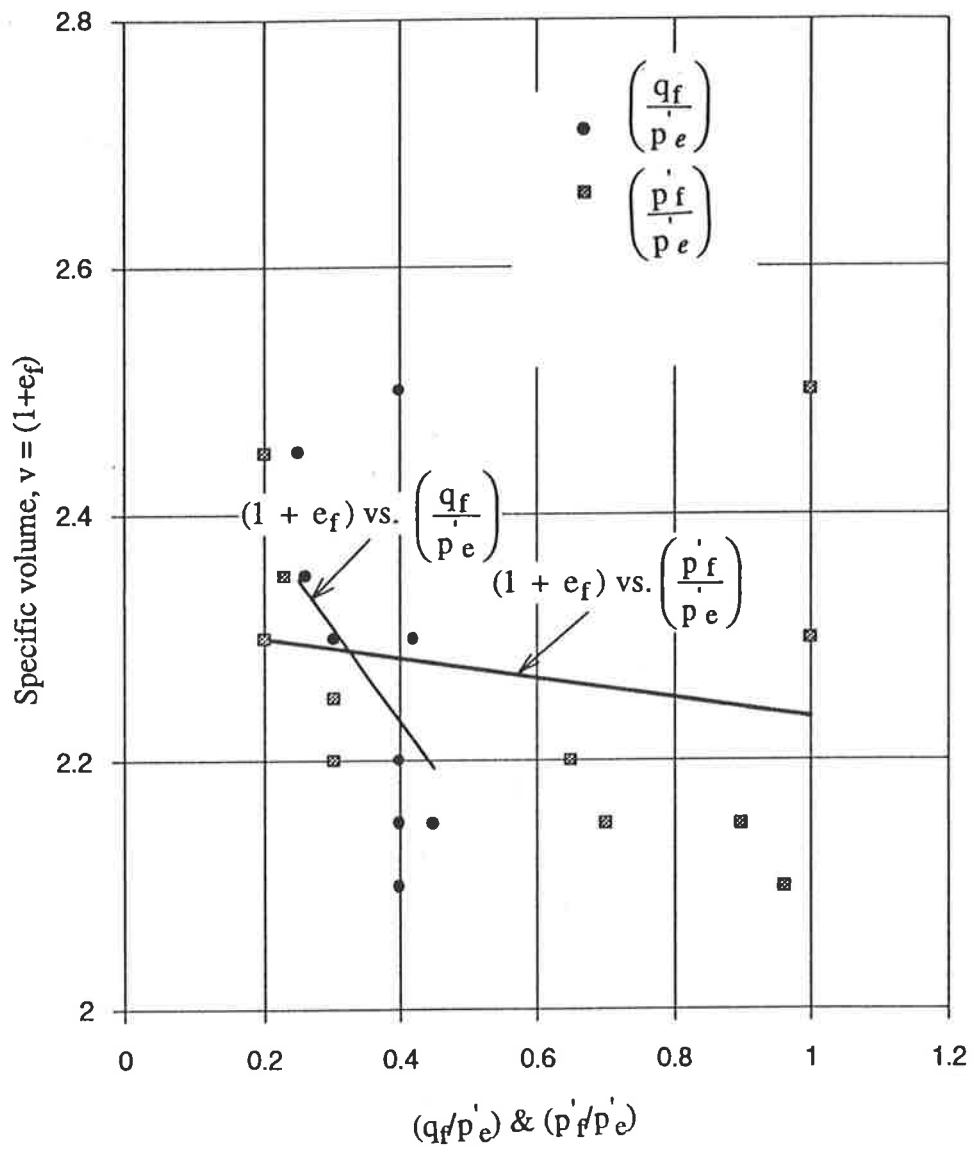


Figure 5.9 Relationships between $(1 + e_f)$, $\left(\frac{p_f}{p_e}\right)$, and $\left(\frac{q_f}{p_e}\right)$, for Keswick Clay.

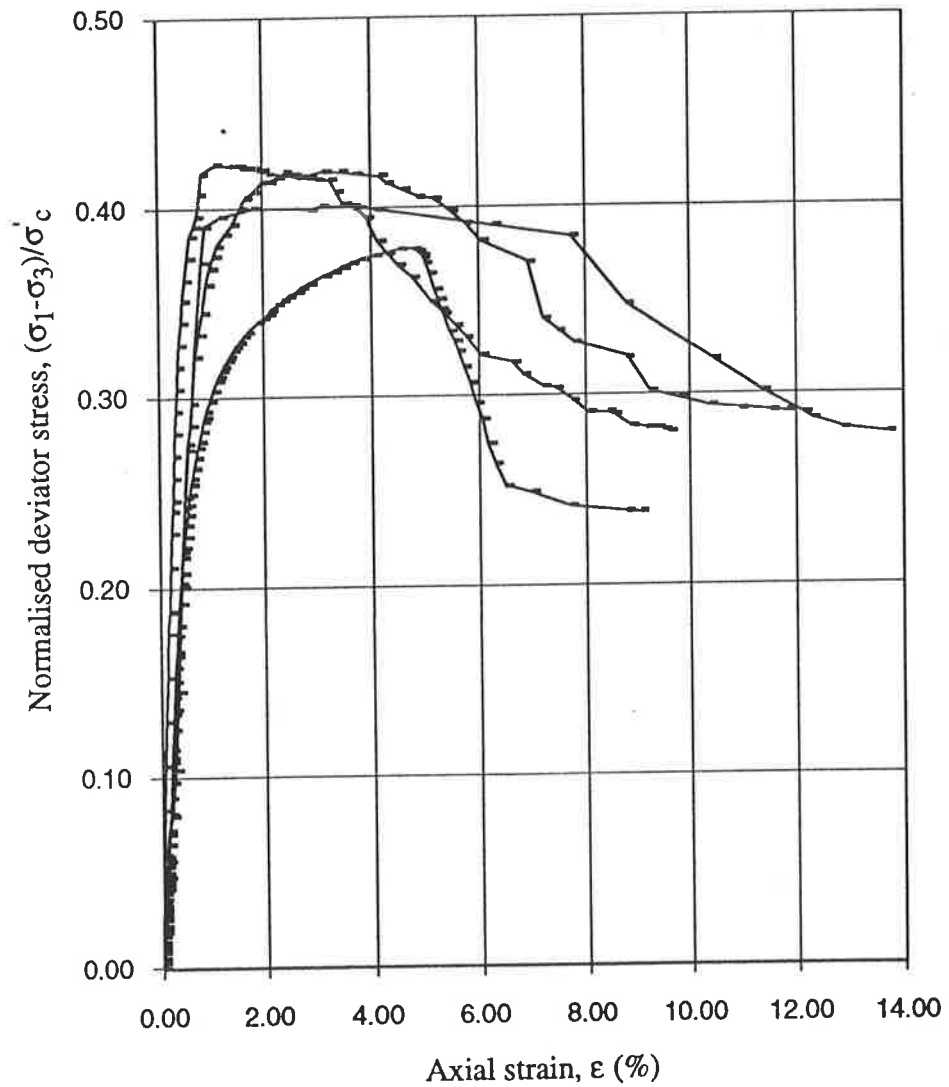


Figure 5.10 Normalised behaviour from the stress-strain data of normally consolidated remoulded Keswick Clay.

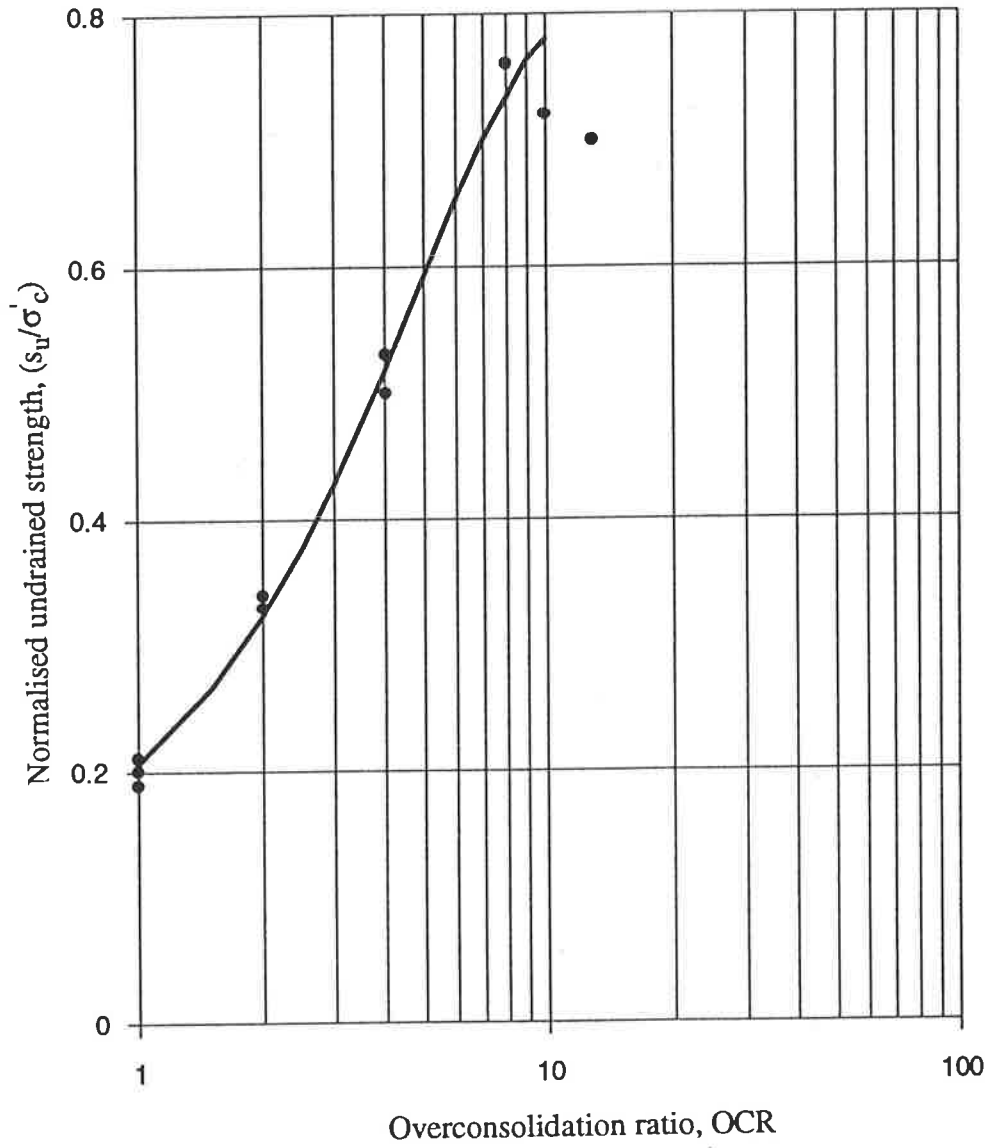


Figure 5.11 Variation of normalised undrained shear strength with overconsolidation ratio

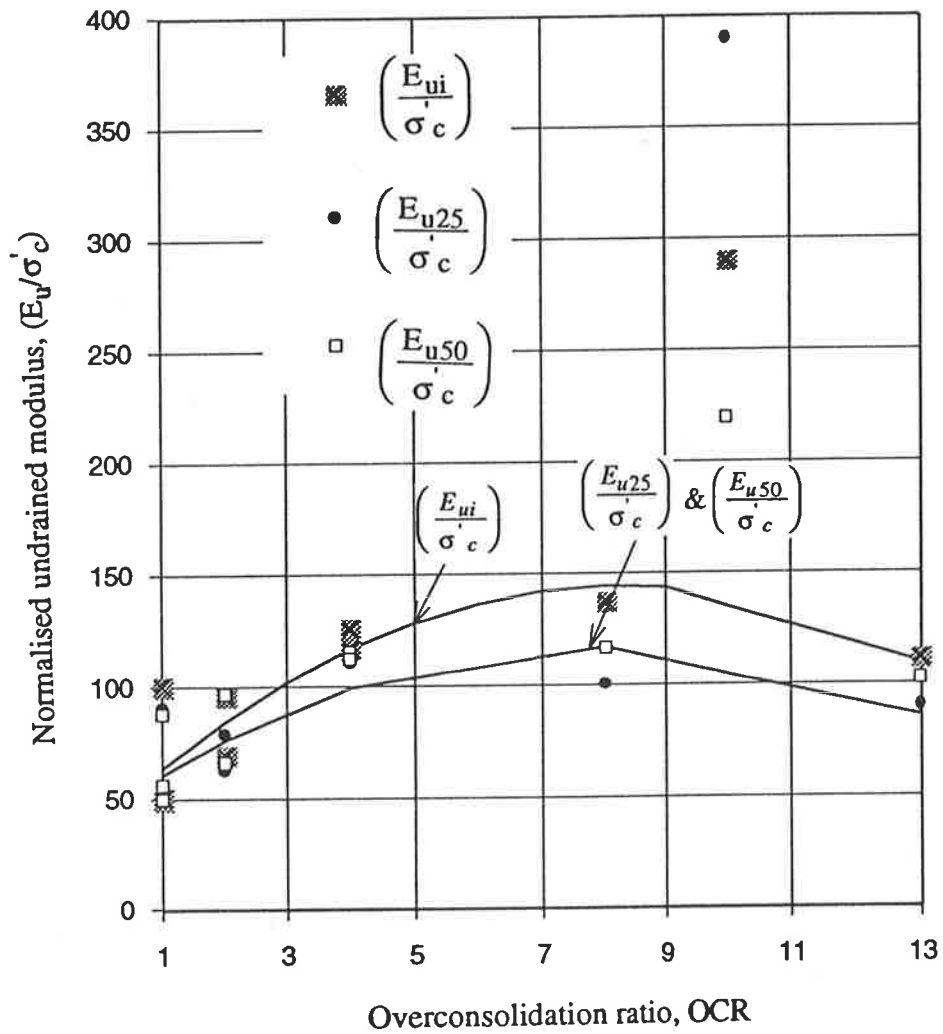


Figure 5.12 Variation of normalised undrained Young's modulus of elasticity with overconsolidation ratio

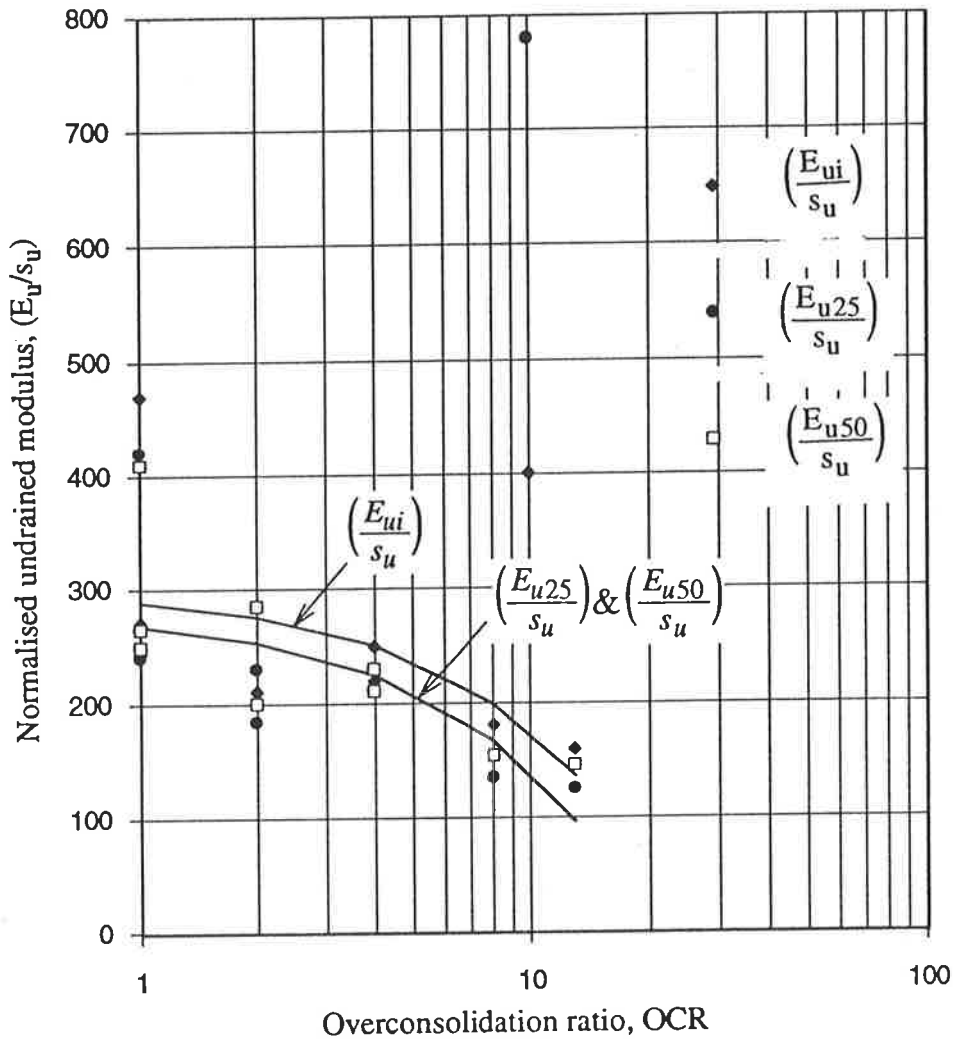


Figure 5.13 Variation of normalised undrained modulus (E_u/s_u) with overconsolidation ratios

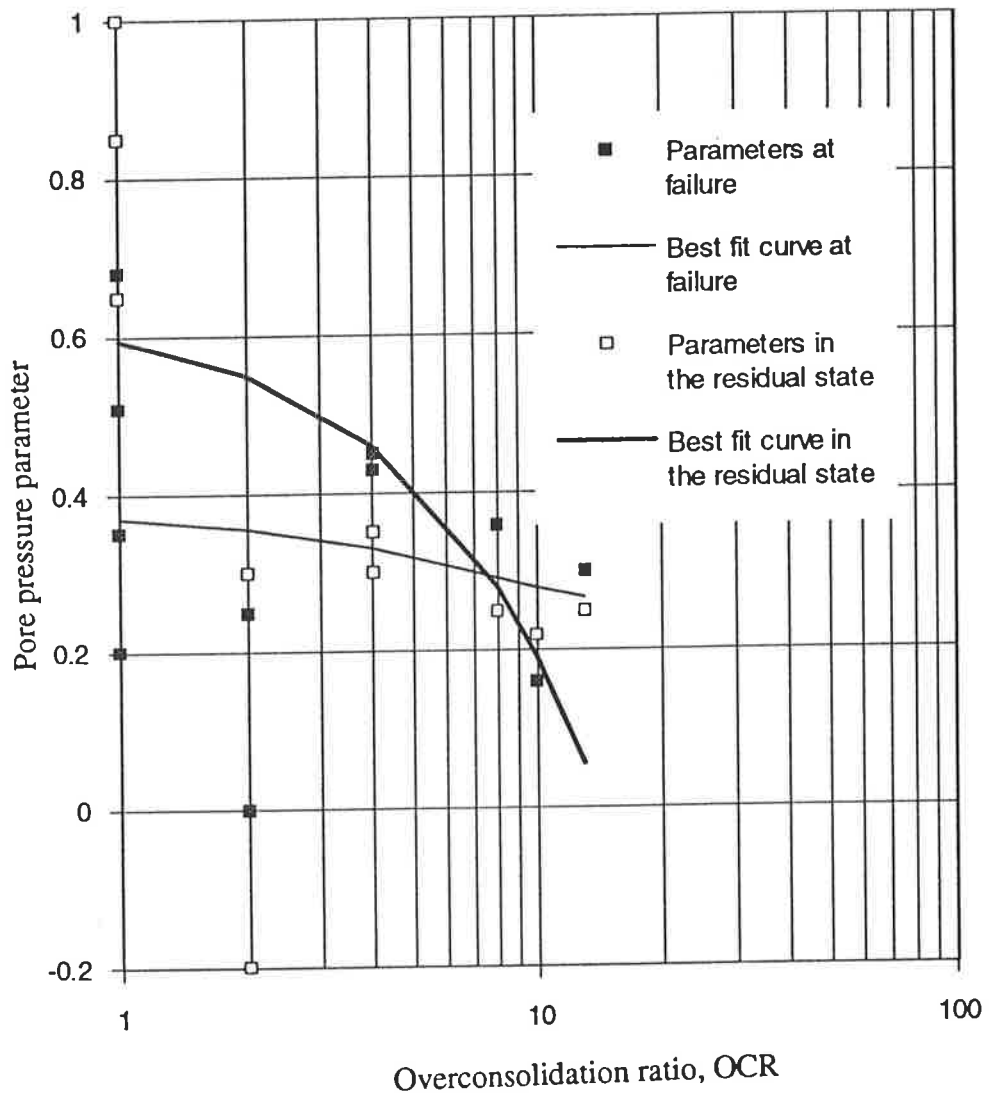


Figure 5.14 Relationship between pore pressure parameter and overconsolidation ratios

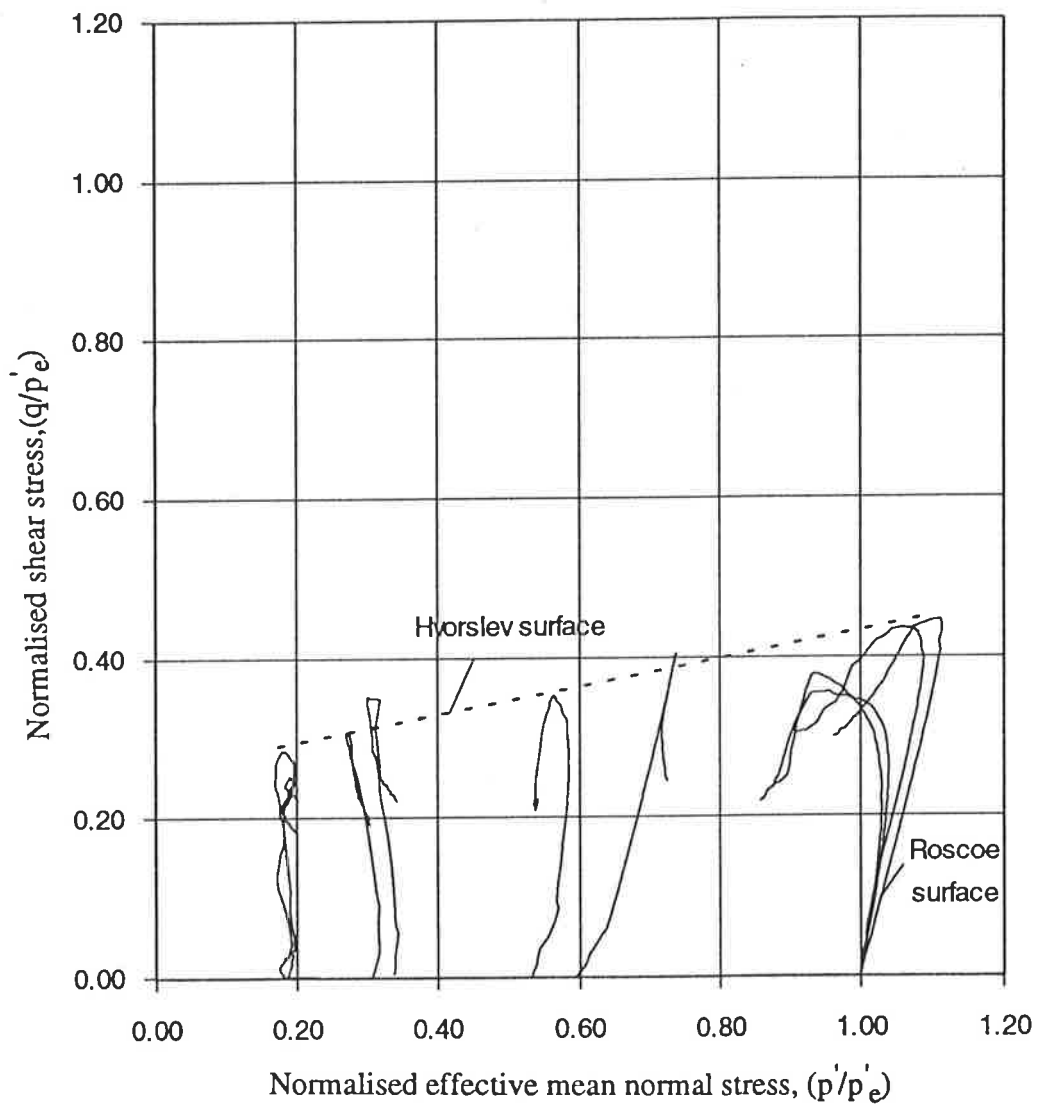


Figure 5.15 Relationship between normalised mean normal stress, p'/p'_e , and normalised shear stress, q/p'_e

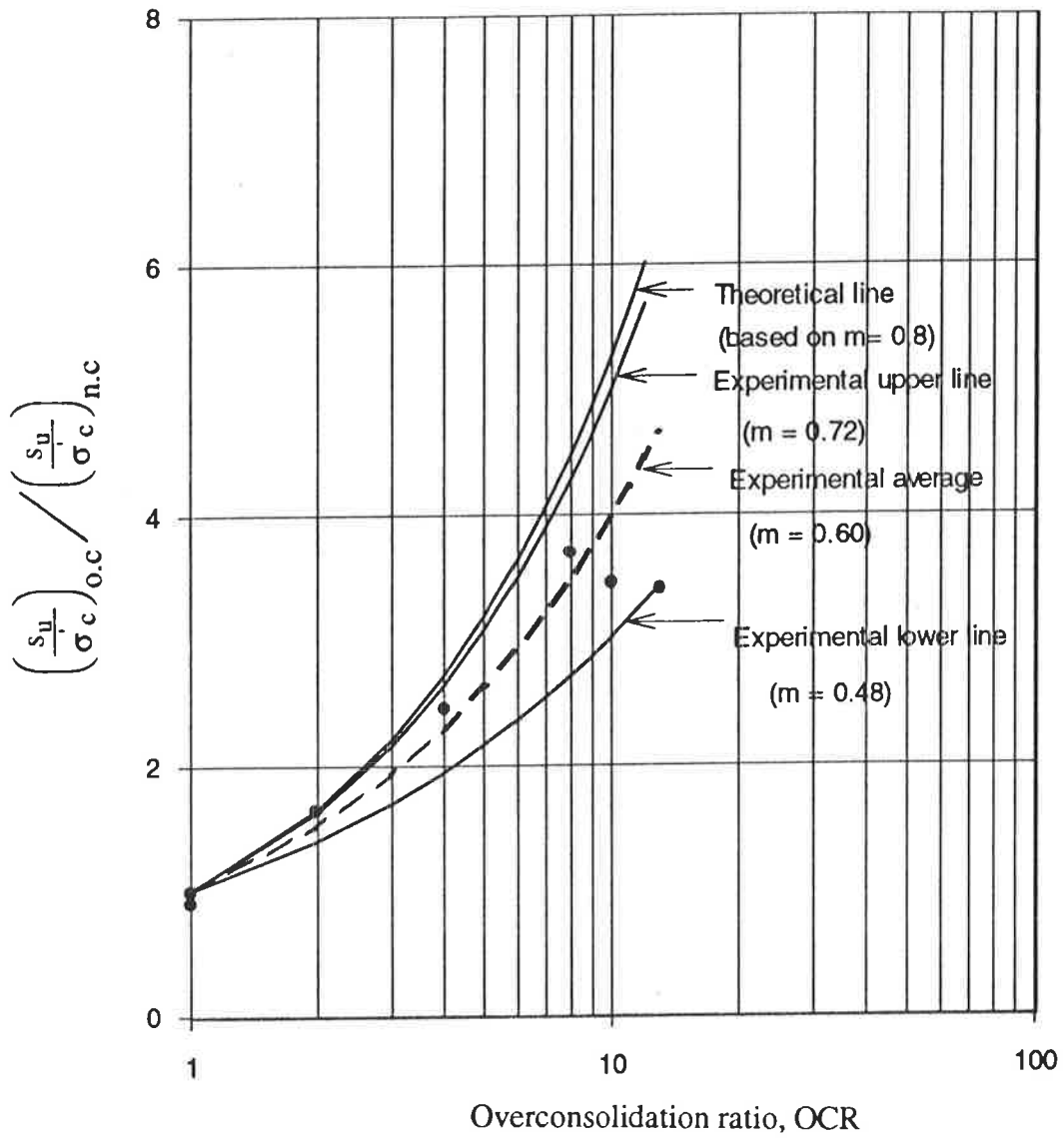


Figure 5.16 Comparison between experimental and m -based theoretical curves of undrained shear strength ratio of remoulded Keswick Clay.

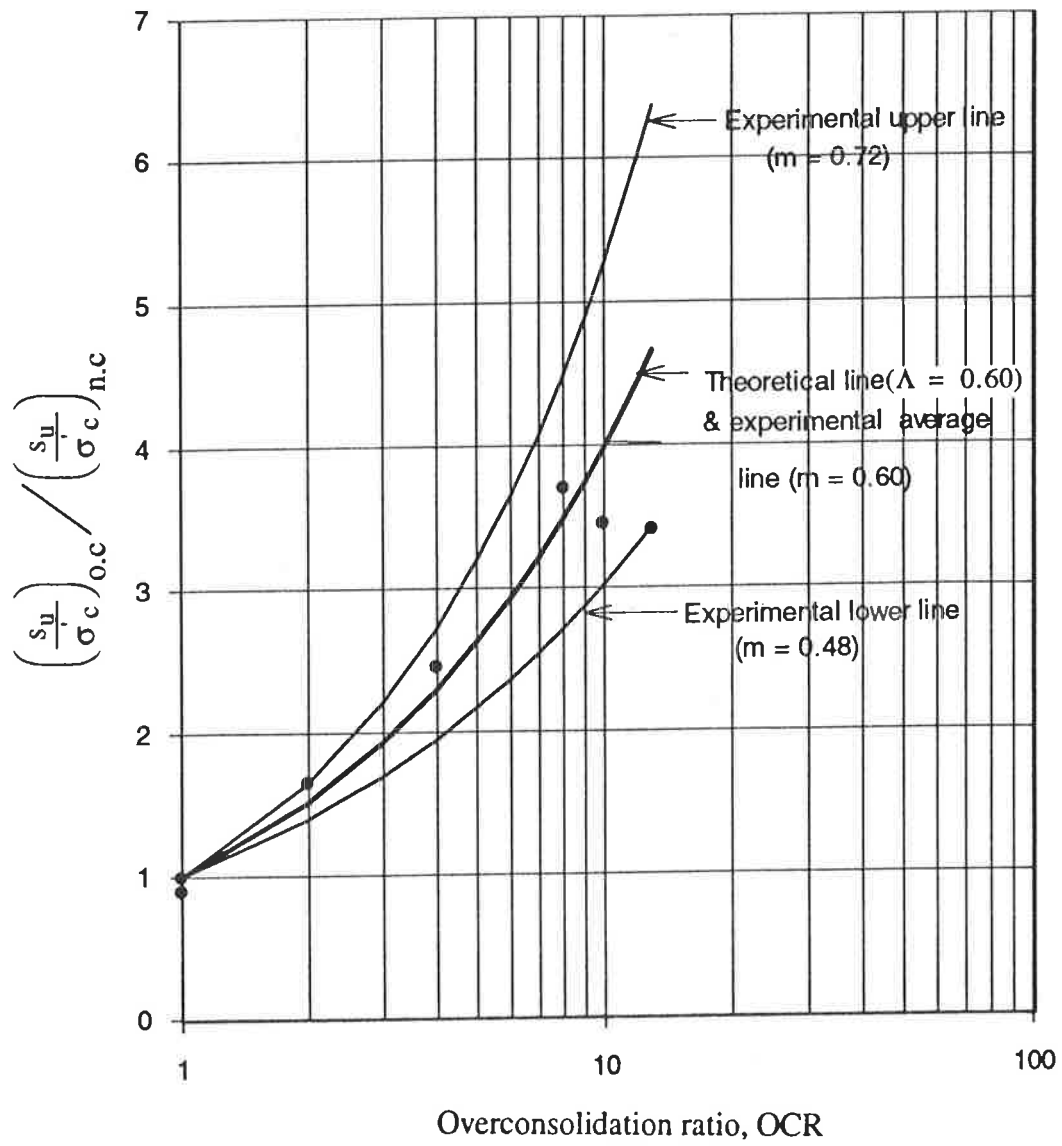


Figure 5.17 Comparison between experimental and Λ -based theoretical curve for undrained shear strength ratio of remoulded Keswick Clay.

Chapter 6

Application of test results to field problems

6.1 Introduction

This chapter describes the use of laboratory triaxial test results presented in the previous chapter to predict the in situ soil properties so that settlement and bearing capacity beneath a circular footing of a typical soil deposit can be determined. The analysis considers three cases of deposits. These cases are:

- (i) a deposit with no surcharge,
- (ii) a deposit with a surcharge of 30 kPa or 1.5 metres of fill, and
- (iii) a deposit with a surcharge of 60 kPa or 3.0 metres of fill.

Following the steps involved in the SHANSEP method, the laboratory test results are extended to in situ soil properties (e.g. undrained shear strength, s_u , and undrained Young's modulus of elasticity, E_u) throughout the deposit for each loading case. Finally, with the interpreted results, the settlements and bearing capacity of a circular footing are predicted with the finite element method and the general bearing capacity equation, respectively.

6.2 The field problem

The field problem is described as the determination of minimum design requirements of a circular footing beneath a natural deposit where emphasis has been given to the soil properties that control the footing design. In order to examine the variations of soil properties with different stresses, the different loading conditions are used to extend the laboratory test results into field conditions. In Figure 6.1(a) the deposit of Keswick Clay having no surcharge has been chosen where the OCR profile of this deposit were used from Figure 3.12. Then, two cases are assumed where an additional surcharge of 30 kPa and 60 kPa are applied to the deposit to examine the effects of surcharge on the soil properties (Figures 6.1 (b) and 6.1 (c)). Details of OCR and effective vertical stress, σ'_v , of the typical natural deposit and the effects of surcharge on OCR and effective vertical stress, σ'_v , which eventually affect the soil properties are subsequently discussed in the following sections.

6.2.1 Typical OCR profile of natural deposit

Many clay deposits (e.g. Keswick Clay, London Clay, Maine Organic Clay) throughout world are lightly to heavily overconsolidated due to the processes of erosion or desiccation in arid and semi-arid climates. Erosion removes the overburden from the top of the deposit

resulting in reduced vertical stress and eventually overconsolidate the clay. In arid regions, drying causes soil suction (negative pore water pressure) near the ground surface, which increases the stress between the particles. Thus when the soil is again wetted during the wet season, the stresses between the particles are reduced and the clay is overconsolidated. These phenomena result in soils, near the ground surface, in most soil profiles, being overconsolidated. This has been shown in Figure 3.12 which is adopted in the following analysis to investigate the significance of the results of remoulded Keswick Clay. Figure 3.12 and Table 3.1 indicate that the OCR of the soil profile decreases with depth of the deposit and the maximum OCR is found near the ground surface.

6.2.2 Effects of surcharging

The soil deposit with low shear strength and high compressibility characteristics can be improved by applying surcharge load on the deposit. The mechanism involved in the process is that excess pore water pressures within the deposit dissipate and the effective stresses increase everywhere within the deposit. Therefore, the shear strength and deformation properties of the deposit increase.

In order to achieve maximum benefit from the surcharge, it is assumed that the fill is left for a period of time to ensure dissipation of excess pore pressures and final consolidation. After final consolidation, this surcharge increases the effective vertical stress which is higher than previous stress that was acting on the deposit. The increased effective vertical stress must be used to determine the OCR of the deposit. Using the data of maximum effective past pressure, σ'_{vm} , and effective vertical stresses for each case, the variation of OCR is plotted against depth of the deposit, as shown in Figure 6.2. The variation of effective vertical stress with depth of the deposit is shown in Figure 6.3. It can be seen from Figure 6.2 that as the surcharge increases from 0 to 30 kPa and 60 kPa the OCR of natural deposit

decreases significantly and in fact becomes normally consolidated over most of the soil depth. Figure 6.3 indicates that the effective vertical stress, σ'_v , increases with increasing surcharge and depth of the deposit. From Figures 6.2 and 6.3 it can be concluded that the effective vertical stress and OCR are largely influenced by the application of surcharge and thus they are different in each case.

6.3 Determination of soil design parameters

6.3.1 Lateral earth pressure coefficient

The coefficient of lateral earth pressure, K_o , of an overconsolidated clay is dependent on the geologic history of the deposit. During primary unloading, that is from the virgin loading, Schmidt, (1966) and Mayne and Kulhawy, (1982) showed that the coefficient of lateral earth pressure, K_o , is related to the effective friction angle, ϕ' , and OCR of the deposit. The relationship between K_o and OCR of overconsolidated clay proposed by Mayne and Kulhawy (1982) can be expressed as follows:

$$K_o = (1 - \sin \phi') (\text{OCR})^{\sin \phi'} \quad (6.1)$$

where

$$\phi' = \text{effective friction angle.}$$

Thus it can be said that K_o is directly related to OCR of the deposit. With the above equation, for each loading case, the lateral earth pressure coefficient, K_o , was determined from the OCR and ϕ' ($\phi' = 12^\circ$, Chapter 5) and plotted against the depth of the deposit. This is shown in Figure 6.4. It can be seen from this figure that without a surcharge, K_o decreases as the depth of the deposit increases and the maximum K_o is found near the top of

the deposit, where the OCR is maximum. For the deposits with surcharges, K_0 is almost constant throughout the depth. This can be attributed to constant OCR of the deposit.

6.3.2 Effective mean normal stress versus depth

The effective mean normal stress, p'_o , can be determined from the following equation:

$$p'_o = \frac{(1+2K_0)}{3} \sigma'_{vo} \quad (6.2)$$

Using the variation of lateral earth pressure, K_0 , and effective overburden pressure, σ'_{vo} , with depth from Figure 6.3 and Figure 6.4, the effective normal stress, p'_o was computed for each loading case throughout the profile and plotted against depth of the deposit. This is shown in Figure 6.5 which indicates that p'_o for each case increases linearly with depth below ground surface.

6.3.3 In-situ soil design parameters

In order to determine the in situ undrained shear strength, s_u , and undrained Young's modulus of elasticity, E_u , from laboratory test results for the different stress conditions shown in Figure 6.1, the following steps were followed:

1. The variation of OCR for each case within the soil profile described in Section 6.2.2 was noted.

2. Using the variation of OCR for each case, the normalised undrained shear strength, (s_u/σ'_c) , was determined from Figure 5.11 at different depths of the deposit.
3. In the same way, the normalised undrained Young's modulus of elasticity, (E_u/σ'_c) , was determined from Figure 5.12. It should be noted that the average normalised undrained modulus of elasticity at different stress levels was used since there are no significant variations of moduli of elasticity when the stress levels are different.
4. Using effective mean normal stress, $p'_{o,} = \sigma'_c$, the undrained shear strength, s_u , and undrained Young's modulus of elasticity, E_u , was determined.

The computed values of the in situ undrained shear strength, s_u , and the undrained Young's modulus of elasticity, E_u , are plotted against depth of the deposit in Figures 6.6 and 6.7. It appears from Figure 6.6 that the effect of OCR on the undrained shear strength, s_u , is more pronounced for no surcharge compared to the 30 kPa and 60 kPa surcharges. In addition, it can be seen that for no surcharge, the undrained shear strength decreases up to a depth of 3.5 m and then, increases slightly. This can be attributed to the variation of the OCR of the deposit which is maximum at the ground surface and decreases with depth. On the other hand, for 30 kPa surcharge, the undrained shear strength also decreases up to a depth of 3.5 m and then increases linearly with depth. This is because at a depth of 2.0 m, the soil is overconsolidated resulting higher undrained shear strength at 3.5 m depth. Below 3.5 m the soil is normally consolidated and shows a linear relationship between s_u , and depth of the deposit. For 60 kPa surcharge, the OCR remains constant throughout the deposit and s_u , increases linearly with depth. Figure 6.6 clearly demonstrates that the undrained shear strength can be increased by applying surcharges to the deposit.

Figure 6.7 shows that without a surcharge, the undrained Young's modulus of elasticity increases linearly with depth and the maximum E_u is found at the bottom of the deposit. The variation of undrained Young's modulus due to OCR for no surcharge is not as pronounced as it is for undrained shear strength, s_u . On the other hand, by using a surcharge of 30 kPa, it can be seen in Figure 6.7, that E_u does not increase linearly up to 3.5 m. For the 60 kPa surcharge, E_u increases linearly with depth of the deposit.

For long term analysis, the obtained undrained Young's modulus was further converted into the drained Young's modulus by the following equation.

$$E' = \frac{E_u(1+v')}{1.5} \quad (6.3)$$

where

$$\begin{aligned} v' &= \text{drained Poisson's ratio,} \\ &= 0.30 \text{ (assumed).} \end{aligned}$$

A detailed summary of effective vertical stress, σ'_v , effective maximum past pressure, σ'_{vm} , effective mean normal stress, p'_o , undrained shear strength, s_u , undrained Young's modulus, E_u , and drained Young's modulus E' , with depth of the deposit for the three load cases are presented in Tables 6.1, 6.2, and 6.3.

The computed drained and undrained soil properties of the deposit are used to determine the settlement of a circular footing using the finite element method, and the bearing capacity via the well known bearing capacity equations. In calculating long term settlement, the drained modulus of elasticity, E' , is used based on a factor of safety of 2.

6.4 The finite element method

The finite element method is a numerical analysis technique for obtaining approximate solutions to a wide variety of engineering problems. The method relies on a discretisation of a field problem into a finite number of elements, connected by nodes. In this method the unknown field variables are expressed in terms of assumed approximate functions (called interpolation functions) within each element. These approximate functions are defined in terms of the values of the field variables at the nodes of the element. The field variables within each element are expressed completely by the nodal values of the field variables and the interpolation functions within the element. For a specific finite element problem, the nodal values of the field variables are the unknowns which are defined by the interpolation functions, throughout the assemblage of elements. The accuracy of the solution depends on both the size and number of elements and on the interpolation functions. The steps involved in the finite element method for solving the settlement beneath a foundation are as follows:

1. Descretisation of the soil and foundation into a system of finite elements.
2. The derivation of the stiffness matrix for an individual element in terms of its nodal variables, using the stress-strain relationship of the material and the interpolation functions.
3. Assembly of the overall stiffness matrix $[K]$ for the entire mesh from the individual element stiffness matrices to obtain the relationship between the total load vector $\{R\}$ and the nodal displacement vector $\{\delta\}$:

$$[K]\{\delta\} = \{R\} \quad (6.4)$$

4. Solution of Equation 6.4 to obtain the nodal displacements.
5. Calculation of element stresses and strains from the nodal displacements.

The numerical computations associated with the analysis are invariably carried out using a computer package with elements already defined. Thus, the most important aspect is to decide what is the best way to discretise the problem for analysis. In the following sections, a soil deposit is discretised to determine the settlement beneath a circular footing.

6.4.1 Descritisation of problem

The field problem described in Section 6.2, was divided into a grid system which was further sub-divided into 4 triangular elements per grid, as shown in Figure 6.8. The node numbers and nodal coordinates are defined using the first quadrant and the elements (element numbers and connecting nodes) are defined in an anticlockwise direction. It can be seen from Figure 6.8 that the soil deposit is represented by 96 triangular elements which are connected by 59 nodes. The spacing of the bays in the Z-direction are 3.0, 3.0, 1.50, 1.50 m, and in the R-direction are 1.0, 1.0, 1.5, 2.0, 3.0, and 4.0 m.

The assumed loadings are applied in the vertical direction through nodes 5, 14, and 23 of the finite element mesh in Figure 6.8 to examine the variations of settlements of circular footing, (4 m in diameter). The boundary conditions include fixity along the axis of loading and a permeable surface at the top of the mesh and it is assumed that the bottom part of the soil deposit is solid rock. The specified boundary conditions for the mesh are as follows.

1. Zero lateral displacements along axis (nodes, 1, 2, 3, 4, and 5)

2. Zero vertical displacement at base of soil (nodes, 1, 10, 19, 28, 37, 46 and 55)
3. Zero excess water pressure at ground surface (nodes, 23, 32, 41, 50 and 59)

6.5 Results of analysis

6.5.1 Settlement of circular footing

A finite element program, *Axcons* (Small, 1977), was used on a personal computer to investigate the displacements and excess pore pressures at the centre and edge of the loaded area using the mesh shown in Figure 6.8. In the computer program *Axcons* the soil is modelled as a linear elastic material. The program solves Biot's equation of consolidation so that solutions of displacement and excess pore pressure can be output at any node of interest at any time. The computer program was run for 12 kPa, 24 kPa, and 48 kPa loading applied to the circular footing. For each case, the vertical displacements have been computed using different effective Young's modulus of elasticity for different surcharges as described in Section 6.2.3. From the computer output the results of the analysis are presented below:

(a) Time dependent settlement at the centre and edge of the foundation

The settlements beneath the centre of the footing (at node 5) for 12 kPa, 24 kPa and 48 kPa loadings with different surcharges, have been plotted against the logarithm of elapsed time in months in Figures 6.9, 6.10 and 6.11. It can be seen from Figure 6.9, that there is an initial settlement of 53 mm followed by 22 mm of consolidation settlement yielding a total

settlement of 75 mm for no surcharge. For the cases of surcharges of 1.5 m fill (30 kPa) and 3 m fill (60 kPa), with an applied load of 12 kPa, the initial settlements were found to be 25 mm and 15 mm respectively, which are lower than those for no surcharge. Also, Figure 6.9 indicates that consolidation settlement is more prominent for the case of no surcharge than for surcharges of 30 kPa and 60 kPa. Figure 6.10 and Figure 6.11 show similar trends of initial and consolidation settlements for 24 kPa and 48 kPa pressure but the amount of initial and consolidation settlement for different surcharges increases substantially as the applied pressure increases. In the same way the settlements at the edge of the footing are plotted in Figures 6.12, 6.13 and 6.14. From the comparison of settlements at the centre and edge of the footing, it can be seen that the edge settlement is significantly lower than the settlement at the centre of the footing for all cases.

From the above discussions, it can be concluded that the settlement of a footing is largely influenced by the soil profile and the applied surcharge. From the study of 98 buildings which were generally old structures of load bearing walls, steel, and reinforced-concrete construction, MacDonald and Skempton (1955), recommended a maximum settlement of 64 mm in a clay soil, which was supported by Grant et al (1974). Thus, in the context of this recommended value, the obtained total settlement for no surcharge is higher for all loading conditions than the recommended values and thus the foundation is considered unsafe. On the other hand, settlements for surcharges of 30 kPa and 60 kPa, are too low for 12 kPa foundation loading than the recommended settlement. For this loading, using surcharges of 30 kPa and 60 kPa make the design highly conservative. The minimum surcharge to meet the design of 50 mm settlement, will be examined in Section 6.5.3.

6.5.2 Bearing capacity of circular footing

The ultimate bearing capacity, q_{ult} , of a footing supported by a cohesive deposit can be determined by various bearing capacity equations, such as Terzaghi (1943), Meyerhof (1951, 1963), Hansen (1970) and Vesic (1973, 1974) equations. From the detailed comparison of computed q_{ult} , by different equations and measured values, Bowles (1988) suggested that Terzaghi's equation is the best for a quick estimate of q_{ult} of highly cohesive soils where $D/B \leq 1$ for concentrically loaded footing. On the other hand, the Hansen, Meyerhof, and Vesic equations can be applied to any situation depending on the designer's preference or familiarity with a particular method (Bowles, 1988). Vesic's equation for determining q_{ult} , can be written as follows:

$$q_{ult} = cN_c s_c d_c i_c g_c b_c + \bar{q} N_q s_q d_q i_q g_q b_q + 0.5 \gamma B N_\gamma s_\gamma d_\gamma i_\gamma g_\gamma b_\gamma \quad (6.5)$$

When $\phi = 0$,

$$q_{ult} = 5.14 s_u (1 + s'_c + d'_c - i'_c - b'_c - g'_c) + \bar{q} \quad (6.6)$$

where

- c = cohesion intercept,
- N_c, N_q, N_γ = bearing capacity factors,
- $N_q = e^{\pi \tan \phi} \tan^2(45 + \frac{\phi}{2})$,
- $N_c = (N_q - 1) \cot \phi$,
- $N_\gamma = 1.5 (N_q - 1) \tan \phi$,
- s_c, s_q, s_γ, s'_c = shape factors,
- d_c, d_q, d_γ, d'_c = depth factors,
- i_c, i_q, i_γ, i'_c = inclination factors,
- g_c, g_q, g_γ, g'_c = ground factors,
- b_c, b_q, b_γ, b'_c = base factors,

- \bar{q} = surcharge pressure,
 B = width of foundation and
 s_u = undrained shear strength.

The above equations were used to determine the short term and long term bearing capacity of a circular footing which was placed 2.0 m below the ground surface. In the case of the short term bearing capacity, the average undrained shear strengths within 2.0 m immediately below the footing were used. The undrained shear strengths below 2.0 m are $s_u = 6.05$ kPa, 8.30 kPa and 12.00 kPa respectively, as shown in Figure 6.6. Using these values together with $\gamma = 17.3$ kN/m³, $s'_c = 0.2$, $d'_c = 0.40$ and neglecting inclination, ground, and base factors, Equation 6.6 gives the short term ultimate bearing capacities of 84 kPa, 132 kPa and 193 kPa respectively for the applied loadings of 12 kPa, 24 kPa and 48 kPa. For determining the long term bearing capacity, the effective strength parameters ($c' = 0$, $\phi' = 12^\circ$) are taken from Chapter 5 which provide the following bearing capacity factors using Vesic's charts:

$$\begin{aligned}N_q &= 3.0, \\N_\gamma &= 1.80, \\s_q &= 1.2, \\s_\gamma &= 0.6, \\d_q &= 1.3, \text{ and} \\d_\gamma &= 1.0.\end{aligned}$$

Using the above values Equation 6.5 yields ultimate bearing capacities of 181 kPa, 321 kPa, and 461 kPa, respectively.

From the determination of short term and long term bearing capacities for different loading applications, it is clear that short term bearing capacity is critical. Thus, in order to make the design safe, the short term bearing capacity has been considered for further analysis.

6.5.3 Recommendations for design pressure

The results presented in Sections 6.5.2 and 6.5.3 are used to determine the minimum design requirements by specifying the minimum thickness of fill in order to ensure that a factor of safety of 3 against bearing capacity failure is provided and the maximum settlement is limited to 50 mm. The settlement at the centre of the footing for 12 kPa, 24 kPa and 48 kPa loading and allowable bearing pressure based on factor of safety of 3, are plotted against surcharge pressure in Figure 6.15. This figure shows that the settlement decreases with increasing surcharge pressure whereas the bearing pressure increases with surcharge pressure. The minimum surcharge to cause less than 50 mm settlement for 12 kPa and 24 kPa loading are 16 kPa and 46 kPa respectively. These surcharges of 16 kPa and 46 kPa result in a bearing capacity of the footing of 38 kPa and 54 kPa. As can be seen from Figure 6.15, for 48 kPa loading, the minimum settlement is 75 mm which demonstrates that the applied surcharge is not large enough to satisfy a maximum design settlement of 50 mm.

6.6 Summary

The extension of laboratory test results to field soil properties for different deposits, presented in this chapter revealed that the OCR profile is changed by the application of surcharge and it increased the in situ undrained soil properties (s_u , E_u). These properties directly affect the calculated settlement and bearing capacity of a footing.

A discussion of a typical OCR profile of arid/semi-arid natural deposit shows that the OCR and coefficient of lateral earth pressure at rest, K_0 , decrease with increasing depth, and that the maximum OCR and K_0 are found close to the ground surface. K_0 is considered in determining the effective mean normal stress, p'_o , which shows higher values particularly near the surface where OCR greater than 1. The interpreted undrained shear strength, s_u , shows an increase with increasing effective vertical stress, σ'_v , and OCR. But OCR decreases as σ'_v increases and so their influence on s_u is negated to some extent as indicated on Figure 6.6, and also that once σ'_v is large enough, the OCR = 1, and s_u increases linearly. The undrained Young's modulus of elasticity, E_u , also increases linearly below the ground surface.

The application of the in situ soil properties to determine design parameters of a circular footing show that the settlement and bearing capacity vary substantially with different surcharges. This is because surcharges affect soil properties significantly by altering the in situ effective stresses. From the analysis of the settlement and bearing capacity of a circular footing for the different stress conditions it was concluded that a surcharge of 16 kPa (1.0 m fill) and 46 kPa (2.5 m fill) are needed for 12 kPa and 24 kPa loading for an adequate design.

Table 6.1 Summary of in situ undrained shear strength, undrained and drained Young's modulus of elasticity for no surcharge.

Depth of the deposit (m)	Effective vertical stress, $\sigma'_v = \sigma'_{vo}$ (kPa)	Maximum past pressure, σ'_{vm} (kPa)	OCR	s_u/σ'_c from Figure 5.11	Effective mean normal stress, p'_o (kPa)	s_u (kPa)	Average E_u/σ'_c from Figure 5.12	E_u (MPa)	E' (MPa)
2.0	9	48	5.4	0.62	9.75	6.05	115	1.12	0.97
3.5	15	38	2.55	0.39	14.60	5.70	89	1.30	1.13
5.0	22	36	1.65	0.29	20.25	5.90	77	1.56	1.39
6.5	28	36	1.30	0.25	24.80	6.20	70	1.75	1.52
8.0	35	37	1.05	0.21	30.35	6.40	66	2.00	1.75

Table 6.2 Summary of in situ undrained shear strength, undrained and drained Young's modulus of elasticity for surcharge of 30 kPa.

Depth of the deposit (m)	Effective vertical stress, $\sigma'_v = \sigma'_{vo} + 30$ (kPa)	Maximum past pressure, σ'_{vm} (kPa)	OCR	s_u/σ'_c from Figure 5.11	Effective mean normal stress, p'_o (kPa)	s_u (kPa)	Average E_u/σ'_c from Figure 5.12	E_u (MPa)	E' (MPa)
2.0	39	48	1.25	0.24	34.60	8.30	69	2.39	2.07
3.5	45	38	1.0	0.20	39.00	7.80	65	2.54	2.20
5.0	52	36	1.0	0.20	45.00	9.00	65	2.93	2.54
6.5	58	36	1.0	0.20	50.25	10.05	65	3.27	2.83
8.0	65	37	1.0	0.20	56.35	11.25	65	3.66	3.17

Table 6.3 Summary of in situ undrained shear strength, undrained and drained Young's modulus of elasticity for surcharge of 60 kPa.

Depth of the deposit (m)	Effective vertical stress, $\sigma'_v = \sigma'_{vo} + 60$ (kPa)	Maximum past pressure, σ'_{vm} (kPa)	OCR	s_u/σ'_c from Figure 5.11	Effective mean normal stress, p'_o (kPa)	s_u (kPa)	Average E_u/σ'_c from Figure 5.12	E_u (MPa)	E' (MPa)
2.0	69	48	1.0	0.20	60.0	12.00	65	3.90	3.38
3.5	75	38	1.0	0.20	65.0	13.00	65	4.25	3.68
5.0	82	36	1.0	0.20	71.0	14.20	65	4.62	4.00
6.5	88	36	1.0	0.20	76.0	15.20	65	4.94	4.28
8.0	95	37	1.0	0.20	82.0	16.40	65	5.33	4.62

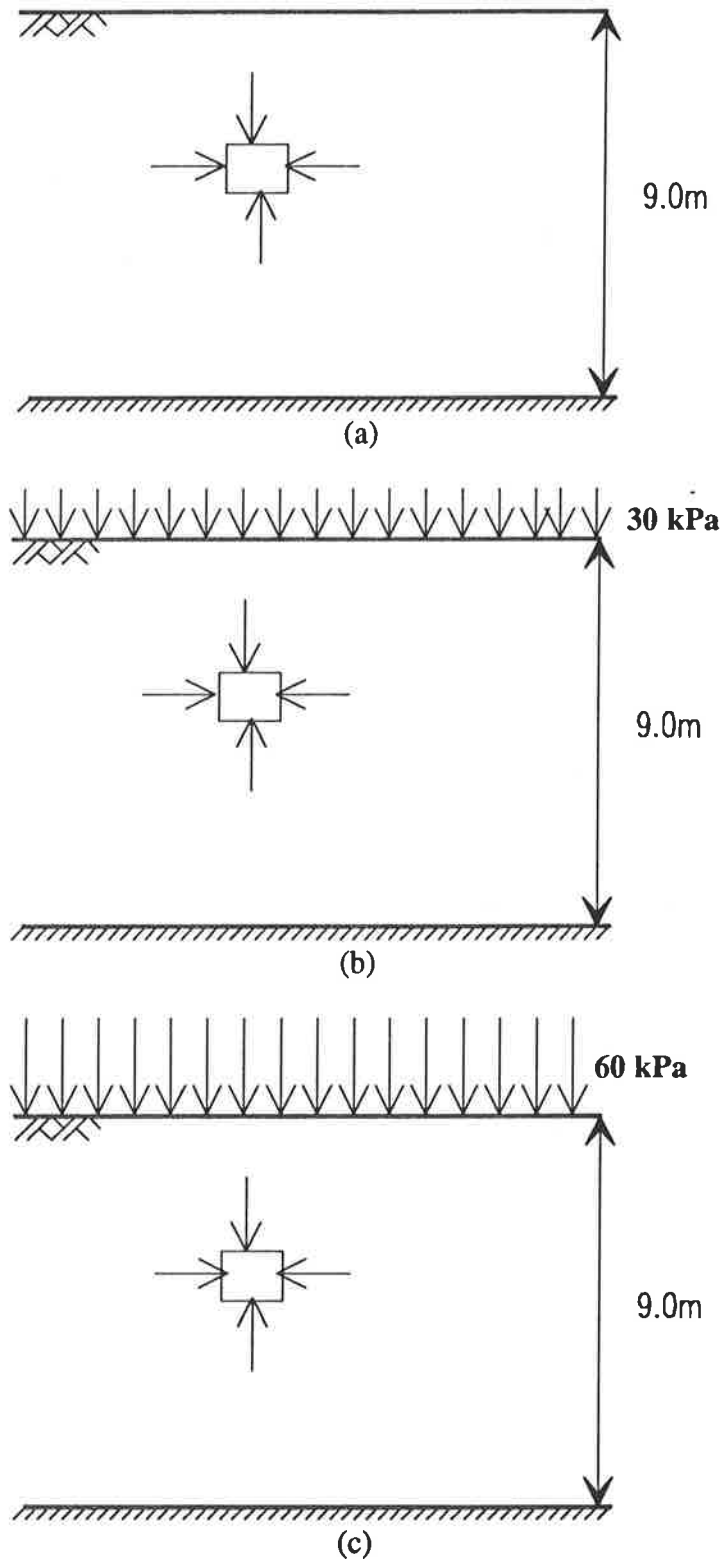


Figure 6.1 Different stress conditions which are used to determine the soil properties

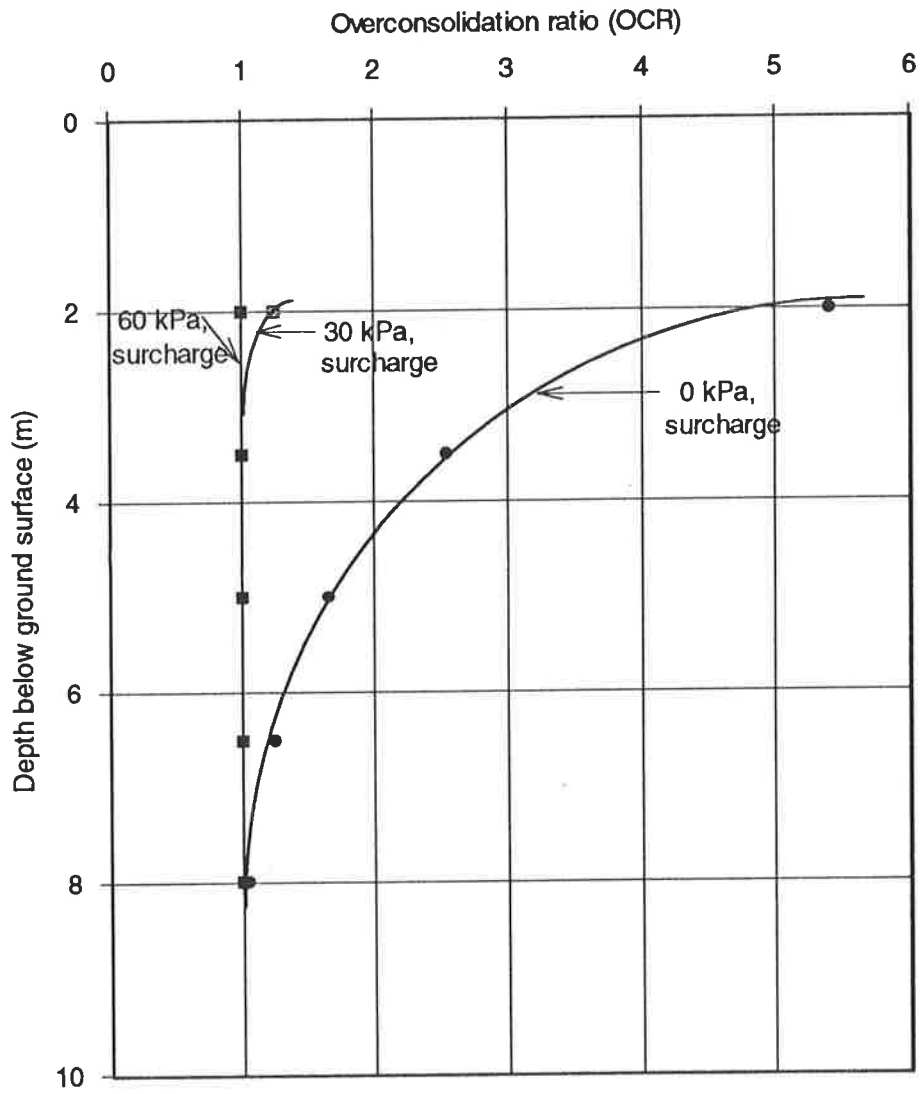


Figure 6.2 Relationship between OCR and depth of the deposit.

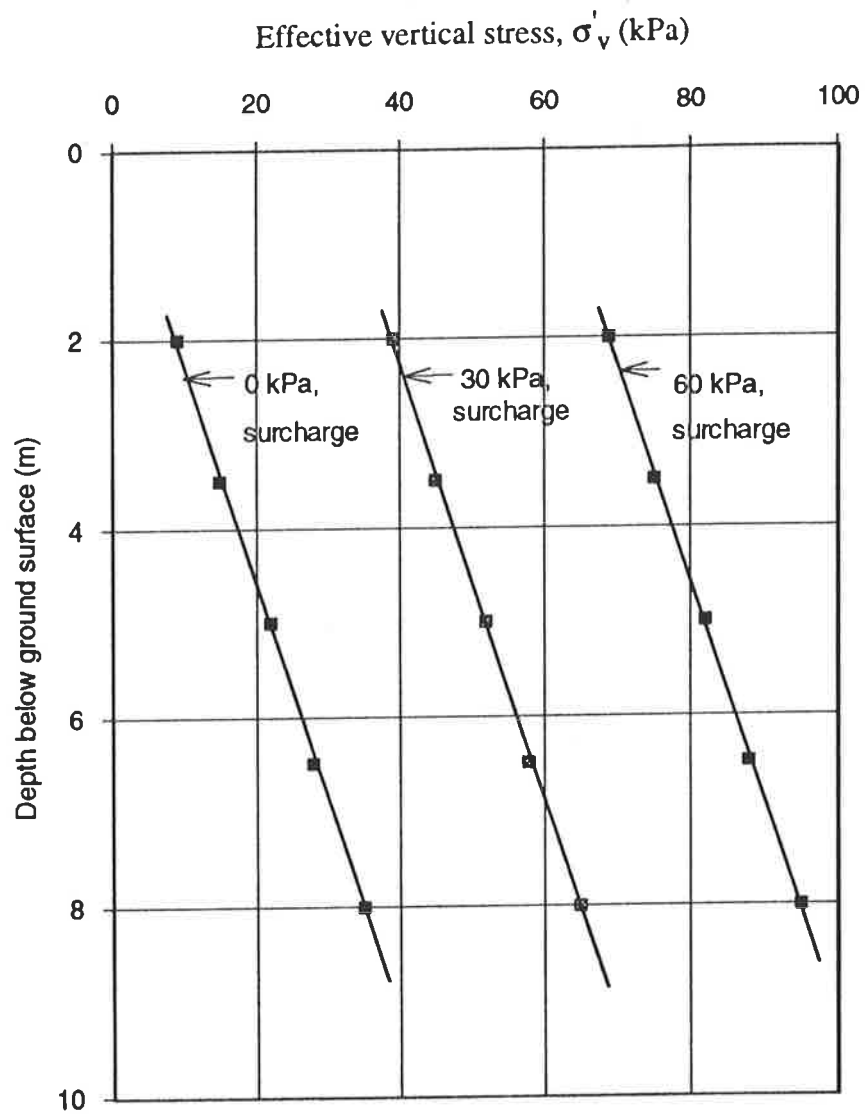


Figure 6.3 Relationship between effective vertical stress, σ'_v for different surcharges with depth of the deposit

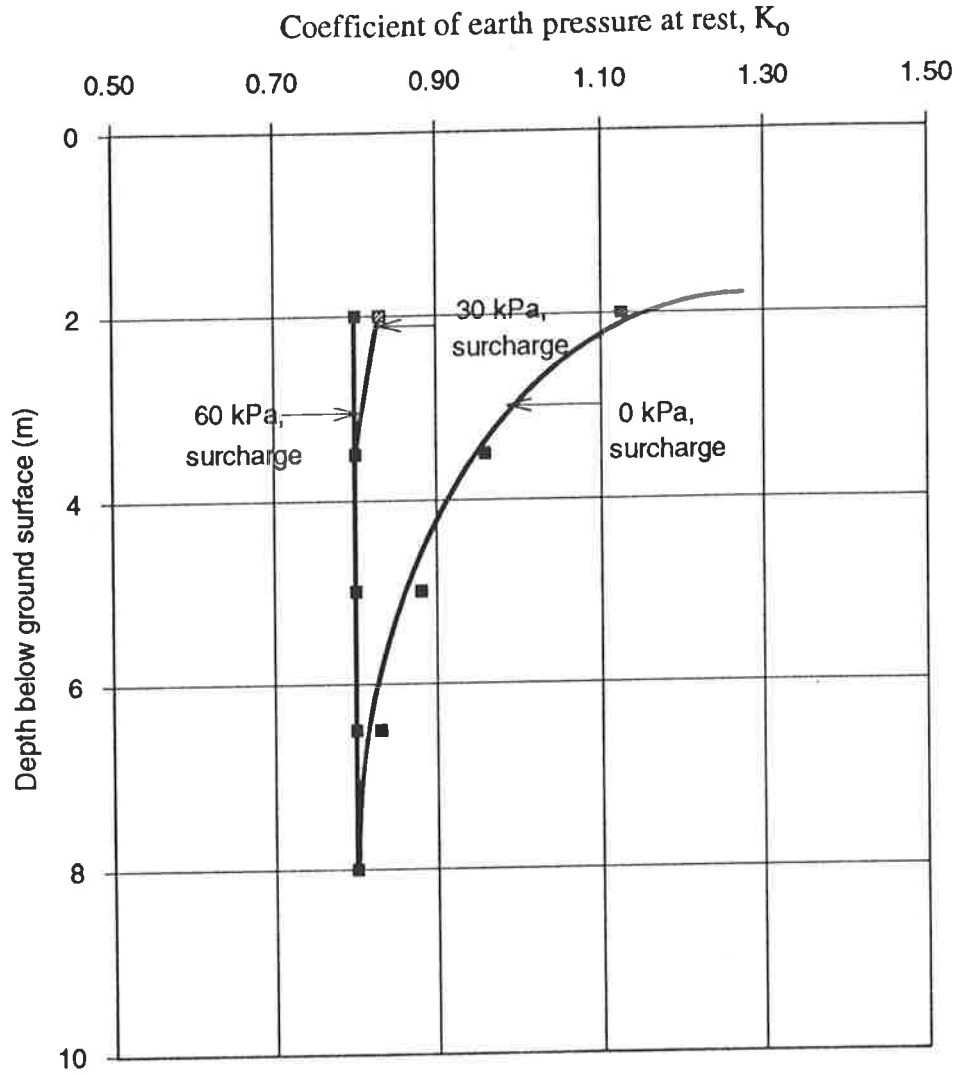


Figure 6.4 Variation of K_0 with depth of the deposit

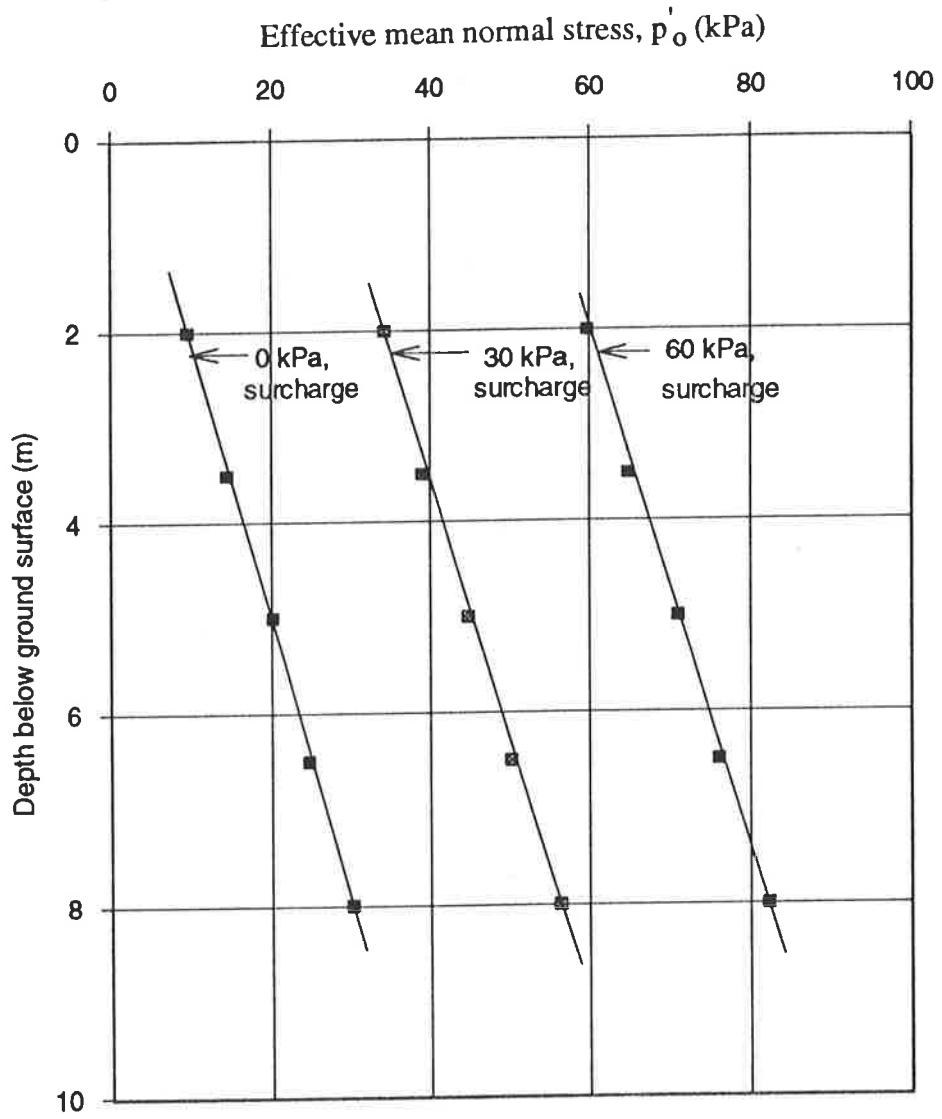


Figure 6.5 Relationship between mean effective stress, p'_o , and depth of the deposit.

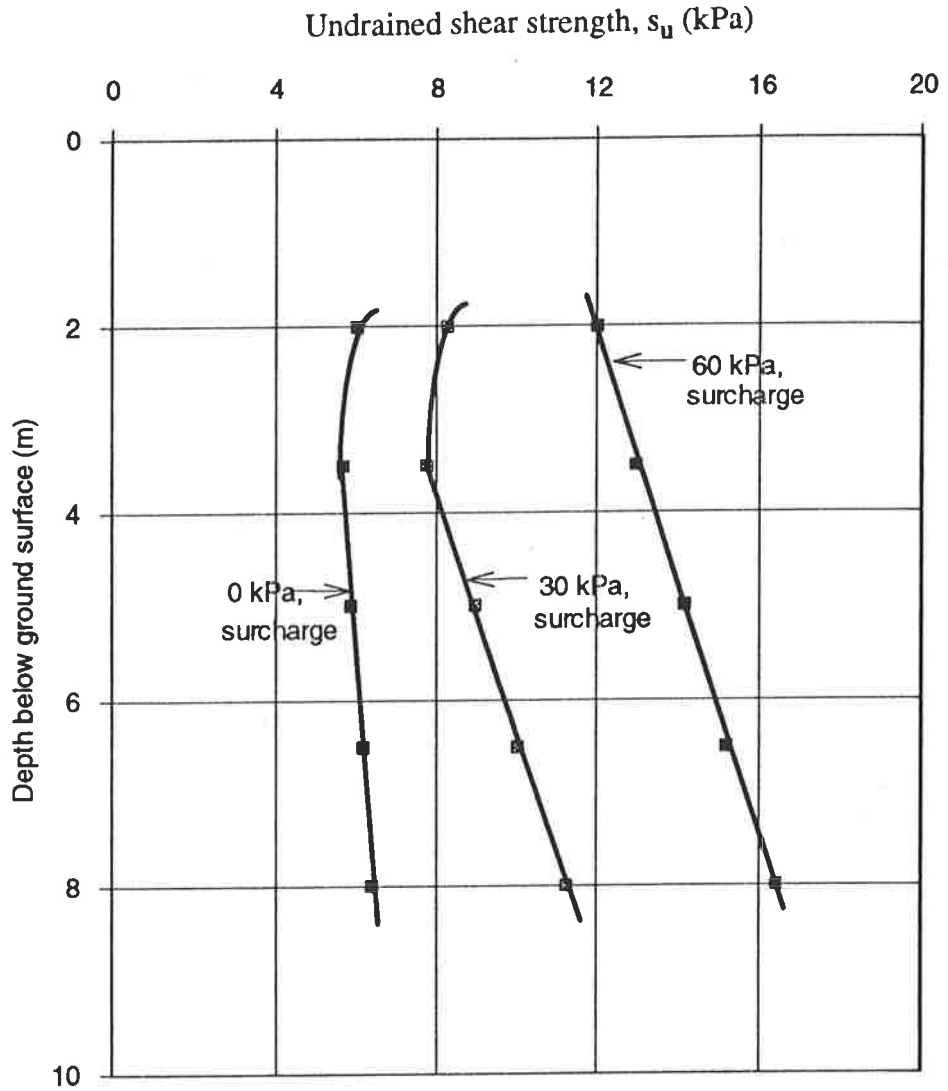


Figure 6.6 Relationship between undrained shear strength, s_u , and depth of deposit

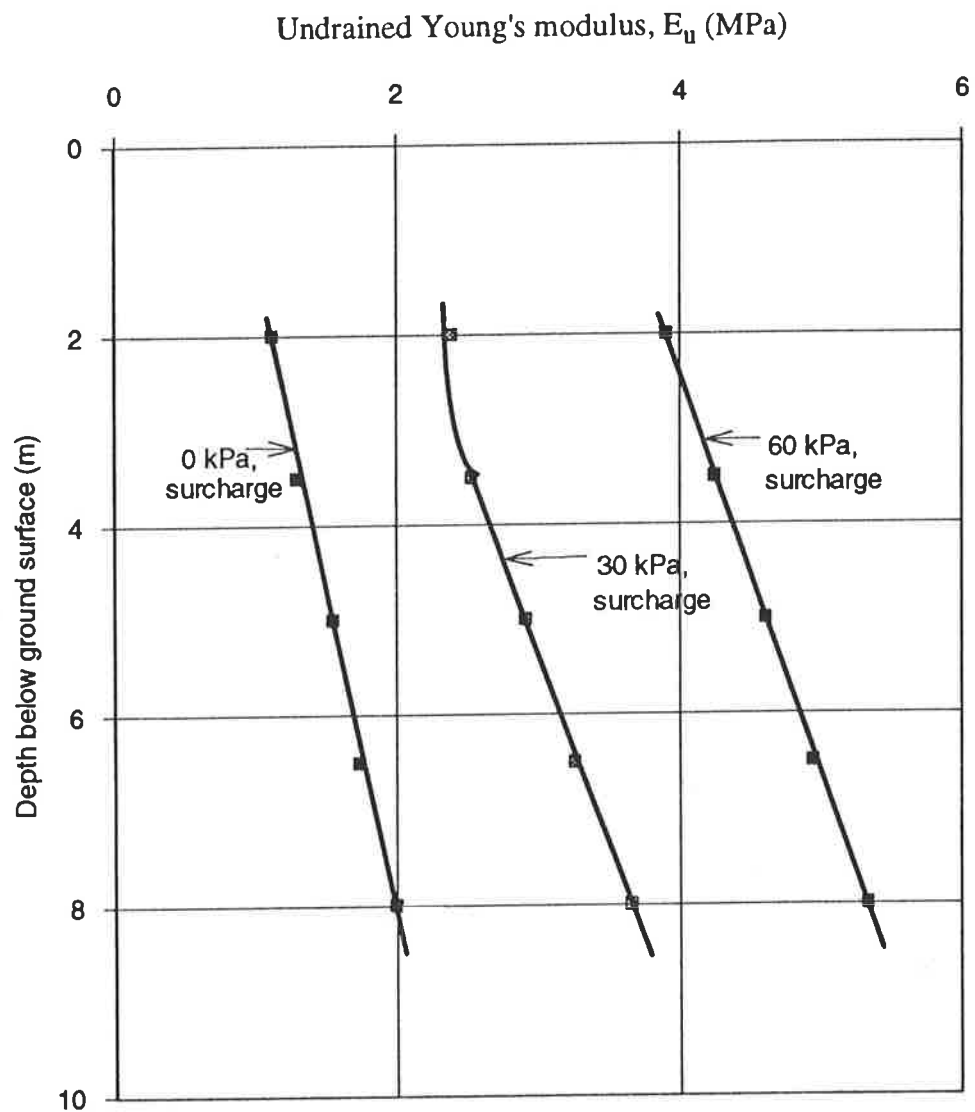


Figure 6.7 Relationship between undrained Young's modulus, E_u , and depth of the deposit.

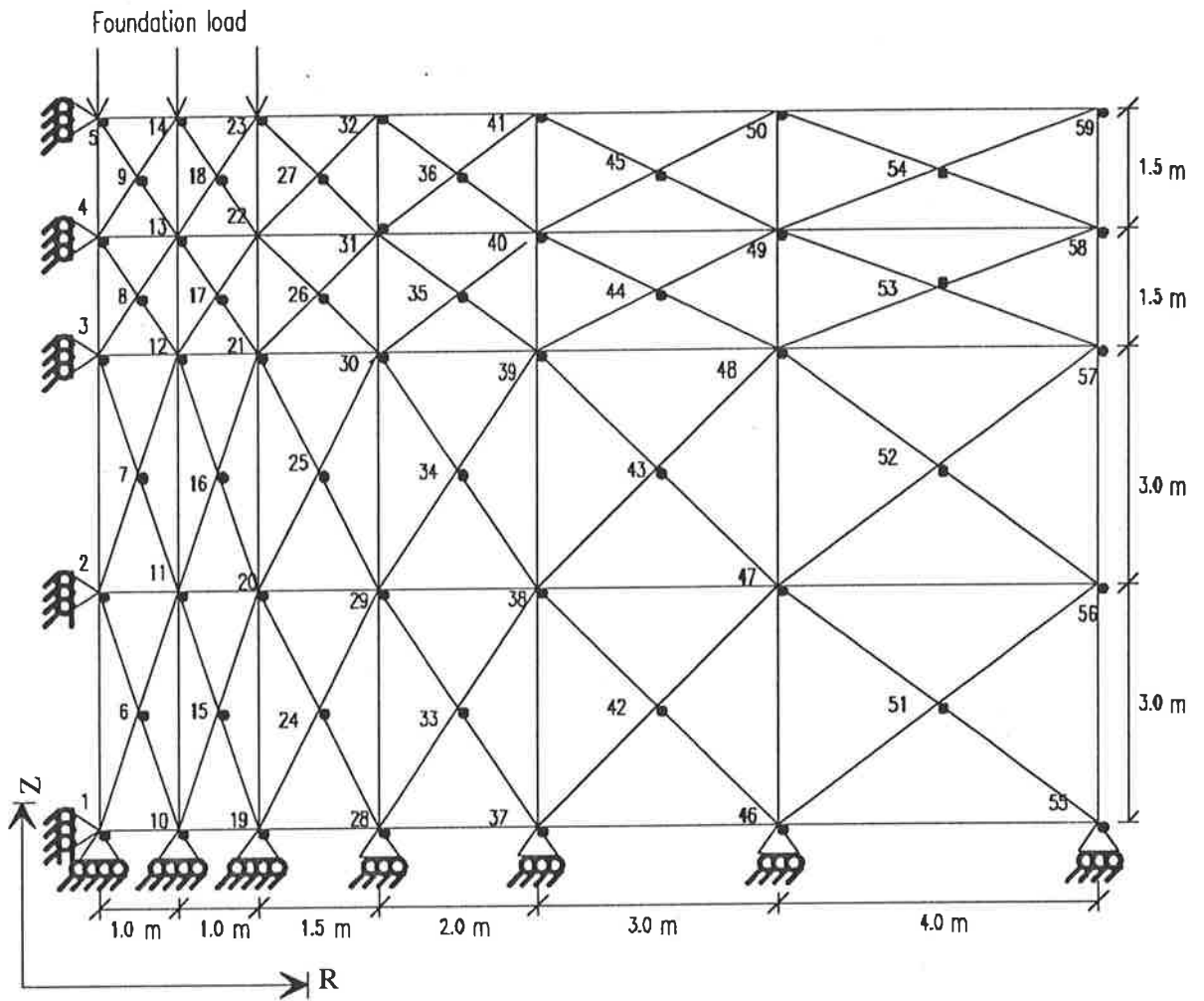


Figure 6.8 Finite element mesh details

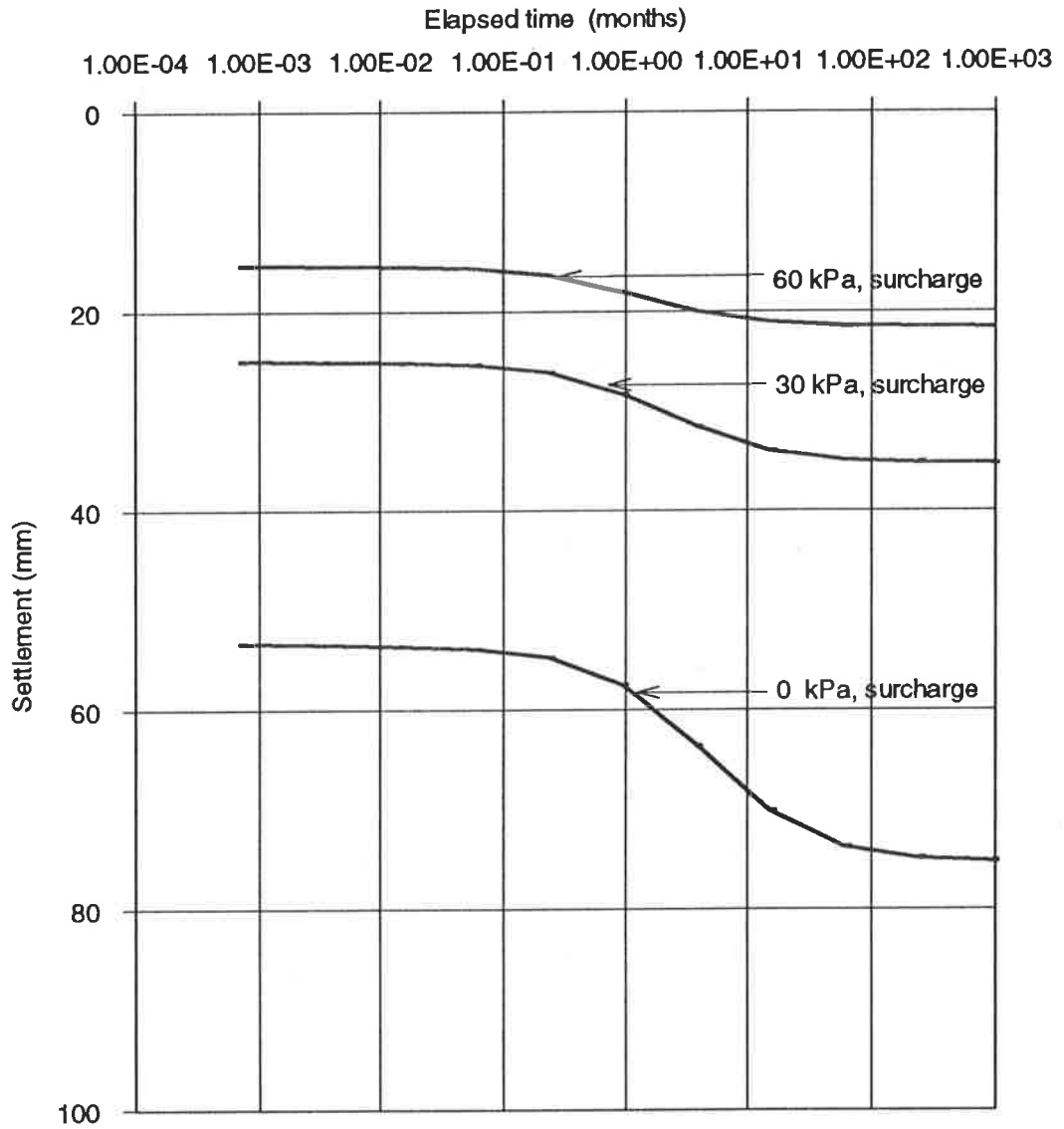


Figure 6.9 Relationship between settlement and elapsed time at the centre of a circular footing for 12 kPa loading.

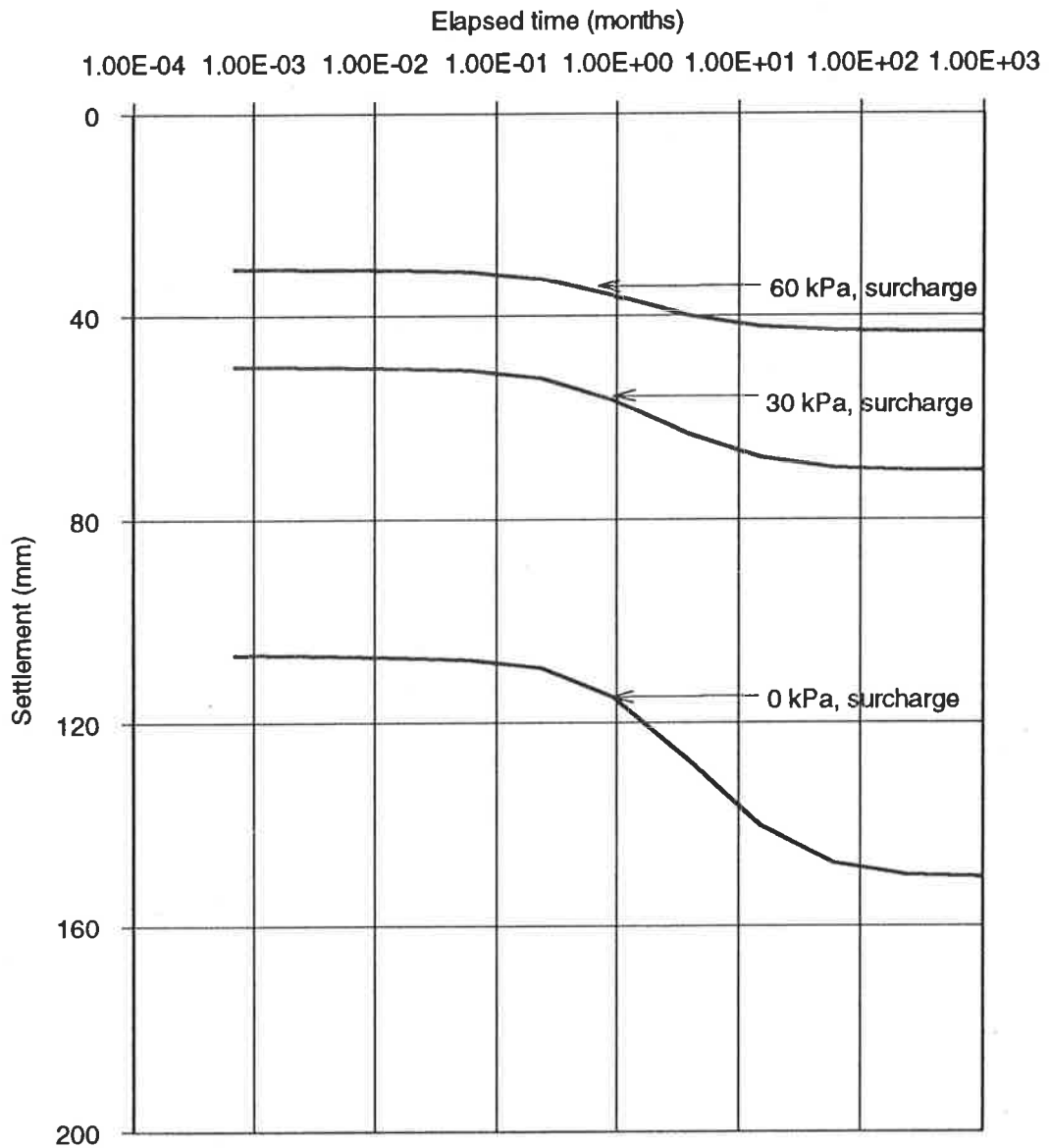


Figure 6.10 Relationship between settlement and elapsed time at the centre of a circular footing for 24 kPa loading.

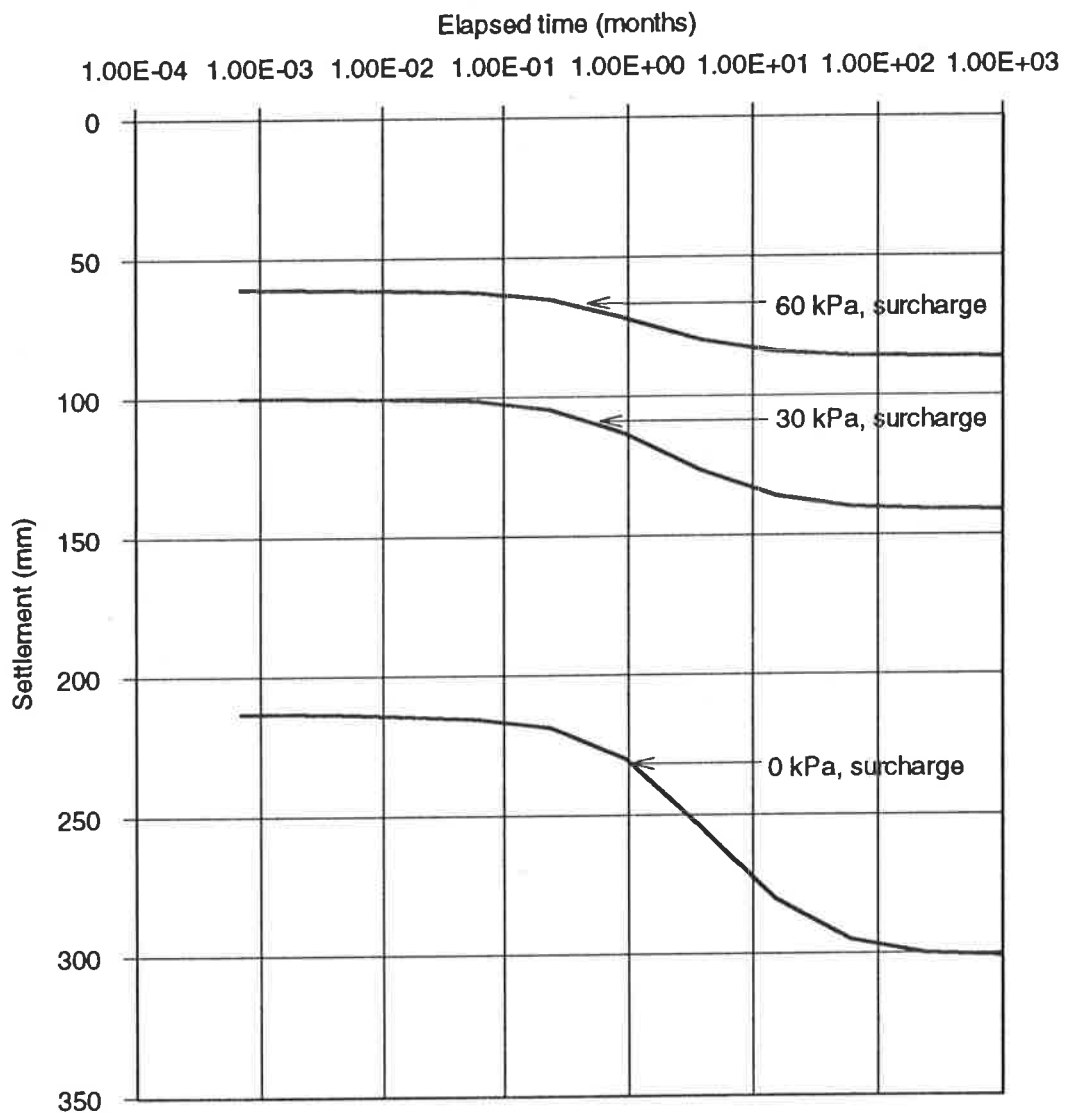


Figure 6.11 Relationship between settlement and elapsed time at the centre of a circular footing for 48 kPa loading.

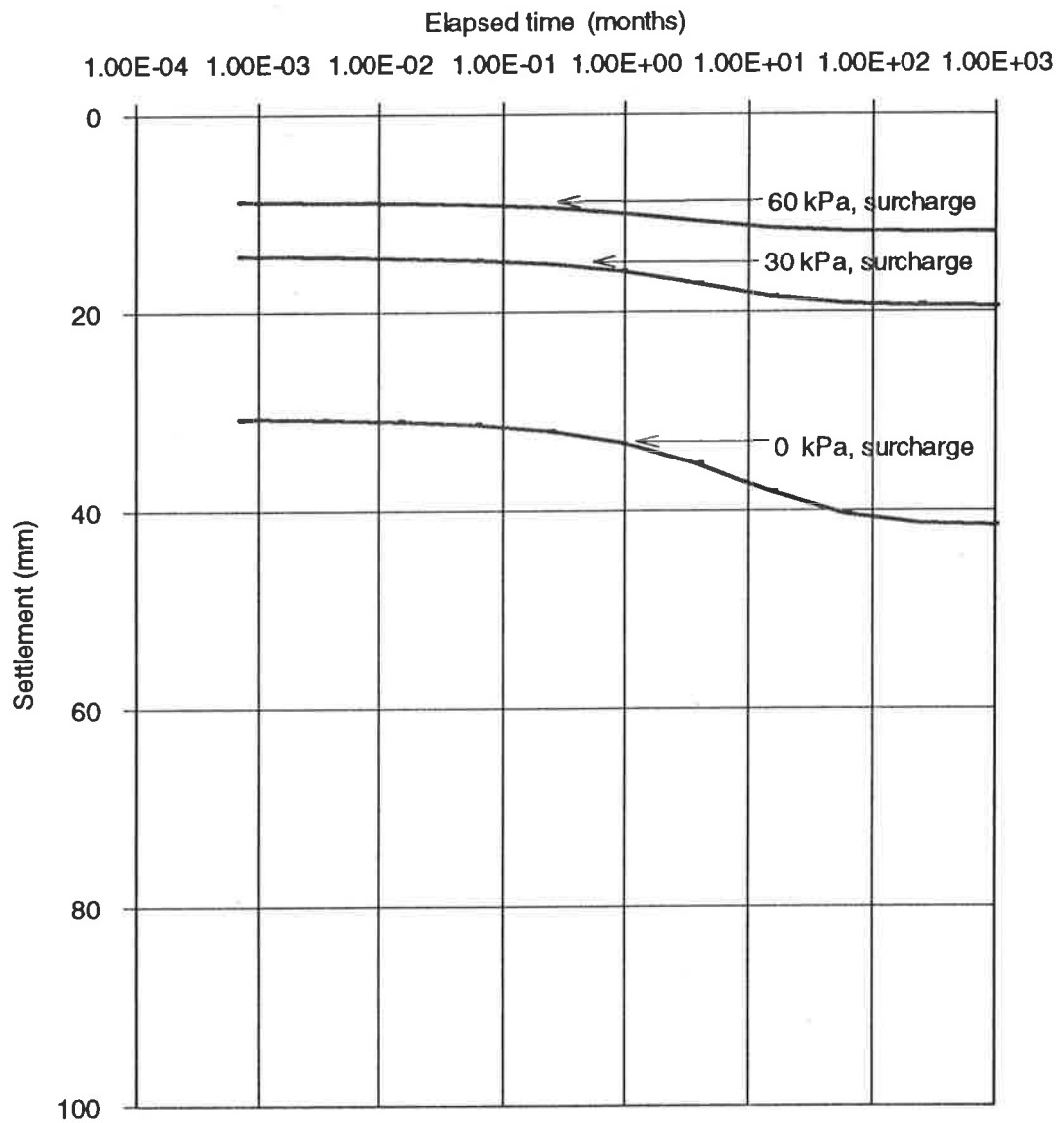


Figure 6.12 Relationship between settlement and elapsed time at the edge of a circular footing for 12 kPa loading.

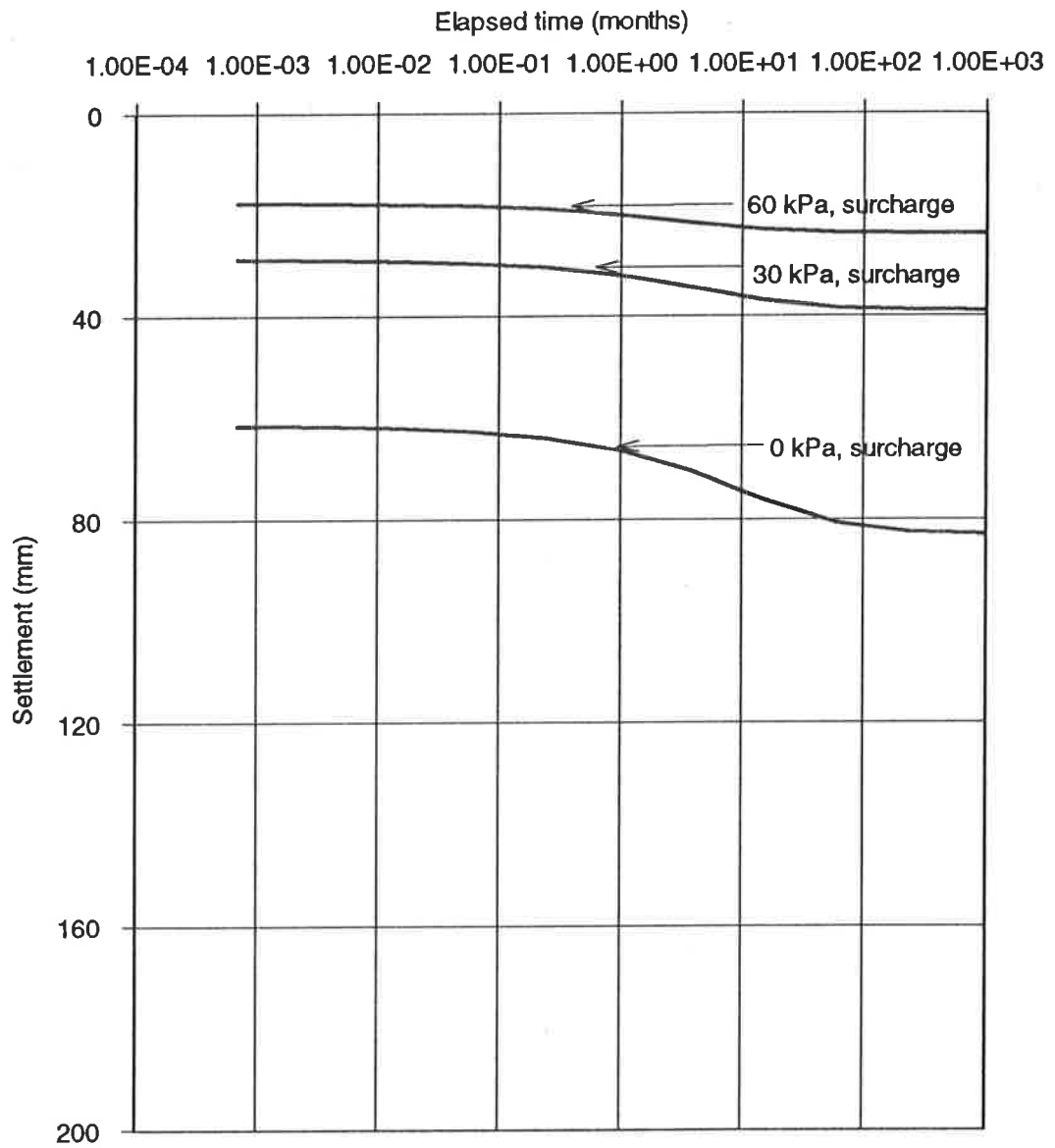


Figure 6.13 Relationship between settlement and elapsed time at the edge of a circular footing for 24 kPa loading.

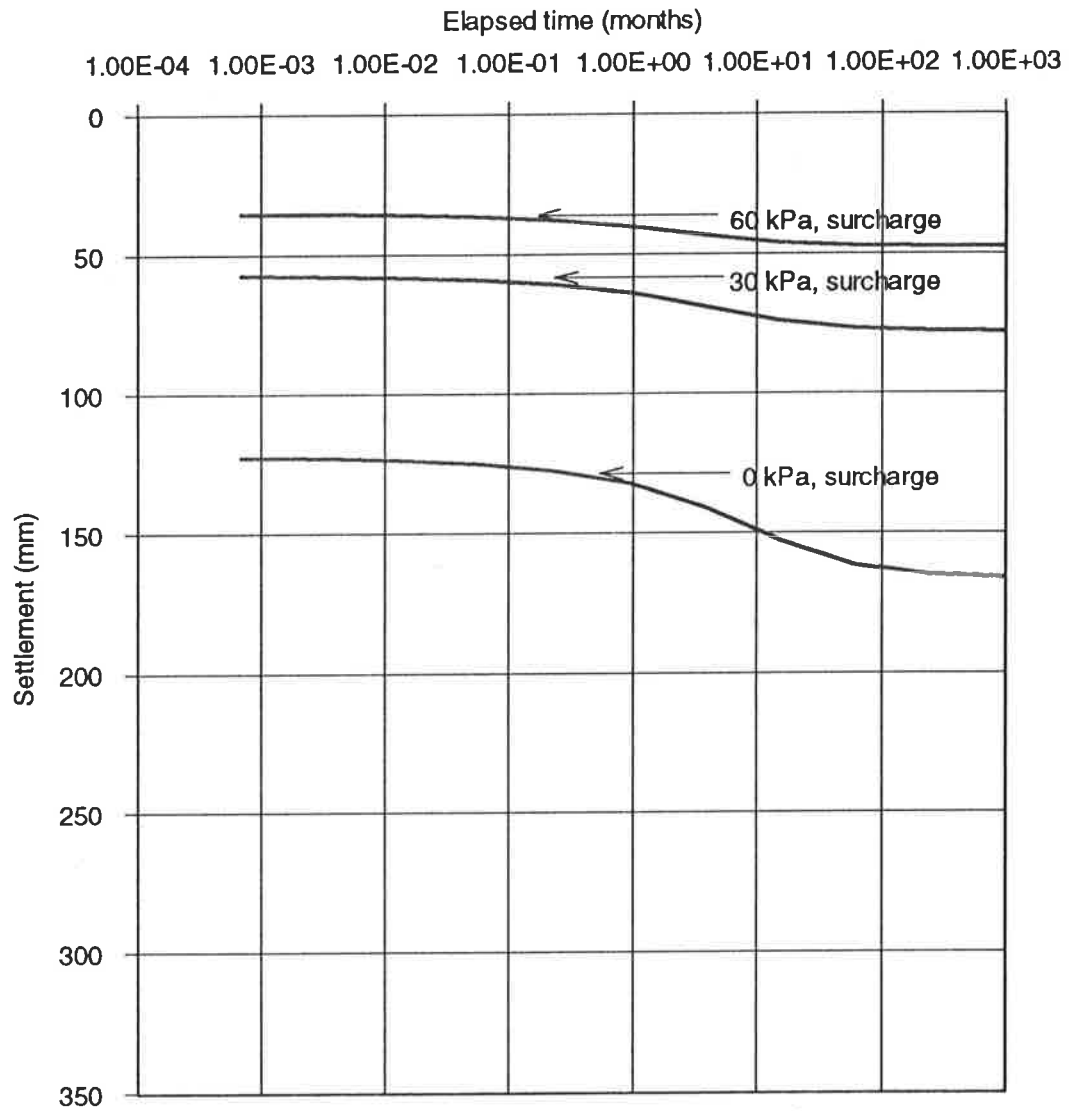


Figure 6.14 Relationship between settlement and elapsed time at the edge of a circular footing for 48 kPa loading.

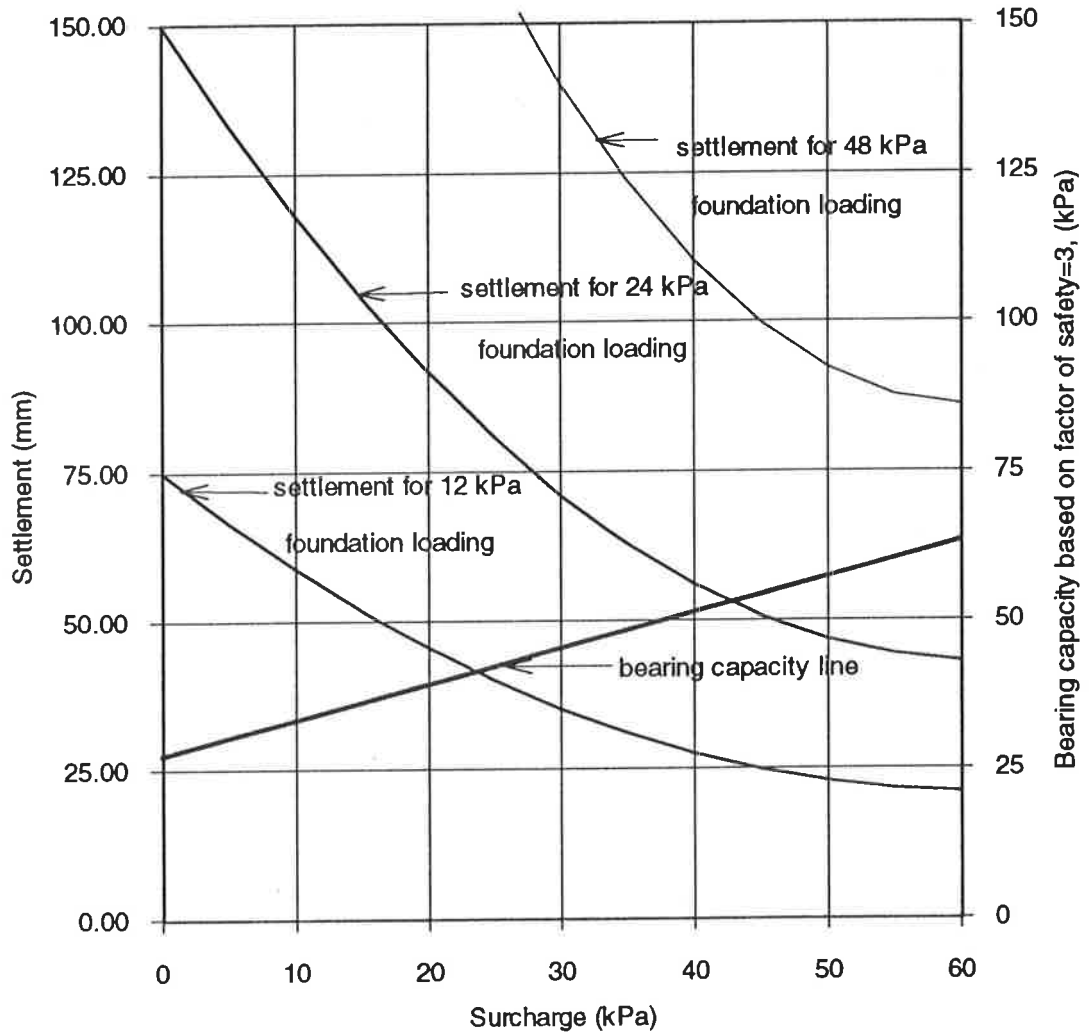


Figure 6.15 Variation of long term settlement and safe bearing pressure of 4m diameter footing with surcharge pressure.

Chapter 7

Summary and conclusion

7.1 Summary

The main objective of this study was to determine the normalised undrained shear strength and deformation parameters of Keswick Clay in the laboratory from isotropically consolidated undrained triaxial compression tests. The second objective was to apply the normalised soil parameters to evaluate the in situ soil properties of a typical soil profile, and to use them in the determination of minimum design requirements of a circular footing.

Information on triaxial testing, presented in Chapter 2, indicated that a range of test types are available, with unconsolidated undrained tests being the simplest. However, emphasis has been given to consolidated undrained tests because the undrained shear strength obtained from UU tests is unreliable, primarily due to sampling disturbance.

Based on CU tests, the detailed testing procedure of the SHANSEP method was described. The main testing technique involved in this method is to consolidate the sample beyond the maximum effective past pressure, σ'_{vm} , that has been experienced by the soil and then shear the normally consolidated sample. If a specified overconsolidation ratio is required to represent in situ overconsolidated condition, then the effective consolidation pressure is lowered and the sample allowed to swell completely. The test results reveal that the normalised soil parameters (s_u/σ'_{v0} , E_u/σ'_{v0}), increase significantly with OCR.

A review of properties of the Keswick Clay from the available literature, followed by standard laboratory test results were presented in Chapter 4 together with the experimental program, which consisted of a series of isotropically consolidated undrained tests, with overconsolidation ratios varying between 1 and 13.

Based on the analysis of the results, the following points emerge:

- There is a linear relation between undrained shear strength and effective consolidation pressure for normally consolidated clay. Values of the effective cohesion, c' of 0, and the effective friction angle, ϕ' of 12° , were obtained.
- The stress-strain curves of normally consolidated clay exhibit normalised behaviour when the deviator stress is normalised with respect to the effective consolidation pressure.
- The relationship between the normalised undrained shear strength (s_u/σ'_{v0}) and OCR shows that the normalised undrained shear strength of Keswick Clay increases with increasing OCR although the values are lower than those reported by Ladd and Edgers (1972) for various cohesive soils. The normalised

deformation parameter (E_u/σ'_{v0}) also increases with OCR, whereas the pore pressure parameter at failure, A_f , decreases slightly with increasing OCR.

The extension of normalised soil parameters (s_u/σ'_{v0}), and (E_u/σ'_{v0}), to field conditions indicated that the undrained shear strength and undrained Young's modulus, which affect the settlement and bearing capacity, significantly increase with increasing surcharge and depth below the ground surface. From considerations of footing settlement and allowable bearing pressure, surcharges of 16 kPa and 46 kPa are needed for the safe design of a 4 m diameter circular footing carrying 12 kPa and 24 kPa average pressures, respectively.

7.2 Future research

Based on the present study, it is recommended that research on normalised behaviour of Keswick Clay should be extended into several areas for a number of reasons. These include:

- The anisotropic nature of in situ soil conditions generates the need for K_0 -consolidation in the laboratory but due to time constraints, isotropic consolidation was adopted in the testing procedure of this research. Therefore, further research is recommended to carry out tests under K_0 consolidation, to examine the effect of initial consolidation on the properties of the soil.
- The interpretation of test results from the present research was based on normalised soil parameters and OCR. However, more research is needed to investigate the elasto-plastic behaviour of Keswick Clay to further quantify the clay's behaviour.

- More complex numerical analyses than those carried out in this study are also needed to account for elasto-plastic behaviour and other conditions such as suction dependent soil movements of the soil under field loading conditions.

7.3 Conclusion

Normalised soil parameters play an important role in evaluating the soil properties of cohesive soils. This study has demonstrated that, for Keswick Clay the correlations between normalised soil parameters and OCR obtained in the laboratory can be extended to determine the in situ soil properties of the profile. Therefore, in conclusion, it can be said that normalised soil parameters are very useful in evaluating the soil parameters of cohesive soils.

References

Andreson, A., Berre, T., Kleven, A. & Lunne, T. (1979), "Procedures Used to Obtain Soil Parameters for Foundation Engineering in the North Sea," March, *Geotechnol*, 3, pp. 201-266.

Atchison, G. D., Peter, P. and Power, R. F. (1977), "Stress Deformation Mechanisms in Clays - Case Histories in Adelaide," *Symposium on How to Live with Geotechnical Risks*, Cooma, Inst. Eng. Aust., pp. 26-33.

Atkinson, J. H. and Bransby, P. L. (1978), "*The Mechanics of Soil: An Introduction to Critical State Soil Mechanics*," McGraw Hill Book Co, pp. 184-209, 210-234.

Berre, T. (1977), "Effect of End Friction on Results of Triaxial Tests on Plastic Clay from Drammen," *NGI Internal Report 56103-9*, (Unpublished).

Berre, T. (1978), "Effect of Rubber Membrane, Side Dram and Specimen Height on Results of Triaxial Tests," *NGI Internal Report 56103-10*, (Unpublished).

References

Bishop, A. W. and Henkel, D. J. (1957), "*The Measurement of Soil Properties in the Triaxial Test,*" Edward Arnold Ltd., London.

Bishop, A.W. and Bjerrum, L. (1960), "The Relevance of the Triaxial Test to the Solution of Stability Problems," *Proceedings, ASCE Research Conference on Shear Strength of Cohesive Soils*, University of Colorado, Boulder, Colo., pp. 437-501.

Bishop, A. W. and Henkel, D. J. (1962), "*The Measurement of Soil Properties in the Triaxial Test,*" Edward Arnold Ltd., 2nd ed., London, pp. 1-29.

Bjerrum, L. (1972), "Embankments on Soft Grounds," *Proceedings, ASCE Specialty Conference on Performance of Earth-Supported Structures*, Vol. 11, Purdue University, West Lafayette, Ind., pp. 1-54.

Bjerrum, L. (1973), "Problems of Soil Mechanics and Construction on Soft Clays," *Proceedings of the 8th International Conference on Soil Mechanics and Foundation Engineering*, Moscow, Vol. 3, pp. 109-159.

Bowles, J. E. (1988), "*Foundation Analysis and Design,*" 4th Edition, McGraw-Hill, International Edition, 295p.

Casagrande, A. (1936), "The Determination of the Pre-consolidation Load and its Practical Significance," *Proceedings of the 1st International Conference on Soil Mechanics and Foundation Engineering*, Cambridge, Mass, Vol. 3, pp. 60-64.

Casagrande, A. W. and Wilson, S. D. (1951), "Effect of Rate of Loading on the Strength of Clays and Shales at Constant Water Content," *Geotechnique*, Vol. 2, No. 3, pp. 251-263.

References

Chen, Yit-Jin and Kulhawy, F. H. (1993), "Undrained strength interrelationships among CIUC, UU, and UC Tests," *Journal of the Geotechnical Engineering Division, Proceedings of the American Society of Civil Engineers*, Vol. 119, No. 11, pp. 1732-1750.

Cox, J. B. (1970), "A Review of the Geotechnical Characteristics of the Soils in the Adelaide City Area," *Proceedings of Symposium on Soils and Structures in Arid Climates, I. E. Aust. and Aust. Geomech. Society*, Adelaide, pp. 72-86.

D' Appolonia, D. J., Lambe, T. W., and Poulos, H. G. (1971), "Evaluation of pore pressure beneath an embankment," *Journal of the Soil Mechanics and Foundation Division, American Society of Civil Engineers*, Vol. 97, No. SM 6, Proc. Paper 8213, pp. 881-898.

Davis, E. H. and Poulos, H. G. (1967), "Laboratory Investigations of the Effects of Sampling," *Civil Engineering Transactions*, Institute of Engineers, Australia, Vol. CE9, No. 1, pp. 67-91.

Donaghe, R. T. and Townsend, F. C. (1978), "Effects of Anisotropic versus Isotropic Consolidation in Consolidated Undrained Triaxial Comparison Tests of Cohesive Soils," *Geotechnical Testing Journal, GTJODJ*, Vol. 1, No. 4, pp. 173-189.

Duncan, J. M. and Dunlop, P. (1969), "Behaviour of Soils in Simple Shear Tests," *Proceedings of the Seventh International Conference on Soil Mechanics and Foundation Engineering*, Mexico, Vol. 1, pp. 101-109.

Duncan, J. M. and Seed, H. B. (1966), "Anisotropy and Stress Reorientation in Clay," *Journal of the Geotechnical Engineering Division, Proceedings of the American Society of Civil Engineers*, Vol. 92, No. SM5, pp. 21-50.

References

Germaine, J. T. and Ladd, C. C. (1988), "Triaxial Testing of Saturated Cohesive Soils," *Advanced Triaxial Testing of Soil and Rock*, ASTM STP 977, Robert, T. Donaghe, Ronald Chaney, and Marshal L. Silver, Eds., *American Society for testing and Materials*, Philadelphia, pp. 421-459.

Grant, R., Christian, J. T. and Vanmarcke, E. H. (1974), "Differential Settlements of Buildings," *Journal of the Geotechnical Engineering Division, Proceedings of the American Society of Civil Engineers*, Vol. 100 No. GT 9, pp. 973-991.

Hansen, J. B. (1970), "A revised and Extended Formula for Bearing Capacity," *Danish Geotechnical Institute Bul.*, No. 28, Copenhagen, 22 p.

Hansen, J. B. and Gibson, R. E. (1949), "Undrained Shear strength of Anisotropically Consolidated Clays," *Geotechnique*, Vol. 1, No. 3, pp. 189-204.

Hanzawa, H. and Tanaka, H. (1992), "Normalised Undrained Strength of Clay in the Normally Consolidated State and in the Field," *Soils and Foundations*, Vol. 32, No. 1, pp. 132-148.

Head, K. H. (1988), "*Manual of Soil Laboratory Testing*," Vol. 2, Pentec Press, London, pp. 616-650.

Henkel, D. J. (1956), "The Effect of Overconsolidation on the Behaviour of Clays During Shear," *Geotechnique*, Vol. 6, p. 139.

Henkel, D. J. (1960), "The Shear Strength of Saturated Remoulded Clays," *Proceedings ASCE Specialty Conference on Shear Strength of Cohesive Soils*, University of Colorado, pp. 533-554.

References

Jacobsen, M. (1967), "The Undrained Shear Strength of Preconsolidated Boulder Clay," *Geotechnical Conference of Shear Strength Properties of Natural Soils and Rocks*, Proceedings, Vol. 1, Oslo, pp. 119-122.

Jaksa, M. B. and Kaggwa, W. S. (1992), "Degree of Saturation of the Keswick Clay Within Adelaide City Area Above the General Ground Water Table," *Proceedings 6th Australia New Zealand Conference on Geomechanics*, Christchurch, pp. 336-341.

Jaksa, M. B., Brooker, P. I., Kaggwa, W. S., van Holst Pellekaan, P. D. A. and Cathro, J. L. (1994), "Modelling the Lateral Spatial Variation of the Undrained Shear Strength of a Stiff, Overconsolidated Clay Using a Horizontal Cone Penetration Test," *Research Report*, Dept. of Civil & Environmental Engg., University of Adelaide (in print).

Jamiolkowski, M., Ladd, C. C., Germaine, J. T. and Lancellota, R. (1985), "New Developments in Field and Laboratory Testings of Soils," *Proceedings of the 11th International Conference on Soil Mechanics and Foundation Engineering*, Vol. 1, pp. 57-153.

Kaggwa, W. S. (1992), "On In-Situ Stresses, Soil Suctions, Shear strength and K_0 of Hindmarsh Formation Clay," *Civil Engineering Transactions*, Institute of Engineers Australia, Vol. CE34, No. 2, pp. 97-105.

Kaggwa, W. S. and Jaksa, M. B. (1992), "Normalised Shear Strength and Compressibility Characteristics of Adelaide Expansive Clay," *Proceedings 6th Australia New Zealand Conference on Geomechanics*, Christchurch, pp. 330-335.

References

Koutsoftas, D. C. and Ladd, C. C. (1985), "Design Strength for Offshore Clay," *Journal of the Geotechnical Engineering Division, Proceedings of the American Society of Civil Engineers*, Vol.111, No. 3, pp. 337-355.

Lacasse, S. and Berre, T. (1989), "Triaxial Testing Methods for Soils," "Triaxial Testing of Saturated Cohesive Soils", *Advanced Triaxial Testing of Soil and Rock*, ASTM STP 977, Robert, T. Donaghe, Ronald, Chaney, and Marshal, L. Silver, Eds., *American Society for Testing and Materials*, Philadelphia, pp. 264-289.

Ladd, C. C. (1964), "Stress Strain Modulus of Clay in Undrained Shears," *Journal of the Soil Mechanics and Foundations Division, Proceedings of the American Society of Civil Engineers*, Vol. 90, No. 5, pp. 103-132.

Ladd, C. C. (1965), "Stress Strain Behaviour of Anisotropically Consolidated Clays During Undrained Shear," *Proceedings of the 6th International Conference on Soil Mechanics and Foundation Engineering*, Vol. 1, pp. 282-286.

Ladd, C. C. and Lambe, T. W. (1963), "The Strength of 'Undisturbed' Clay Determined from Undrained Tests," *American society for testing and materials*, STP 361, pp. 342-371.

Ladd, C. C., Aldrich, H. P., and Johnson, E. G. (1969), "Embankment Failure on Organic Clay," *Proceedings of the 7th International Conference on Soil Mechanics and Foundation Engineering*, Vol. 2, Mexico City, Mexico, pp. 627-634.

Ladd, C. C. and Edgers, L. (1972), "Consolidated-Undrained Direct-Simple Shear Tests on Saturated Clays," *Research Report R72-82*, No. 284, Department of Civil Engineering, Massachusetts Institute of Technology, Cambridge, 354 p.

References

Ladd, C. C. and Foott, R. (1974), "New Design Procedure For Stability of Soft Clays," *Journal of the Geotechnical Engineering Division, Proceedings of the American Society of Civil Engineers*, Vol. 100 No. GT 7, pp. 763-786.

Ladd, C. C., Foott, R., Ishihara, K., Schlosser, F., and Poulos, H. G. (1977), "Stress Deformation and Strength Characteristics," *Proceedings of the 9th International Conference on Soil Mechanics and Foundation Engineering*, Vol. 2, pp. 421-495.

Ladd, C. C. and Foott, R. (1980), Discussion of "The Behaviour of Embankments on Clay Foundations," *Canadian Geotechnical Journal*, Vol. 17, No. 3, pp. 454-460.

Lade, P. V. (1986), "*Advanced Triaxial Testing of Soils*," School of Civil and Mining Engineering, The University of Sydney, New South Wales, Australia, pp. 1-33, 149-200.

Lambe, T.W. and Whitman, R. V. (1979), "*Soil Mechanics*," John Wiley and Sons, Inc., pp. 304-317, 423-438.

Loudon, P. A. (1967), "Some Deformation Characteristics of Kaolin", *Ph.D Thesis*, University of Cambridge.

MacDonald, D. H. and Skempton, A. H. (1955), "A Survey of Comparisons between Calculated and Observed Settlement of Structures on Clay," *Conference on Correlation of Calculated and Observed Stresses and Displacements*, Institute of Civil Engineers, London, pp. 318-337.

Mayne, P. W. (1979), Discussion of "Normalised Deformation Paramaters for Kaolin," *Geotechnical Testing Journal, GTJODJ*, Vol. 2, No. 2, pp. 118-121.

References

Mayne, P. W. (1985), "Stress Anisotropy Effects on Clay Strength," *Journal of the Geotechnical Engineering Division, Proceedings of the American Society of Civil Engineers*, Vol. 111, No.3, pp. 356-366.

Mayne, P. W. and Kulhawy, F. H. (1982), " K_0 -OCR Relationship in Soils," *Journal of the Geotechnical Engineering Division, Proceedings of the American Society of Civil Engineers*, Vol.108, No. GT6, pp. 851-872.

Mesri, G. (1975), Discussion on "New Design Procedure for Stability of Soft Clays," *Journal of the Geotechnical Division, Proceeding of the American Society of Civil Engineers*, Vol. 101, No. GT4, pp. 409-412.

Meyerhof, G. G. (1951), "The Ultimate Bearing Capacity of Foundations," *Geotechnique*, Vol. 2, No. 4, pp.-301-331.

Meyerhof, G. G. (1963), "Some Recent Research on the Bearing Capacity of Foundations," *Canadian Geotechnical Journal*, Ottawa, Vol. 1, No. 1, pp. 16-26.

Mitachi, T. and Kitago, H. (1979), "The Influence of Stress History and Stress System on the Stress-Strain-Strength Properties of Saturated Clay," *Soils and Foundations*, Vol. 19, No. 2, pp. 45-61.

Nakase, A. and Kamei, T. (1988), "Undrained Shear Strength of Remoulded Marine Clays," *Soils and Foundations*, Vol. 28, No. 1, pp. 29-40.

Parry, R. H. G. (1960), "Triaxial Compression and Extension Tests on Remoulded Saturated Clays," *Geotechnique*, London, England, Vol. 10, No. 4, pp. 166-180.

References

Poulos, H. G. (1978), "Normalized Deformation Parameters for Kaolin," *Geotechnical Testing Journal*, GTJODJ, Vol. 1, No. 2, pp. 102- 106.

Richards, B. G. and Kurzeme, M. (1973), "Observations of Earth Pressures on a Retaining Wall at Gouger St. Mail Exchange, Adelaide," *Australian Geomechanics Journal*, Vol. G3, No. 1.

Richardson, A. M., and Whitman, R. V. (1963), "Effect of Strain-Rate Upon Undrained Shear Resistance of a Saturated Remoulded Fat Clay," *Geotechnique*, London, Vol. 13, No. 4, pp. 310-324.

Saada, A. S. and Townsend, F. C. (1981), "In Laboratory Shear Strength of Soils," *American Society for Testing and Materials*, STP 740, Philadelphia, ASTM, pp. 7-77.

Schmidt, B. (1966), Discussion of "Earth Pressure at Rest Related to Stress History," *Canadian Geotechnical Journal*, Vol. 3, No. 4, pp. 239-242.

Selby, J. and Lindsay, J. M. (1982), "*Engineering Geology of the Adelaide City Area*," Dept. Mines & Energy, Bulletin 51, 48p.

Sheard, M. J. and Bowman, G. M. (1987a), "Definition of Keswick Clay: Adelaide/Golden Grove Embayment, Para and Eden Blocks, South Australia," *Q. Geological Notes, Geological Survey South Australia*, 103, pp. 4-9.

Sheard, M. J. and Bowman, G. M. (1987b), "Redefinition of the Upper Boundary of the Hindmarsh Clay: Adelaide Plains Sub-Basin and Adelaide/Golden Grove Embayment," *Q. Geological Notes, Geological Survey South Australia*, 103, pp. 9-16.

References

Shibata, T. and Karube, D. (1965), "Influence of the Variation of the Intermediate Principal Stress on the Mechanical Properties of Normally Consolidated Clays," *Proceedings of the 6th International Conference on Soil Mechanics and Foundation Engineering*, Vol. 1, pp. 359-363.

Skempton, A. W. (1948), "The $\phi = 0$ Analysis of Stability and Theoretical Basis," *Proceedings of the 2nd International Conference on Soil Mechanics and Foundation Engineering*, Vol. 1, pp. 72-78.

Skempton, A. W. (1954), "The Pore Pressure Coefficients A and B," *Geotechnique* 4, pp. 143-147.

Skempton, A. W. and Bishop, A. W. (1954), "Soils in Building Material-Their Elasticity and Inelasticity," *North Holland Publication Co.*, Amsterdam, pp. 417-482.

Skempton, A. W. and Sowa, V. A. (1963), "The Behaviour of Saturated Clays During Sampling and Testing," *Geotechnique*, Vol. 13, No. 4, pp. 269-290.

Small, J. C. (1977), "Axcons, A Finite Element Software that Analyses Axi-Symmetric Consolidation within Triangular Elements," *School of Civil Engineering*, University of Sydney.

Standards Association of Australia (1977), "*Methods for Testing Soils for Engineering Purposes, 1289*," Sydney.

Terzaghi, Karl and Peck, R.B. (1962), "*Soil Mechanics in Engineering Practice*", John Wiley & Sons Inc., New York.

References

Terzaghi, K. (1943), "Evaluation of Coefficient of Subgrade Reaction," *Geotechnique*, Vol. 5, No. 4, pp. 297-326.

Vaid, Y. P. and Campanella, R. G. (1974), "Triaxial and Plane Strain Behaviour of Natural Clay," *Journal of Geotechnical Engineering Division, American Society of Civil Engineers*, Vol. 100, No. GT3, pp. 207-224.

Vesic, A. S. (1973), "Analysis of Ultimate Loads of Shallow Foundations," *Journal of the Soil Mechanics and Foundation Division, American Society of Civil Engineers*, Vol. 99, SM 1, pp. 45-73.

Vesic, A. S. (1974), Chap. 3: "Bearing Capacity of Shallow Foundations, in *Foundation Engineering Handbook*, Van Nostrand Remhold Book Co., New York, 751p.

Wroth, C. P. (1984), "The Interpretation of In Situ Soil Tests," *Geotechnique*, Vol. 34, No. 4, pp. 449-489.

Corrigenda for Masters Thesis
 "Normalised Undrained Shear Strength and Deformation Properties of
 Remoulded Keswick Clay"

by

MD. ZAHRUL ISLAM

Page	Paragraph	Line	
10	2-4		replace 'Poisson' with 'Poisson's'
11	2		σ'_{cm} is the effective maximum confining pressure
11	2	9	replace 'and shear stress, $q = (\sigma_1 - \sigma_3)$.' with 'and mean shear stress, $q = \frac{(\sigma_1 - \sigma_2)}{2}$.'
27	2	9	replace 'pore pressure during sampling' with 'pore pressure parameters during sampling'
29			UC stands for unconfined compression
30	1		read as different paragraph 'The results from plane strain
30	1	9	replace 'decreases' with 'decreased'
30	1	10	replace 'changes' with 'changed'
31	1	1	replace 'heavily OCR' with 'high OCR'
32	1	1	σ'_D is the maximum overburden pressure
32	3	2	read sentence as 'Parry (1960) evaluated the shear strength characteristics of normally consolidated and overconsolidated samples of remoulded London Clay and Weald Clay. He found that samples with the same overconsolidation ratio, but different effective consolidation pressures, exhibit constant $\frac{(\sigma_1 - \sigma_3)}{\sigma'_c}$ when the deviator stress, $(\sigma_1 - \sigma_3)$, is normalised with respect to the effective consolidation pressure, σ'_c .'
35	1	Last sentence	read sentence as 'The SHANSEP method is described in Figure 3.3 with regard to stresses used in the in situ, UU tests and CK_0U compression tests.'
35	3	6	replace 'consolidate' with 'consolidation of'
37	3	last line	replace 'between a normalised' with 'between normalised'
40	2	6	replace 'dependant' with 'dependant on'

page	paragraph	line	
43			τ_h is the horizontal shear stress
67	3	5	replace 'pointed out' with 'indicated'
68	1	3	replace 'dissipate' with 'is dissipated'
68	2	3	replace 'clay laboratory' with 'clay, laboratory'
69	3	9	read sentence as 'The shear strength data give an apparent cohesion at the surface of 18 Kpa, and at depth, 192 Kpa showing an increase in strength with depth.'
70	1	3	replace 'dried' with 'air-dried'
70	footnote		replace 'centre' with 'centres'
72	1	16	replace 'shear strength increases' with 'shear strength should increase'
72	1	18	read (ii) as 'The soil is very difficult to compact when wet and impossible to drain by ordinary means.'
75	3	third sentence	read sentence as 'Generally with an increase in the particle size the sample size required will also increase.'
76	1	point (a)	read (a) as 'The samples with smooth ends and (h/d) ratio had similar strength as the sample with rough ends and (h/d) ratio of 2 upto an axial strain of 10%. Beyond an axial strain of 10% the sample with smooth ends and (h/d) ratio of 1 showed higher strength.'
76	1	point (b)	read (b) as 'The smooth ended samples showed more pronounced false deformation than rough ended samples for the initial part of the stress strain curve. Also the determination of Young's modulus at low strain is more reliable with high sample and rough ends.'
76	footnote		read 3) as 'The term 'rough 'means a filter paper placed between the sample ends and the pedestal and top cap.'
76	4	2	replace 'Initially the moisture' with 'Initially, the moisture.'
79	2	7	read sentence as 'As mentioned in chapter 3, it should be noted that isotropically consolidated undrained test can be used as a 'reference' test and the results can be used to estimate parameters for K_0 condition.'
81		10	replace 'are plotted' with 'were plotted'
92	2	6	replace 'where there' with 'at which point there'

page	paragraph	line	
97	1	6	replace 'For some effective' with 'For the same effective'
97	1	7	replace 'show higher' with 'have higher'
97	2	4th last	replace 'But for' with 'However for'
98	2	2	read sentence as 'As can be seen from the figure, normally consolidated clay samples form a straight line passing through the origin.'
99	1	7	delete 'which decreases'
101	2	7	replace 'non-linear relationships' with 'non-linear relationship'
102	4	2	replace 'produce identical' with 'produce an identical'
103	2	7	replace 'found lower' with 'found to be lower'
104		last line	replace 'homogeneity' with 'homogenous nature'
108	1	2nd last sentence	replace 'A value of ' with 'The experimental value of'
108	4	4	replace 'conn. valey' with 'conn. valley'
108	4	5	replace 'Sydney Kaolin which was examined by Poulos (1978)' with 'the results of Sydney Kaolin reported by Poulos (1978)'
109	3		replace 'OCR increases' with 'OCR increased'
110	3	8	replace ϕ'_r with c'_r
134	2	6	read sentence as 'In Figure 6.1(a) the deposit of Keswick Clay with no surcharge has been chosen, having the OCR profile shown in Figure 3.12.'
134	2	last sentence	'The OCR and the effective vertical stress, σ'_v affect the soil properties. Details of the OCR and the effective vertical stress σ'_v and the effect of surcharge on them is discussed in the following sections.'
134	3	2	replace 'throughout world' with 'throughout the world'
135	3	4	replace 'higher than previous' with 'higher than the previous'
135	3	9	replace 'the OCR of natural deposit' with 'the OCR of the natural deposit'
137	2	7	replace 'below ground surface' with 'below the ground surface'
138	point 3	4	replace 'no significant variations' with 'no major variations'
138	4	10	replace 'resulting higher' with 'resulting in higher'
139	2	2	replace 'by the following equation' with 'using the accepted expression'



page	paragraph	line	
140	1	2, point 1	replace 'descretisation' with 'descretisation'
145	1	9	d' _c = 0.2
145	1	10	replace 'bearing capacities of 84 kPa, 132 kPa and 193 kPa' with 'bearing capacities of 48 kPa, 66 kPa and 96 kPa.'
147	1	8	read sentence as 'But OCR decreases as σ'_v increases and so their influence on s_u is negated to some extent as indicated on Figure 6.6. Also once is large enough, the OCR=1 and s_u increases linearly.'
165	2		replace 'properties of the Keswick Clay' with "properties of Keswick Clay"
166	2		ignore last sentence of 7.1